MINERALOGICAL, GEOCHEMICAL, AND ISOTOPIC EVIDENCE OF DIAGENETIC ALTERATION, ATTRIBUTABLE TO HYDROCARBON MIGRATION, RAVEN CREEK AND REEL FIELDS, WYOMING

By

JOHN CONRAD MARKERT II

Bachelor of Science
Oklahoma State University
Stillwater, Oklahoma
1974

Bachelor of Science
Oklahoma State University
Stillwater, Oklahoma
1979

Submitted to the Faculty of the Graduate College
of the Oklahoma State University
in partial fulfillment of the requirements
for the Degree of
MASTER OF SCIENCE
May, 1982

MINERALOGICAL, GEOCHEMICAL, AND ISOTOPIC

EVIDENCE OF DIAGENETIC ALTERATION,

ATTRIBUTABLE TO HYDROCARBON

MIGRATION, RAVEN CREEK

AND REEL FIELDS,

WYOMING

Thesis Approved:

Zuhair al-Shaieb
Thesis Adviser

Douglas C. Kent

Gary J. Stewart

Norman N. Durham
Dean of the Graduate College

PREFACE

Hydrocarbon migration exerted a limited influence on diagenetic mineralization in the upper Minnelusa sandstones of the Raven Creek and Reel oil fields in northeastern Wyoming. Alteration of sandstones by hydrogen sulfide gas associated with petroleum resulted in the formation of disseminated euhedral pyrite crystals. Cementation by anhydrite, dolomite, and authigenic clays reduced reservoir potential. Secondary porosity resulted from the dissolution of anhydrite cement. The results of this study were obtained through detailed examination and description of cores, petrographic studies, scanning electron microscopy, sulfur, carbon, and oxygen isotopic analysis, x-ray diffraction, and formation water analysis.

The author wishes to express his appreciation to his thesis adviser, Dr. Zuhair Al-Shaieb, for his guidance and assistance during this study. Suggestions and critical review of the manuscript by Dr. Gary F. Stewart and Dr. Douglas C. Kent, advisory committee members, are gratefully acknowledged. Partial financial support was provided by the Shell Development Company.

Appreciation is expressed to Mr. Bill Linenberger of the United States Geological Survey and Mr. John Christianson of the Shell Development Company who provided access to cores during this investigation. Dr. Fred Witz is acknowledged for his assistance in the preparation of the WATEQF program.

The author's parents deserve special appreciation for their encouragement and financial support. Special gratitude is extended to the author's wife, Wendy, for her drafting, encouragement, patience, and sacrifices too numerous to list.

TABLE OF CONTENTS

LIST OF TABLES

LIST OF FIGURES

LIST OF PLATES

CHAPTER I

INTRODUCTION

Location of the Study Area

The area of study is located in northeastern Wyoming, on the northeastern flank of the Powder River basin, and includes parts of Campbell, Crook, and Weston Counties (Fig. 1). The majority of the study focused on the Raven Creek and Reel oil fields, which trend northwest through the area of investigation.

Statement of the Problem

The principle objective of this investigation was to identify the diagenetic minerals which can be attributed to the migration of hydrocarbons at the Raven Creek and Reel oil fields. This petroleum originated in Permian rocks and migrated through central Wyoming into the Powder River basin (Barbat, 1967; Sheldon, 1967; Momper and Williams, 1979). The stable isotope geochemistry of sulfur from diagenetic pyrite was related to hydrocarbon migration in upper Minnelusa sandstones.

Previous Investigations

The structure of rocks in the subsurface of the Powder River basin has been studied by many investigators, including Curtis et al. (1958), Thomas (1963), and Glaze and Keller (1965). Structural features controlling hydrocarbon accumulation in the northeastern part of the basin

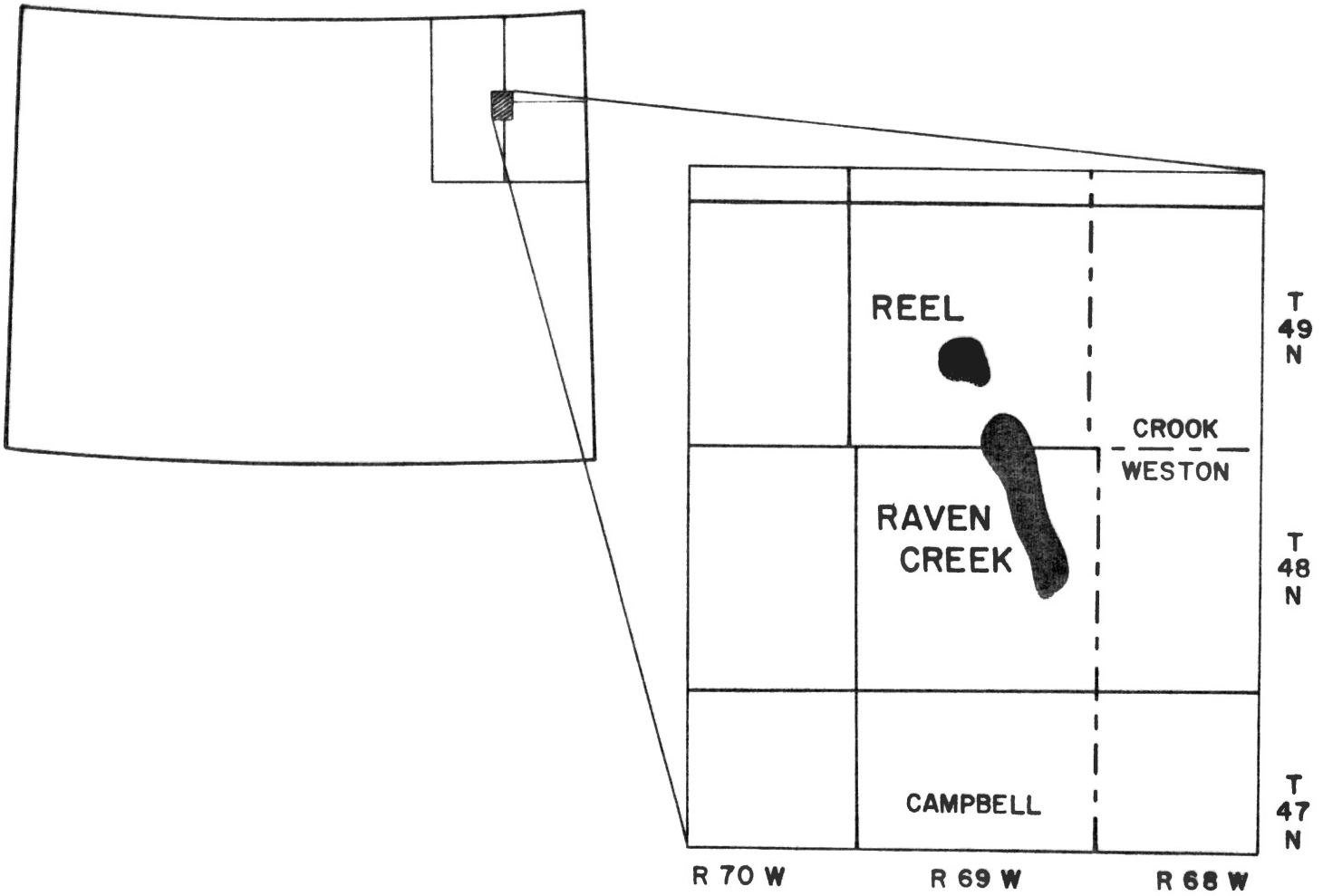

Fig. 1.--Index map of the study area.

have been described by Slack (1981).

The stratigraphy of Pennsylvanian and Lower Permian sediments in the Powder River basin has been studied by Branson (1939), Agatston (1954), Mallory (1967), Maughan (1978) and others. Foster (1958) divided the Minnelusa Formation into three members and described each in detail. The stratigraphy and structure of Minnelusa and adjacent strata in the Raven Creek field were described by Tranter (1963). Glaze and Keller (1965) studied the geologic history of the Powder River basin. Tenney (1966) described the geologic history and depositional environments of Lower Permian sediments in the Powder River basin. Stone (1969) studied the composition and depositional environments of Minnelusa sandstones.

Barbat (1967) presented evidence which indicates that the Phosphoria Formation is the source of petroleum trapped in Minnelusa sandstones. Sheldon (1967), Barbat (1967), and Momper and Williams (1979) described the mechanisms of migration of hydrocarbons into the Minnelusa. The structural and stratigraphic framework responsible for hydrocarbon entrapment in the Raven Creek oil field was described by Tranter (1913). The composition of oil from the Minnelusa was studied by Curtis et al. (1958), Stickland (1958), and Wenger and Reid (1958).

Methods and Procedures

The large number of cores taken from wells in the study area facilitated this investigation. The cores were obtained from the United States Geological Survey Core Library and Shell Development Company, both of Denver, Colorado.

Twenty-eight wells were selected for the investigation (Table I).

TABLE I

WELL LOCATIONS AND SAMPLE INTERVALS

Well Number	Location	Interval Studied
1. Mobil Oil Government No F12-6-G	NW, SW, NW 6-48N-68W	8051' - 8148'
2. Mobil Oil Krause No. F12-2-P	C, SW, NW 2-48N-69W	8339' - 8413'
3. Mobil Oil Krause No. F21-2-P	C, NE, NW 2-48N-69W	8306' - 8696'
4. Mobil Oil Krause No. F23-2-P	C, NE, NW 2-48N-69W	8347' - 8384'
5. Mobil Oil Krause No. F41-3-P	C, NE, NE 3-48N-69W	8464' - 8395'
6. Mobil Oil Krause No. F32-3-P	C, SW, NE 3-48N-69W	8371' - 8421'
7. E. M. Davis Talley No. 1	C, NE, NE 5-48N-69W	8654' - 8674'
8. Kewanee Oil Krause No. C-1	C, NE, NE 10-48N-69W	8415' - 8513'
9. Mobil Oil Krause No. F12-11-P	C, NE, NW 11-48N-69W	8366' - 8398'
10. Mobil Oil Krause No. F34-11-G	C, SW, SE 11-48N-69W	8333' - 8383'
11. Clark Oil No. F-48-69-13-C4	C, SW, SE 13-48N-69W	8451' - 8521'
12. Kewanee Oil Norman No. 1	C, NE, NW 14-48N-69W	8344' - 8452'
13. Kewanee Oil Government Bell No. 1	C, SW, NE 14-48N-69W	8317' - 8451'
14. Clark Oil No. F-48-69-24-B1	C, NE, NW 24-48N-69W	8380' - 8493'
15. Clark Oil Pickrel No. P-48-69-29-A4	C, SW, SW 29-48N-69W	8992' - 9042'

TABLE I (continued)

Well Number	Location	Interval Studied
16. McCulloch Oil Bishop No. 1-31	SW, SE, NE 31-48N-69W	9014' - 9074'
17. Ashland Oil Government Neuenschwander No. 1	C, NE, SW 1-48N-70W	9378' - 9427'
18. Mobil Oil State No. F34-16-S	C, SW, SE 16-49N-69W	8443' - 8560'
19. Mobil Oil Reel No. F14-21-P	C, NE, SW 21-49N-69W	8527' - 8570'
20. Grace-Ford Oil Reel No. 1	C, NE, SW 21-49N-69W	8450' - 8494'
21. Stuarco Oil Wolfe No. 1	C, NE, NE 22-49N-69W	8341' - 8393'
22. Clark Oil Bryant No. P-49-69-27-A4	C, SW, SW 27-49N-69W	8447' - 8465'
23. Shell Oil Reel Government No. 23-28A	SE, NE, SW 28-49N-69W	8546' - 8585'
24. Shell Oil Reel Government No. 21-28A	C, NE, NW 28-49N-69W	8502' - 8551'
25. Shell Oil Reel No. 32-28A	C, SW, NE 28-49N-69W	8470' - 8498'
26. Mobil Oil Krause No. F14-34-P	C, SW, SW 34-49N-69W	8449' - 8498'
27. Mobil Oil Krause No. F34-34-P	C, SW, SE 34-49N-69W	8390' - 8488'
28. Prenalta Government No. 14-1	C, SE, SW 14-49N-70W	9052' - 9097'

Twenty-one of these were in or near the main trend of the Raven Creek and Reel oil fields (Plate 1). Seven wells served as control wells to determine if changes in diagenetic mineralization occurred away from the producing trend. The selection of these wells was based on the availability of cores and electric logs. Petroleum Information Inc. was the source of all electric logs used.

The cores were examined with a binocular microscope and described in detail. Lithologic sections representing approximately 1,500 feet of core were constructed with emphasis placed on lithology, texture, color and diagenetic mineralization.

Samples of the core were subjected to x-ray diffraction analysis. Bulk samples and clay extractions were analyzed to determine total mineral percentages and to identify the clay fractions, respectively (Appendix A).

Several samples from each well were subjected to detailed petrographic analysis (Appendix A). Thin sections were made by Central Petrographic Service, Inc., Dallas, Texas. The samples were impregnated with blue epoxy to show porosity and provide a basis for inferring permeability. Thin sections were stained with potassium ferrous cyanide to distinguish iron-bearing dolomite. Photomicrographs were made of the more obvious diagenetic mineral relationships.

Several samples were examined with a scanning electron microscope (SEM and EDXA) to identify diagenetic minerals and determine their textural relationships.

Formation-water analyses were subjected to WATEQF (Truesdell and Jones, 1974; Plummer et al., 1976), a computer technique for calculating chemical equilibria of natural waters. The results were used to

construct contour maps of the saturation indices of anhydrite-gypsum and dolomite (Plates 2 and 3).

Samples of diagenetic pyrite and dolomite were selected for isotopic analysis. These samples provided two δS^{34} values from pyrite and seven δO^{18} and δC^{13} values from dolomite cement. One sample from an anhydrite bed was analyzed for δS^{34} content. Two samples from dolomite beds were analyzed for δO^{18} and δC^{13} content. Histograms were constructed to show the frequency distributions of δS^{34}, δC^{13}, and δO^{18} of the pyrite and dolomite samples. All isotopic analyses in this study were done by Geochron Laboratories, Cambridge, Massachusetts.

Five cross sections were constructed (Plates 4, 5 and 6) using electric logs, lithologies, abundance of diagenetic minerals and isotopic analyses. They were designed to show diagenetic imprints in upper Minnelusa sandstones and their lateral and vertical extent in the subsurface.

CHAPTER II

GEOLOGIC SETTING

The geologic framework within which the Minnelusa Formation developed must be considered in any interpretive study of its strata. The Minnelusa Formation ranges in age from Atokan to Wolfcampian, and encompasses the strata between the unconformity at the base of the Permian Goose Egg Formation and the erosional top of the Mississippian Pahasapa Limestone. In the discussion of the geologic setting major emphasis is placed on the Lower Permian Minnelusa sandstones in the Raven Creek and Reel oil fields.

Tectonic Setting

The Wyoming structural province is part of the Cordilleran foreland. The foreland is an extension of the Mid-Continent craton but has been more severely deformed and is intermediate between the geosyncline and the craton (Sales, 1968). The foreland differs from the Cordilleran geosyncline to the west, in that it is characterized by thinner, more persistent, more unconformity-bounded Paleozoic and Mesozoic strata and by large uplifts in which the deep basement is exposed. A mechanically integrated tectonic system which resulted from the Pacific block being driven under the North American craton is responsible for Laramide and pre-Laramide deformation in the Wyoming structural province (Sales, 1968).

Regional Tectonic Setting

The study area is located on the eastern flank of the Powder River basin (Fig. 2). The basin, which trends northwesterly across northeastern Wyoming, into southeastern Montana, is the second largest structural basin in the Rocky Mountain province. The Powder River basin is bounded on the north by the Miles City arch. The broad arch of the Black Hills uplift and the continuing folds to the north of that uplift form the eastern boundary of the basin. The southern part of the basin is bounded by the Hartville uplift and the Denver basin to the southeast and the Laramie Range to the southwest. The Casper arch and Big Horn Mountains form the western boundary.

The Powder River basin is markedly asymmetric with the synclinal axis adjacent to the Casper arch and Big Horn Mountains. The eastern and northern flanks of the basin are devoid of strong structural features. On the eastern flank the beds are relatively undisturbed and dip gently westward off the Black Hills uplift, at approximately one degree.

The basin is bounded by zones of stronger deformation along the margins of the Laramie, Hartville and Black Hills uplifts on the south, and the Casper arch and Big Horn Mountains on the west. High-angle reverse faulting is associated with steep basin flanks on the south. Faulting was most intense near the Big Horn Mountains where displacement along thrust faults is as much as one and a half to two miles (Curtis et al., 1958). A broad structural terrace southeast of the Big Horn Mountains is dissected by a system of transverse tension faults.

Gentle to sharp anticlinal closures were formed in these structural belts. The southeast margin of the basin contains folds which parallel the Hartville uplift. On the western margin of the basin steeply

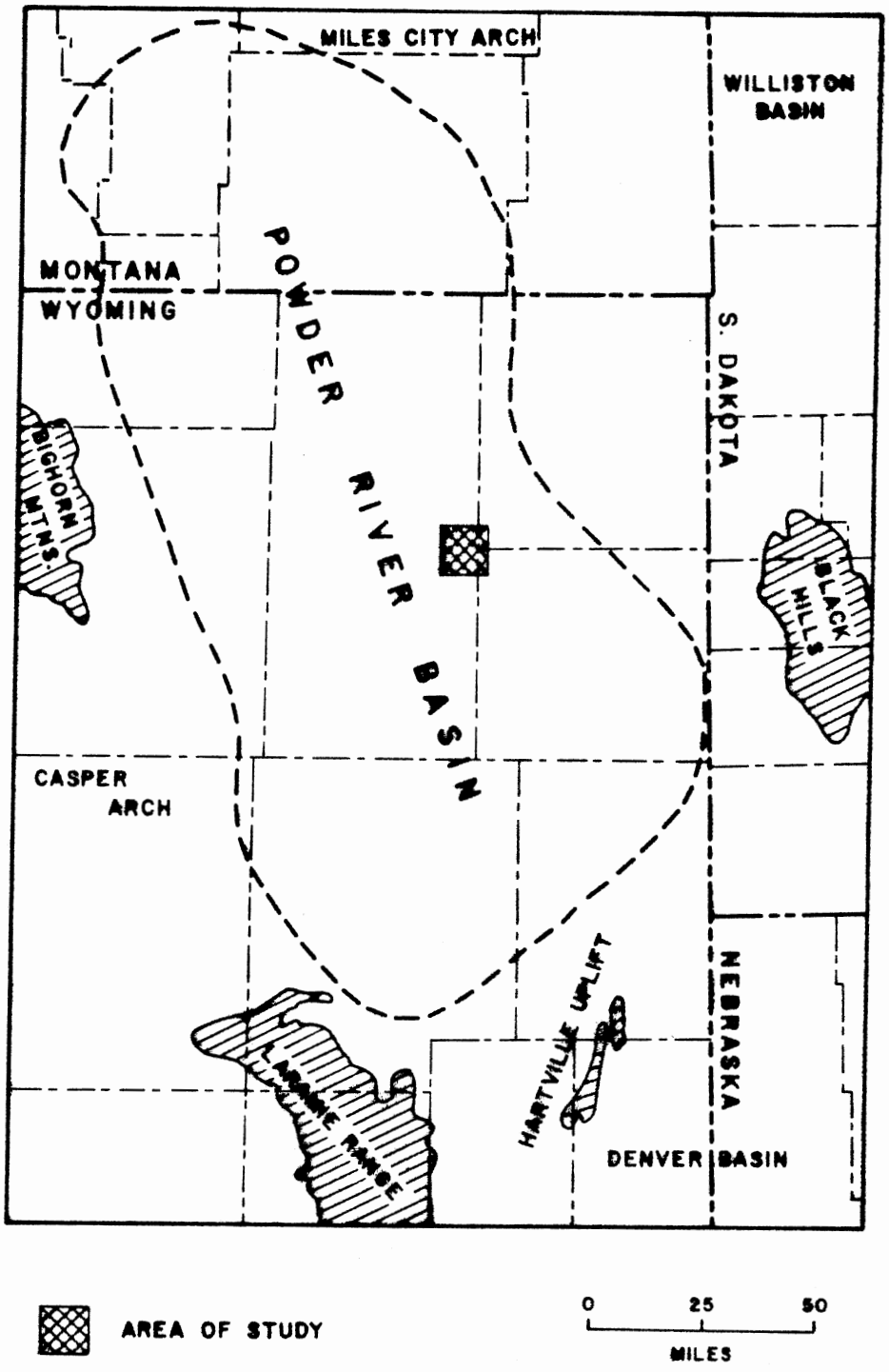

Fig. 2.--Powder River basin and surrounding structural features.

dipping and overturned strata form northwesterly trending hogbacks. A series of en echelon folds has formed on the basin flank adjacent to the Big Horn Mountains, and a major belt of folds has formed adjacent to the Casper arch.

The present configuration of the Powder River basin is the result of Late Cretaceous and Early Tertiary deformation. The first major indication of Laramide orogeny in the Powder River basin is suggested by relatively strong subsidence of the basin during latest Cretaceous time (Glaze and Keller, 1965). During the Paleocene the Big Horn Mountains, Black Hills, and Laramie Range began to rise. As the uplifted areas came into being, they were subjected to erosion, and a large volume of sediment was transported into the newly formed basin (Thomas, 1963). By the end of the Paleocene all of the major basin features were delineated (Love et al., 1963). Strong folding and faulting during the early Eocene formed most of the present major structures in the basin. The basin was tilted westward by renewed uplift in the Black Hills in late Eocene time (Glaze and Keller, 1965). Curtis et al. (1958) suggested that renewed uplift, downwarping, and regional tilting extended into the Miocene.

Although the present form of the Powder River basin is principally a result of Late Cretaceous and Early Tertiary deformation, the general configuration of the basin developed as a result of structural movements dating back as far as Early Paleozoic. Pre-Late Cretaceous structural movements occurred episodically in the form of localized deformation accompanying broad regional downwarps (Curtis et al., 1958). At least 12 episodes of stratal warping occurred before deposition of Cretaceous rocks, with the possibility of many more such movements having occurred

which are now imperceptible (Strickland, 1958). Isopachous maps of Mississippian, Pennsylvanian and Lower Permian, Upper Jurassic, and Upper Cretaceous rocks in the basin reflect gentle warpings with northwest trends similar to the present dominant structural grain (Curtis et al., 1958). Blackstone (1963) suggested that Paleozoic and Upper Cretaceous movements were minor, but that a major arching occurred during the Jurassic. These trends were recurrent with marked persistence through geologic time.

Local Tectonic Setting

The Raven Creek and Reel oil fields are located on the Black Hills monocline which dips gently westward off the Black Hills uplift. The east limb of the Powder River basin is structurally simple with many flexures that are uncomplicated and of low magnitude (West, 1964). The most prominent structural feature in the northeast part of the basin is the Belle Fourche arch. Subtle differential uplift along lineaments has formed the gentle northeast-trending arch (Slack, 1981).

The Black Hills monocline is shown by a set of outcrop patterns with average trends of N30°W and N48°E (Robinson et al., 1964). The monocline is considered to be an immature drape fold; therefore, the linear outcrop pattern represents the configuration and orientation of the basement blocks along which uplift occurred. Recent stream drainages in the Black Hills area and in Tertiary sediments throughout the northern half of the basin trend N23°W and N42°E. On the basis of these observations Slack (1981, p. 733) concluded that:

> . . . the fracture system which yielded the Black Hills monocline is also present in the basement complex of the Powder River basin and that the fracture system has readjusted through time, effectively controlling surface drainage patterns.

Structural patterns of Black Hills monocline segments are mirrored by linear topographic escarpments which reflect boundary basement blocks of the uplift. West of the monocline outcrop, topographic escarpments follow the same trend as those in the Black Hills. Slack (1981) interpolated these trends across the intervening area to form a northeast-trending system (Fig. 3). Linear drainage segments which appear to connect these two systems support this interpolation.

The following synopsis of the tectonic development of the Belle Fourche arch was suggested by Slack (1981). A set of shear zones developed in Precambrian time, probably in response to the Hudsonian orogeny. Minor movement occurred during depositon of Pennsylvanian and Lower Permian sediments in a subtle basinal area on the present crest of the Belle Fourche arch, west of the Black Hills monocline outcrop. Upward movement of the Belle Fourche arch was initiated during deposition of Lower Cretaceous sediments, and continued into the Late Cretaceous. Movement along the lineaments during the Laramide orogeny was minor, but sufficient to ingrain the structural trend into Laramide synorogenic basin-fill sediments and to control recent stream drainage.

Stratigraphic Setting

Upper Mississippian, Pennsylvanian, and Lower Permian shelf deposits are preserved today in most areas of Wyoming and parts of adjoining states. The total section averages less than 1000 feet in thickness on the Wyoming shelf. Much thicker sediments were deposited in the Cordilleran geosyncline in southwestern Wyoming and parts of adjacent Idaho and Utah. These sediments made up a multiplicity of rock types. This variation in lithology has led to a complex of formational

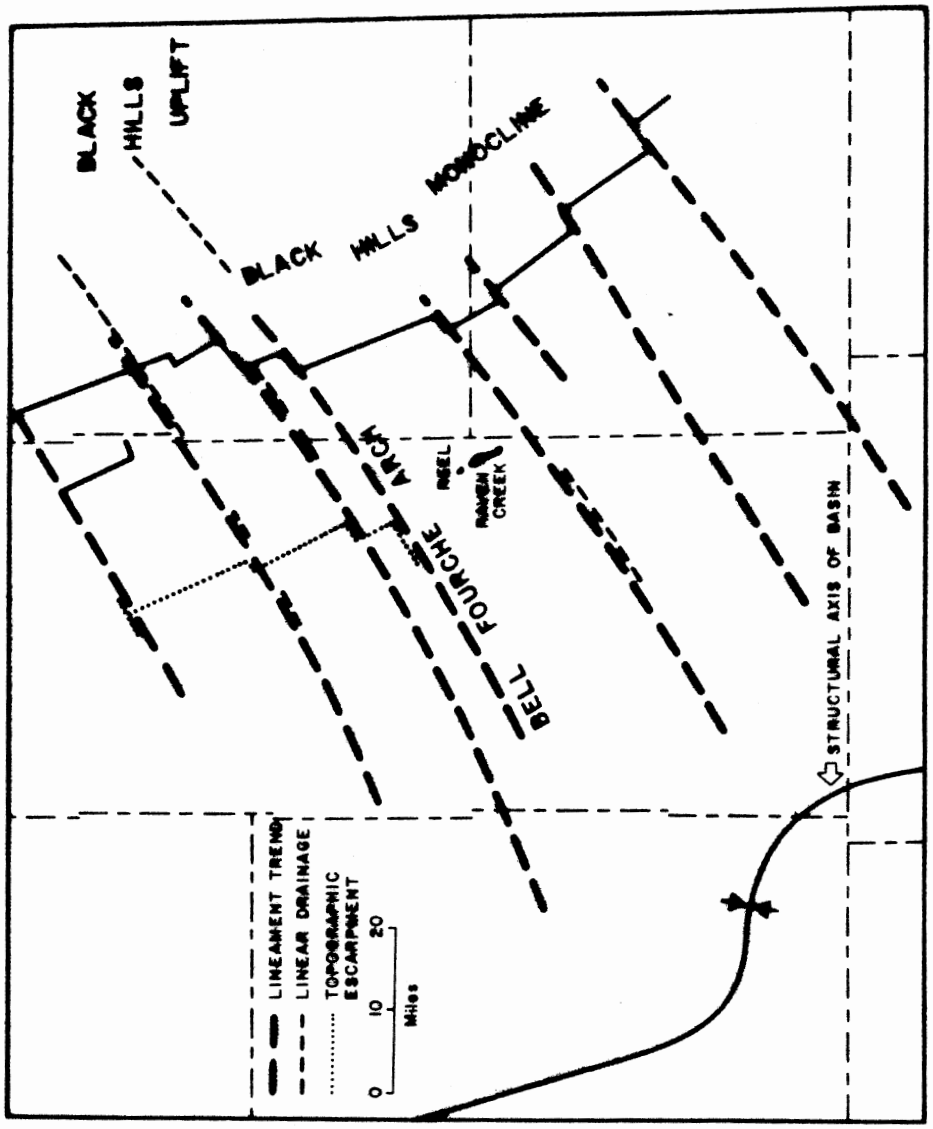

Fig. 3.--Paleotectonic trends in the Black Hills monocline area (after Slack, 1981).

names, including the Amsden, Tensleep, Quadrant, Weber, Morgan, Casper, Hartville, and Minnelusa Formations. These rocks include all sediments between the Permian Phosphoria Formation and its lateral equivalent, the Goose Egg Formation, and the Mississippian evaporite and carbonate sequence comprising the Charles, Guernsey, Madison, and Pahasapa Formations.

Regional Stratigraphic Setting

The major uplifts flanking the Powder River basin have different nomenclatures applied to the outcropping Pennsylvanian and Lower Permian strata (Fig. 4). These strata include the Minnelusa Formation in the Black Hills, the Hartville Formation in the Hartville uplift, the Tensleep and Amsden Formations in the Big Horn Mountains, and the Casper Formation in the Laramie Range. These are briefly described and correlated here for purposes of reference in discussing regional equivalents of the Minnelusa.

Amsden and Tensleep Formations. The Amsden Formation is composed of interbedded red shale, limestone, dolomite, sandstone, and chert that lie unconformably upon the Madison Limestone and are overlain by the Tensleep Formation. The Amsden, as described by Mallory (1967), is divided into three members. The basal unit, the Darwin Sandstone Member, consists predominately of sandstone. The Darwin is unconformably overlain by red mudstones, siltstones, and sandstones of the Horseshoe Shale Member. The Ranchester Limestone Member is the upper unit of the Amsden. The Ranchester consists of cherty and dolomitic limestone.

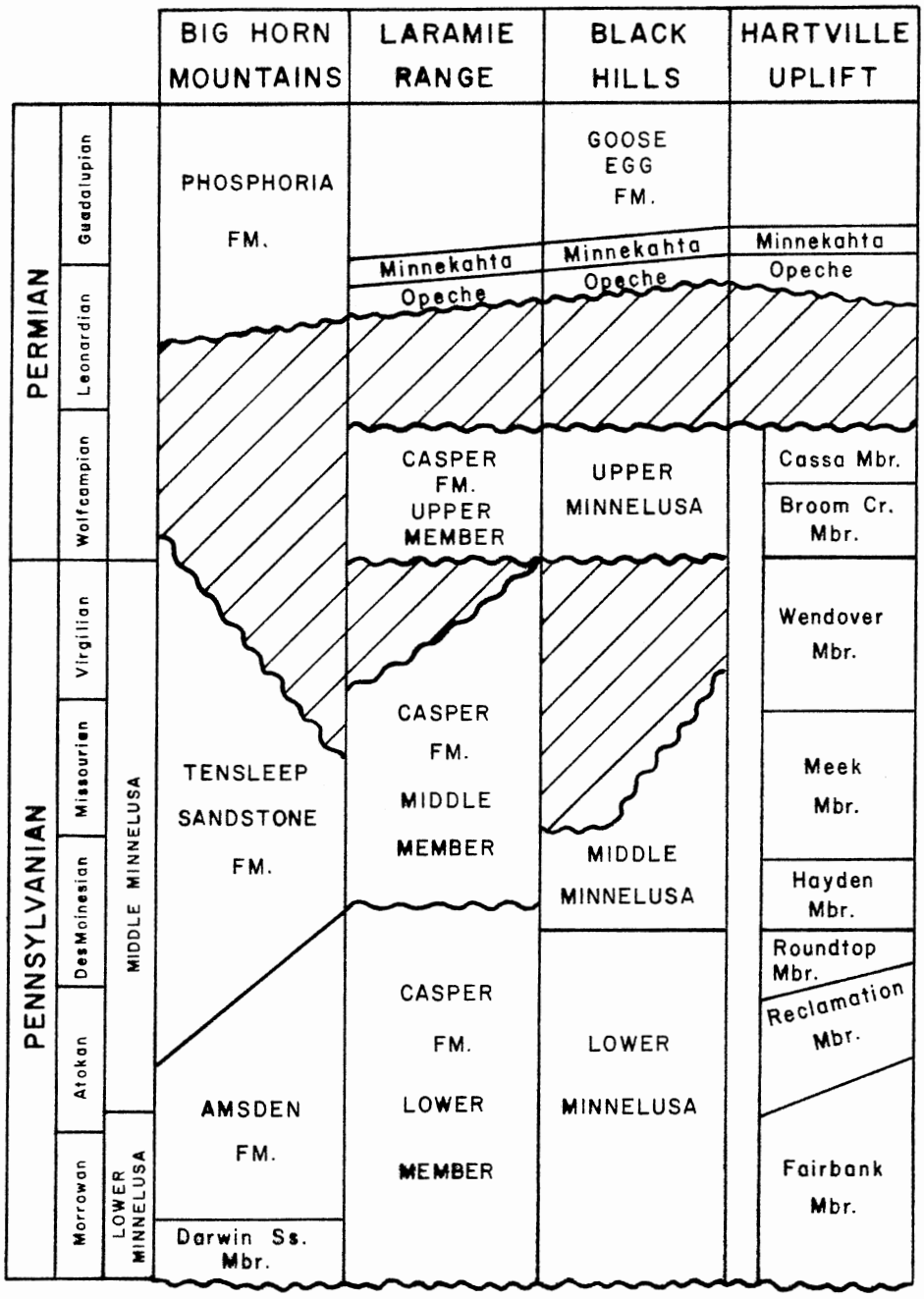

Fig. 4.--Columnar section of the Pennsylvanian and Permian in the uplifts surrounding the Powder River basin (after Tranter and Petter, 1963).

The Darwin Sandstone is considered to be Mississippian, probably early Chesterian, in age. The Horseshoe Shale and Ranchester Limestone are Morrowan in age (Maughan, 1978). The Horseshoe Shale and the lower unit of the Ranchester Limestone correlate with the lower member of the Minnelusa Formation (Foster, 1958) and, where present in the western part of the Powder River basin, make up the Lower Pennsylvanian sequence.

The Tensleep Formation consists of sandstone, dolomite, limestone, shale, and anhydrite that occur above the Amsden Formation and below the red beds of the Goose Egg Formation of Permian and Triassic age. Dolomite beds occur mostly in the lower part of the Tensleep. Sandstone beds are increasingly abundant in upper parts of the unit. Locally the bulk of the lower member (Maughan, 1978) is composed of sandstone and mudstone. The upper part of the Tensleep is a series of massive, cross-bedded sandstones, with some interbedded dolomite (Branson, 1939). Thin, planar beds of dolomitic sandstone and arenaceous dolomite are at the top of the Tensleep and they unconformably overlie the cross-bedded sandstone.

Abundant evidence indicates that the age of the Tensleep is Desmoinesian (Henbest, 1954; Agatston, 1954). Locally the age of the base of the formation is very latest Atokan (Henbest, 1956). In a narrow belt trending approximately northeast through the center of Wyoming, the Tensleep contains strata of Missourian, Virgilian, and Wolfcampian ages (Mallory, 1967).

In the Powder River basin the Tensleep grades by facies changes along the east margin of this belt into the middle and upper members of the Minnelusa Formation. An increase in the number of limestone beds in

the lower part of the Tensleep, on the southeast flank of the Big Horn Mountains (Agatston, 1954) can be attributed to gradation from the mostly sandstone facies of the Tensleep into the interbedded carbonate rock and sandstone facies of the middle member of the Minnelusa (Maughan, 1978). The planar sandstone and dolomite strata occurring at the top of the Tensleep are Wolfcampian in age (Verville, 1957), and are equivalent to the upper member of the Minnelusa (Maughan, 1978).

Casper, Hartville, and Minnelusa Formations. Because of their lithologic and sequential similarity the Casper, Hartville, and Minnelusa Formations should be identified as a single formation (Maughan, 1978). The name "Minnelusa" has gained wide acceptance by the petroleum industry for most of the Pennsylvanian and Lower Permian strata in the Powder River basin, with the exception of the west flank and the Casper arch (Fig. 5). The Minnelusa has been divided into three members separated by regional unconformities (Foster, 1958).

The lower Minnelusa member includes the strata between the unconformity at the base of the middle member and the erosional top of the Mississippian Pahasapa Limestone (Foster, 1958). Basal strata consist predominately of red mudstone, interstratified with fine-grained sandstone, and thin beds of limestone (Maughan, 1978). Detrital sediments are more common in the southwest part of the basin, whereas carbonate rocks predominate in the central and eastern part of the basin. In the southern and eastern part of the basin the lower member can be subdivided, in ascending order, into units equivalent to the Fairbanks, Reclamation, and Roundtop divisions of the lower member of the Hartville Formation (Foster, 1958). These units are a basal sandstone, a middle

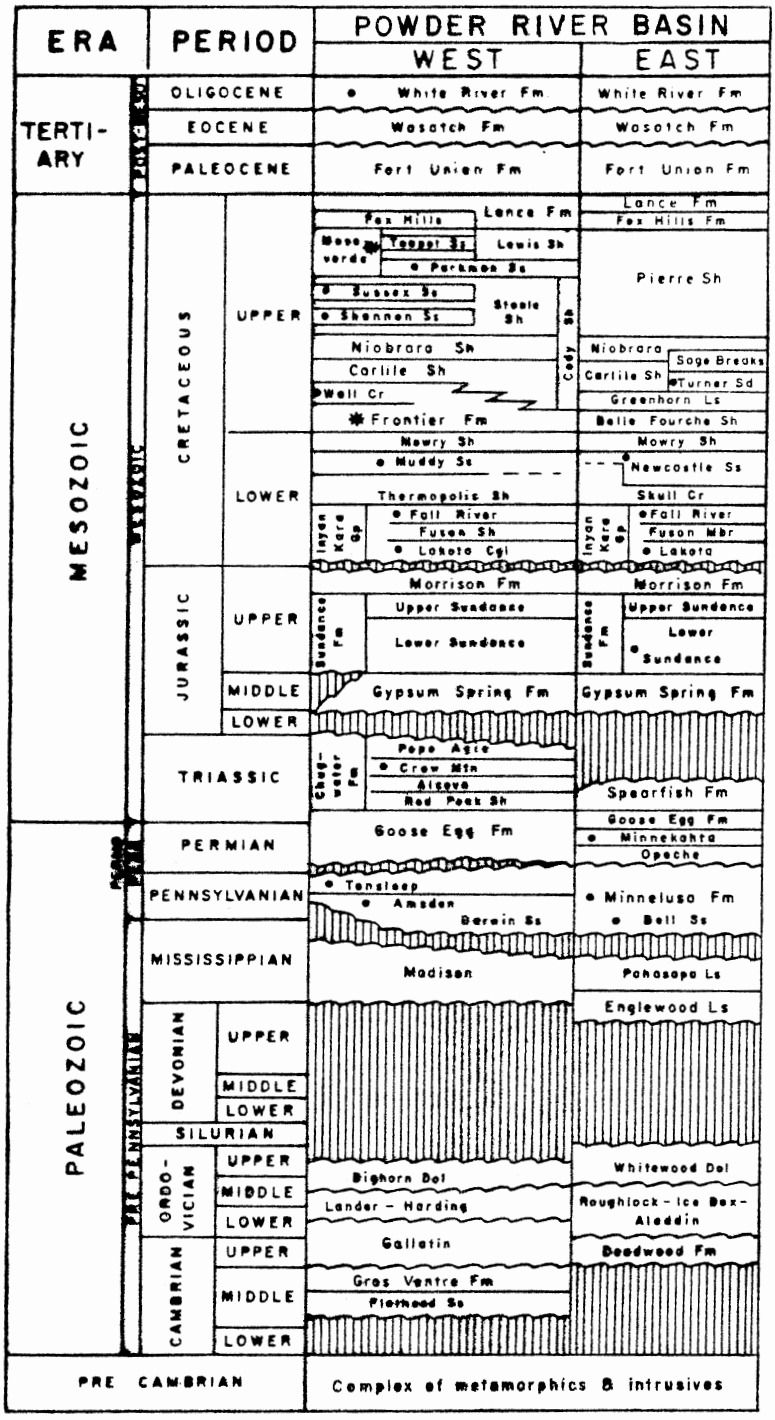

Fig. 5.--Columnar section of the Powder River basin (Kinnison, 1971).

unit of cherty limestone, and an upper unit composed of interbedded cherty carbonates and red shales. Elsewhere in the basin the boundary between the two upper units is indistinguishable.

The lower Minnelusa member includes rocks of predominately Atokan age (Foster, 1958). The basal sandstone may be Morrowan (Agatston, 1954).

The middle Minnelusa member encompasses the strata between the unconformity at the base of the upper member and the unconformity at the top of the lower member. The middle member is an interbedded sequence of dolomite, argillaceous dolomite, quartzose sandstone, and thin but persistent, radioactive black shales (Foster, 1958; Maughan, 1978). The member is thickest in the southeast part of the basin where the "Leo" sandstone zones are located. The greatest percentage of carbonate is in the southeast part of the basin, whereas the highest concentration of sandstone is toward the west and southwest (Foster, 1958).

The middle Minnelusa is Desmoinesian, Missourian, and Virgilian (Foster, 1958). Truncation at the top and onlap at the base have resulted in rocks representing only parts of these ages being preserved in some portions of the Powder River basin.

A red arenaceous to argillaceous mudstone known as the "red shale marker" is at the base of the upper Minnelusa member in most of eastern Wyoming (Foster, 1958). The "red shale marker" delineates an erosional contact between Pennsylvanian and Permian rocks. The marker crops out in the northern Laramie Range, the Hartville uplift, and the southern Black Hills (Maughan, 1978). It extends northward into the middle part of the Powder River basin, where it appears to die out. The marker extends westward, terminating a short distance from the flank of the Big Horn

Mountains. The top of the upper member is marked by the unconformity which separates the Minnelusa from the overlying Opeche Shale Member of the Permian and Triassic Goose Egg Formation.

The upper member of the Minnelusa is composed of sandstone, dolomite, and anhydrite. Sandstone predominates on the periphery of the Powder River basin (Tenney, 1966), with the highest percentage occurring on the western flank of the basin (Foster, 1958). The percentage of carbonate increases basinward. The carbonate grades laterally toward the south, through penesaline sediments into halite deposits (Tenney, 1966).

Maughan (1967) observed several ways in which the Permian upper Minnelusa differs from the Pennsylvanian units below. Thick beds of anhydrite are common in the Permian rocks but are minor constituents in the Pennsylvanian strata. The upper Minnelusa does not contain radioactive dark shale beds which are common in the lower and middle members. The sandstones of Pennsylvanian age are characterized by uniformity in grain size. Permian sandstones are heterogeneous. Thicker sandstone beds in the upper Minnelusa result in a higher clastic ratio. Although dolomite is common throughout the Minnelusa, limestone is a minor constituent in the upper member.

Paleontological evidence derived from the Hartville uplift (Love et al., 1953), the Laramie Range (Agatston, 1954), and the Big Horn Mountains (Verville, 1957) indicates that the upper Minnelusa is Wolfcampian.

Local Stratigraphic Setting

The producing stratigraphic units in the Raven Creek and Reel oil

fields are in the upper member of the Minnelusa Formation. In this area Wolfcampian age strata are composed of sandstone beds separated by beds of microcrystalline dolomite and anhydrite containing thin beds of red and black shale. The sandstones are white to light gray, fine- to very fine-grained, rounded to subrounded and are cemented by anhydrite and dolomite. The sandstones, which are variable in thickness, comprise the majority of upper Minnelusa rock types. The dolomite beds are gray to pink, stylolitized, fractured, and contain chert and anhydrite inclusions. The anhydrite beds are white to pink and range from microcrystalline to sucrosic in texture.

The Minnelusa is overlain by the red, anhydritic, and locally arenaceous shales of the Opeche Member of the Goose Egg Formation. Locally, a rubble zone composed of chert, dolomite, sandstone, and anhydrite pebbles in a red shale matrix is present at the base of the Opeche (Hudson, 1963). The Opeche is overlain by the Minnekahta Limestone Member. This stratigraphic marker is approximately 30 feet thick and is composed of gray to pink, dense to finely crystalline limestone with fractures and anhydrite inclusions (Barkley and Gosman, 1958).

The terms "A" and "B" sandstones were applied to the upper two producing units of the upper Minnelusa by Barkley and Gosman (1958) in their study of the Donkey Creek oil field. The "B" sandstone is possibly the productive unit in the Raven Creek (Tranter, 1963) and Reel oil fields (Fig. 6). Overlying the "B" sandstone is a dense impermeable dolomite. The productive sandstones are isolated from the water-bearing sandstones in the lower portion of the upper Minnelusa by a unit consisting of beds of dolomite and anhydrite with thin beds of shale (Tranter, 1963).

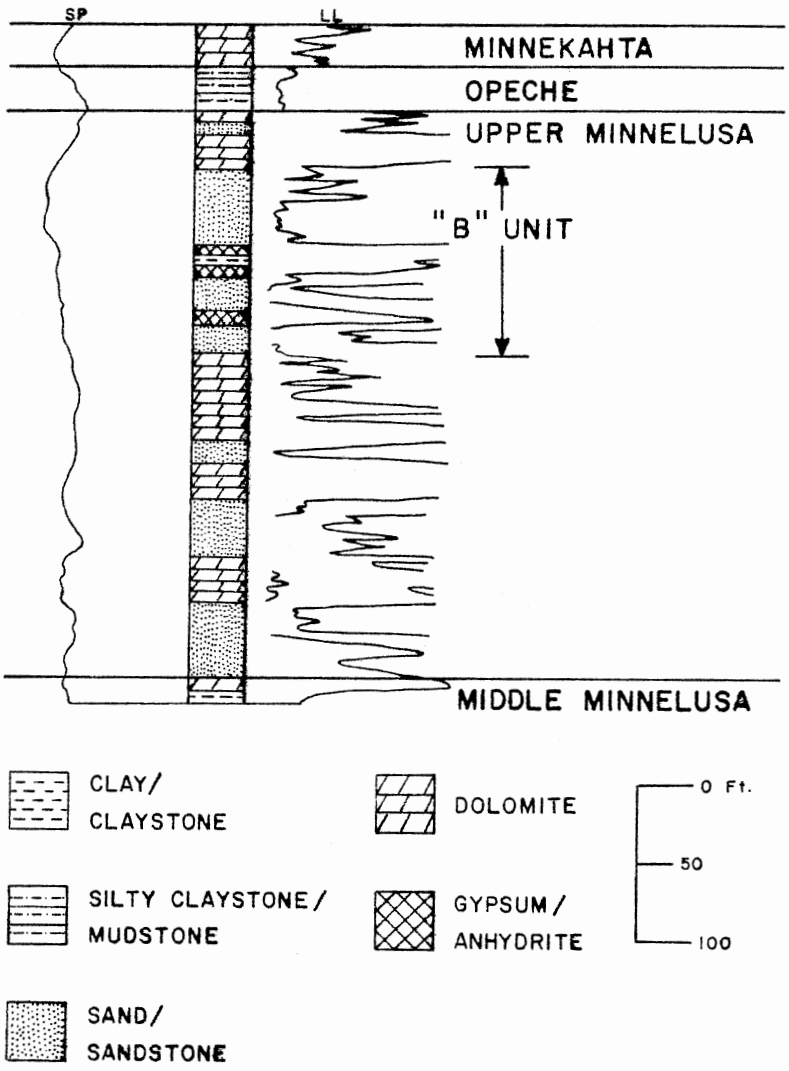

Fig. 6.--Electric log section of the productive unit in the Raven Creek oil field (after Tranter, 1963).

Geologic History and Depositional Environments

During the Paleozoic, Wyoming and the Powder River basin occupied a position on a shelf area between the Transcontinental arch to the east and the Cordilleran geosyncline to the west. The greatest change in Paleozoic sedimentation occurred at the close of the Mississippian when deposition of primarily fine-grained clastic and carbonate rocks gave way to deposition of non-marine clastic sediments (Glaze and Keller, 1965).

In his study of Pennsylvanian and Lower Permian deposition in the Powder River basin, Tenney (1966) concluded the following. Erosion and truncation of the Mississippian surface was followed by tilting of the entire shelf area toward the north. Seas approaching from both the southeast and the southwest transgressed much of Wyoming. Positive areas in central Wyoming, together with the Rosebud arch in Montana and the Black Hills-Chadron arch trend restricted the transgression of the eastern sea and delineated the Powder River depositional basin. This basin occupied an area similar in outline to the present day structural configuration of the Powder River basin. Essentially continuous deposition resulted in the accumulation of a complete sequence of Permian and Pennsylvanian sediments. The shallow sea that occupied eastern Wyoming migrated slowly toward the west near the end of the Wolfcampian. This migration was contemporaneous with downwarping in northwestern Wyoming and regional westward tilting of the eastern part of the state. Westward migration of the sea resulted in truncation of sediments in the northern and eastern parts of the basin. Truncation was followed by deposition of the red bed facies of the Goose Egg Formation.

Lower Permian sediments in the Powder River basin are sandstones, carbonates, and evaporites. The lowering of sea level combined with continued deposition of sediments to restrict the marine environment and resulted in conditions conducive to deposition of anhydrite (Tenney, 1966). The margins of the basin were characterized by littoral and nearshore marine environments where sand deposition was predominant but smaller amounts of dolomite and anhydrite were deposited (Berg and Tenney, 1967). These interbedded sequences probably were the results of minor fluctuations in sea level (Tenney, 1966).

The maturity of upper Minnelusa sandstones indicates that they resulted from the reworking of a former sedimentary section (Stone, 1969). Tenney (1966) suggested that the primary source was the previously deposited Tensleep sediments of Desmoinesian age in central Wyoming. Other source areas existed to the south and east of the present basin.

Stone (1969) concluded that upper Minnelusa sandstones were deposited in separate but closely related environments such as the fore beach, dune, eolian flat, and back beach components of a barrier island complex. Tenney (1966) suggested that lower Permian Minnelusa sandstones displaying high-angle cross-bedding and excellent sorting were deposited in an eolian environment.

The upper Minnelusa in the study area represents deposition in eolian and associated sabkha environments. Sandstones in the Raven Creek and Reel oil fields are massive but finely laminated, exhibit high-angle cross-stratification, and on visual inspection, appear to be well sorted to very well sorted. These observations suggest that upper Minnelusa sandstones in the study area represent eolian dune sands.

Although most of the sandstones in the upper Minnelusa appear to have been deposited in eolian environments, some of the sandstones are thin and wavy-laminated. These units and the thin arenaceous dolomites observed in the study area probably are analogous to the sabkha-wind flat deposits reported by Mankiewicz and Steidtmann (1979) in the Tensleep in the Big Horn basin. These deposits represent groundwater-controlled deflation surfaces upon which dune forms migrated (Stokes, 1968).

Arenaceous dolomites containing chert nodules and lenses of sucrosic anhydrite are common in the cores studied. Mankiewicz and Steidtmann (1979) noted similar rock types in the upper Tensleep and attributed their origin to interdunal pond deposition. Interdunal ponds occur where depressions in the deflation surfaces were deep enough to allow ponding to occur. Schreiber et al. (1976), in reference to similar sediments in the Sicilian basin, suggested subaqueous deposition in hypersaline waters which were periodically freshened by flooding, thus allowing the formation of algal mats.

CHAPTER III

PETROLOGY AND DIAGENESIS

The petrology and diagenesis of upper Minnelusa sandstones were investigated in the subsurface in the Raven Creek and Reel oil fields. Approximately 1,500 feet of strata were examined using electric logs and cores.

Petrologic and diagenetic information incorporated in this chapter were obtained by several analytical techniques and procedures. These include scanning electron microscopy (SEM and EDXA), computer treatment of water analyses, detailed petrologic analysis using stained thin sections, binocular microscope, carbon, oxygen, and sulfur isotope studies, and x-ray diffraction of bulk samples and extracted clay fractions.

General Lithologies

The rocks studied consist of shale, sandstone, dolomite and anhydrite. Primary attention in this part of the study was directed to analyses of sandstones in the upper Minnelusa, which total approximately 65 percent of the rock types within the cores studied. Shales are the least abundant rock type in the upper Minnelusa, constituting less than five percent. Dolomite and anhydrite make up the remainder of the upper Minnelusa section. Red Opeche shale constitutes the remainder of rock types in the cores studied.

Detrital Constituents

The detrital mineralogy of the upper Minnelusa sandstones is essentially the same in all cores examined, although some variation exists in the relative mineralogical proportions (Appendix A). The majority of the framework grains are quartz, with the remainder mostly alkali feldspar (Fig. 7). These rocks would be classified as quartz arenites. Rounded chert grains are present but are volumetrically negligible. Although heavy and accessory minerals are generally present, they rarely exceed one percent of the total composition. Zircon is the most common heavy mineral; it occurs as well-rounded grains which barely reflect the original crystal shape. Biotite and rounded grains of tourmaline are less common.

Of the total mineralogy, detrital quartz is about 77 percent, on the average, of upper Minnelusa sandstones. It is mostly fine to very fine, subrounded to rounded sand. The grains are commonly frosted. The types of quartz observed were unstrained monocrystalline grains, strained monocrystalline grains displaying undulatory extinction, and composite or polycrystalline grains. Strained single grains of quartz make up approximately two-thirds of the total quartz. Polycrystalline quartz is the least abundant variety.

Feldspar constitutes, on the average, two percent of the mineral grains in upper Minnelusa sandstones. Untwinned orthoclase is the most common variety, followed in abundance by rare grains of twinned microcline. No plagioclase was observed. Feldspar grains are subrounded, and are invariably somewhat larger than the mean grain size of samples in which they occur. Two distinct natural populations of detrital feldspar are recognized. Most of the orthoclase grains show

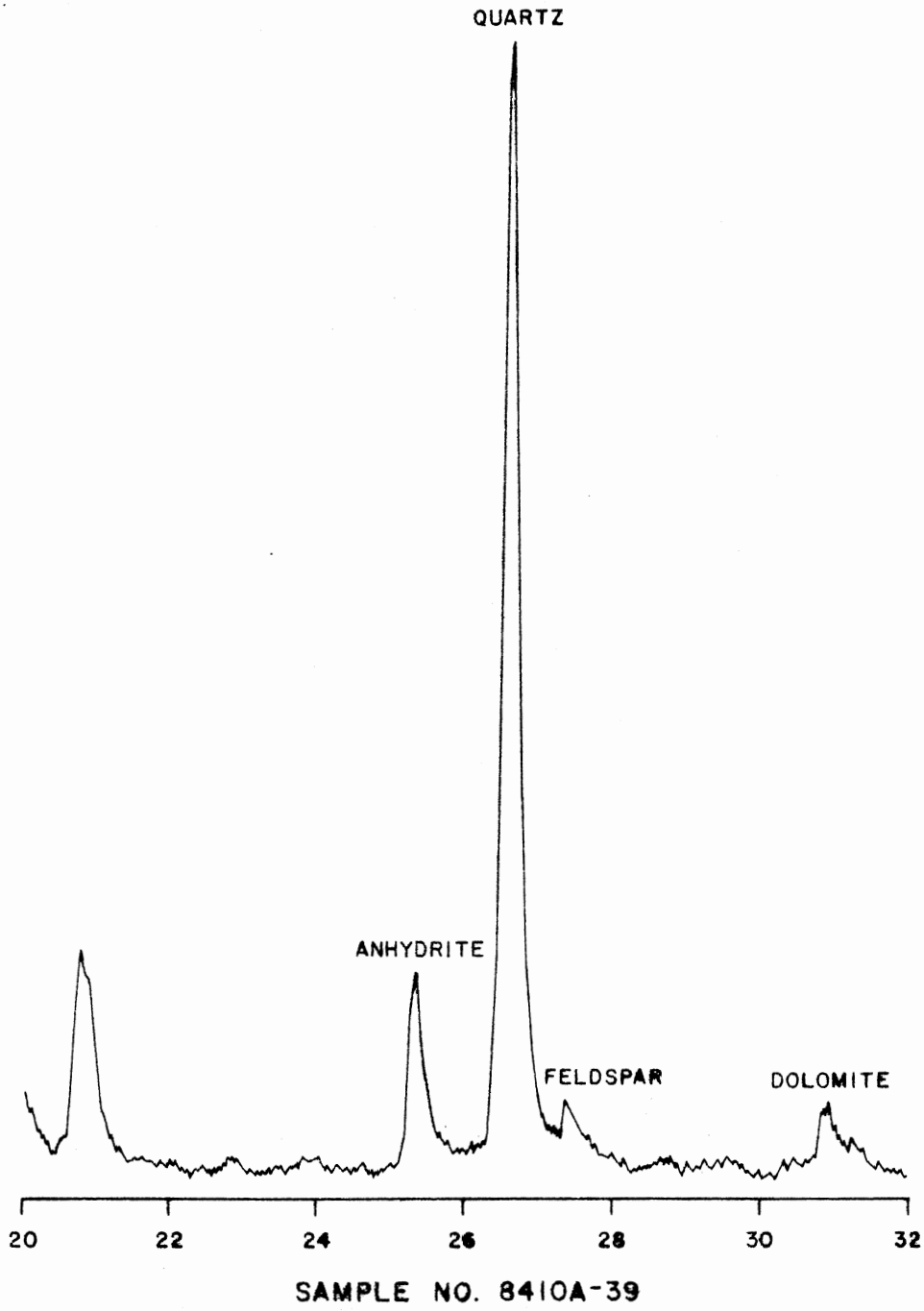

Fig. 7.--X-ray diffraction analysis of sample 8410A-39. Upper Minnelusa sandstone.

signs of weathering and/or chemical alteration. The effects most frequently observed were alteration to sericite and dissolution. The microcline grains are commonly unaltered. The presence of altered and unaltered grains suggests that there were two sources of feldspar, and that alteration of orthoclase occurred in the source area or during transport.

Diagenetic Constituents

Porosity and permeability are the most important bulk properties of potential hydrocarbon reservoirs. These properties of the sediment are dependent on the post-depositional chemical and mechanical alteration of the rock fabric. In the Raven Creek and Reel oil fields the dominant modifications of original depositional fabric are porosity reduction by cementation, and porosity enhancement by dissolution of chemically unstable cement. The most common diagenetic cements are anhydrite and dolomite. Clay minerals, pyrite, and silica are less abundant.

Anhydrite Cement

Anhydrite is the most conspicuous sandstone cement in the study area (Fig. 8), constituting an average of 12 percent. It occurs as poikilotopic masses enclosing and replacing detrital quartz (Fig. 9). Dissolution of anhydrite deposits and secondary precipitation of calcium sulfate in the porous adjacent sands may be the most obvious explanation for the anhydrite cement (Stone, 1969).

De Groot (1973) documented the occurrence of anhydrite and dolomite which are being precipitated from interstitial brines in sediments

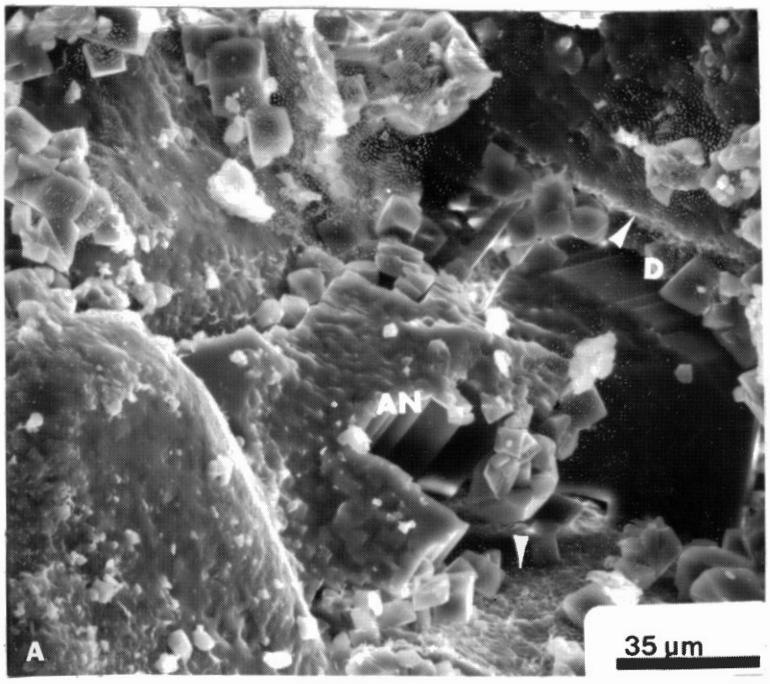

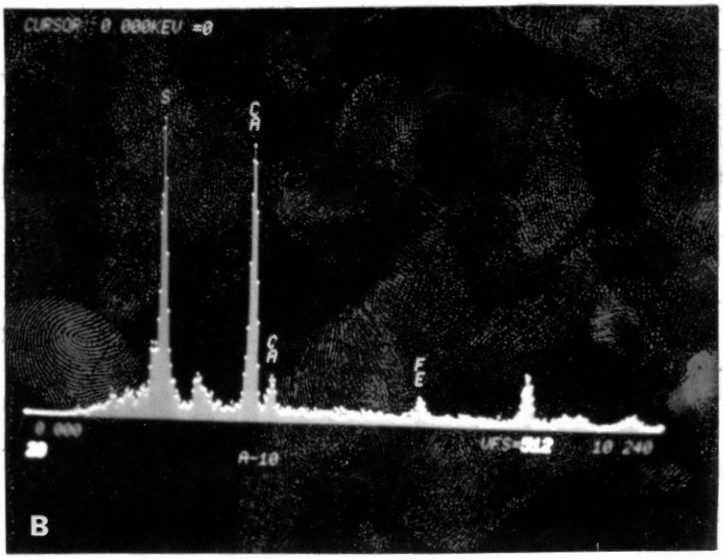

Fig. 8.--SEM photomicrograph of authigenic minerals. A. Anhydrite (AN), dolomite (D), and pore-lining mixed-layer illite-smectite (arrows). B. EDXA of the anhydrite cement.

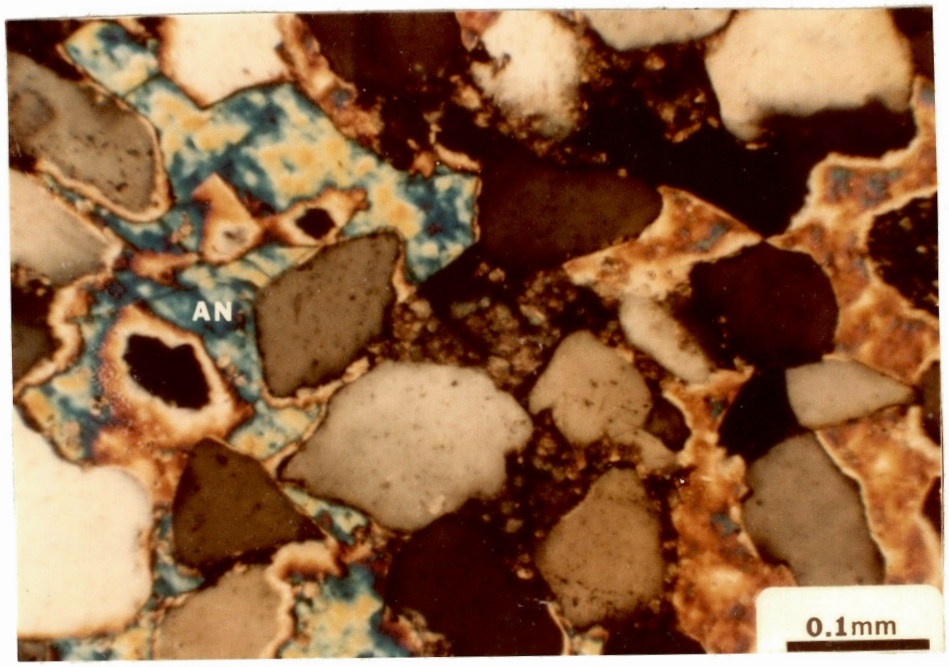

Fig. 9.--Light photomicrograph of poikilotopic anhydrite (AN). Crossed polarizers.

beneath the siliciclastic sabkha surface in the Persian Gulf. Anhydrite may have been introduced into upper Minnelusa sandstones during deposition of supratidal sediments in a geochemical setting analogous to that observed by de Groot. Such an origin has been suggested by Mankiewicz and Steidtmann (1979) for the anhydrite cement observed in the Tensleep sandstone in the eastern Big Horn basin.

Dolomite Cement

Dolomite is also a common cement in upper Minnelusa sandstones. Dolomite content of the sandstones averages approximately 10 percent. It is present as euhedral rhombohedra, which indicate a diagenetic origin (Fig. 10). The rhombs are generally much smaller than the quartz grains. The rhombs occur as aggregates that occupy significant parts of the pore space, or as single crystals that line pores or replace anhydrite (Fig. 11 and 12). Their ferroan nature is indicated, when upon staining with potassium ferrous cyanide, a typical blue color develops (Fig. 13). The ferroan nature of dolomite is explained by the incorporation of Fe^{++} ions in the dolomite lattice to produce ferroan dolomite as dictated by the following reaction:

$$4CaCO_3 + Fe^{++} + Mg^{++} \quad 2CaFe_{.5}Mg_{.5}(CO_3)_2 + 2Ca^{++} \qquad (1)$$

Ferroan Dolomite

An increase in the Fe^{++}/Mg^{++} ratio in solution (Al-Shaieb and Shelton, 1978) and a corresponding minimal level of magnesium ion activity (Katz, 1971) are required to form ferroan dolomite. The maintenance of an elevated concentration of Fe^{++} in solution is dependent on the pH and Eh regime. If the present pH of the formation water, which is approximately

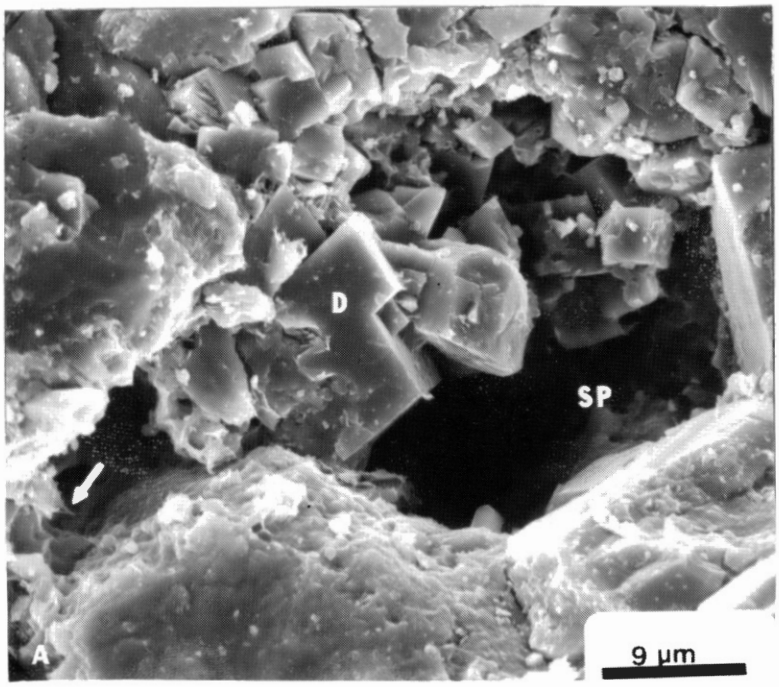

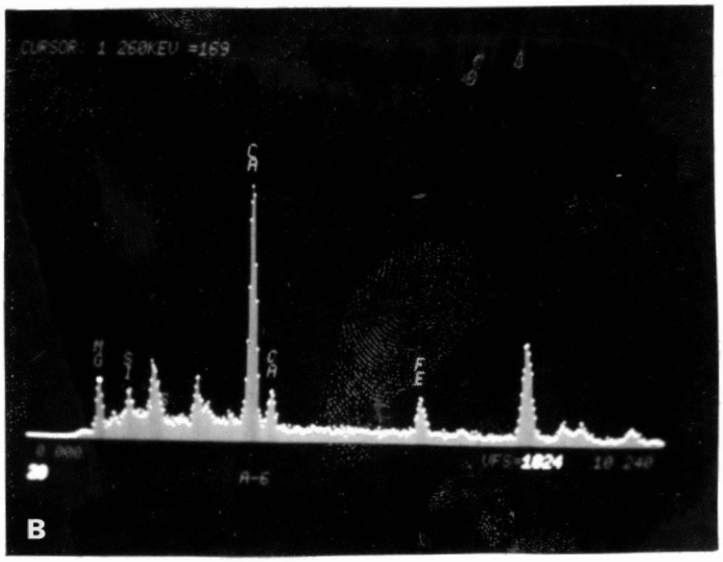

Fig. 10.--SEM photomicrograph of authigenic minerals and secondary porosity. A. Dolomite (D), mixed-layer illite-smectite (arrow), and secondary porosity. B. EDXA of the euhedral dolomite.

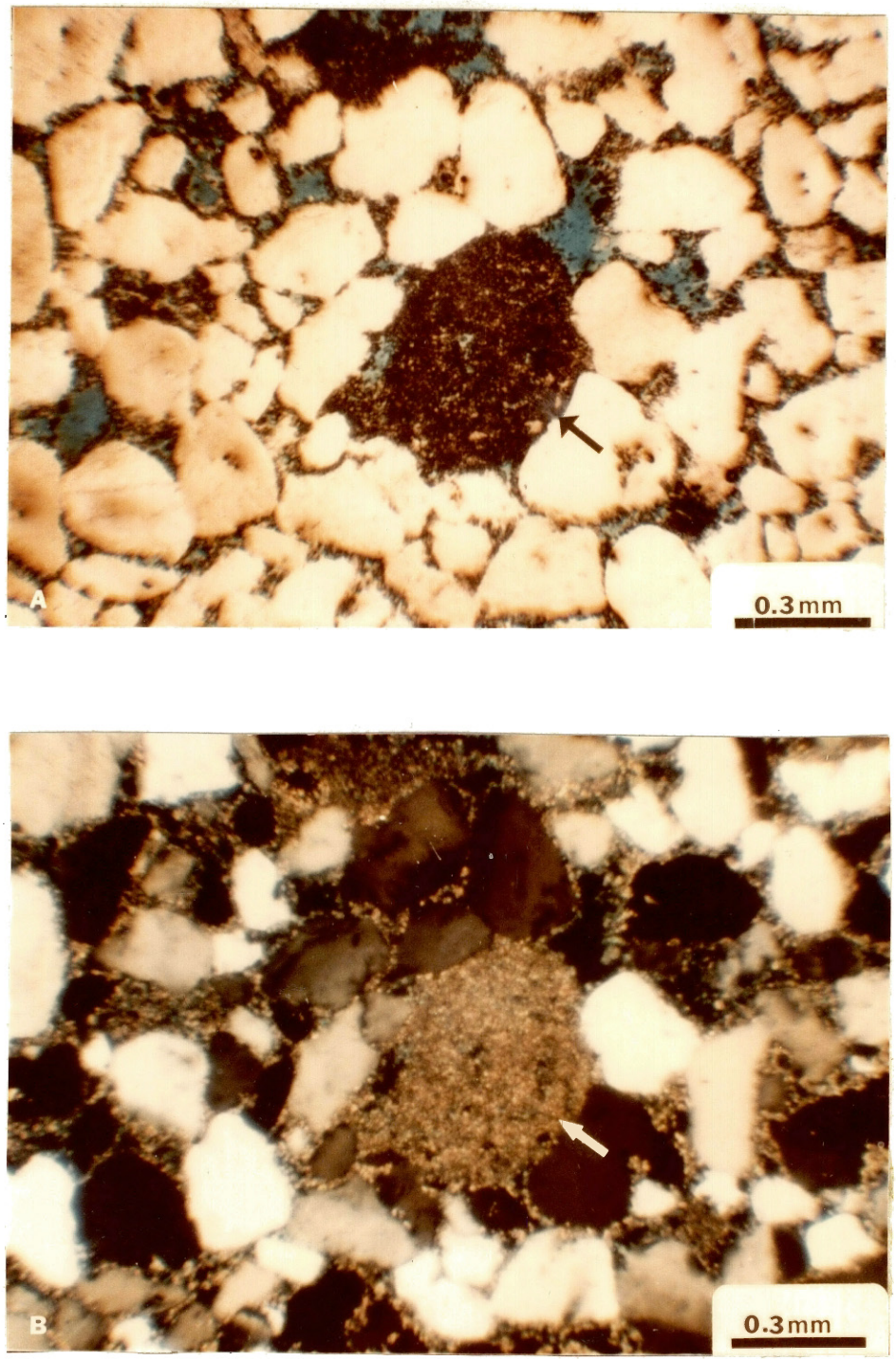

Fig. 11.--Light photomicrographs of pore-filling dolomite aggregates (D). A. Plane light B. Crossed polarizers.

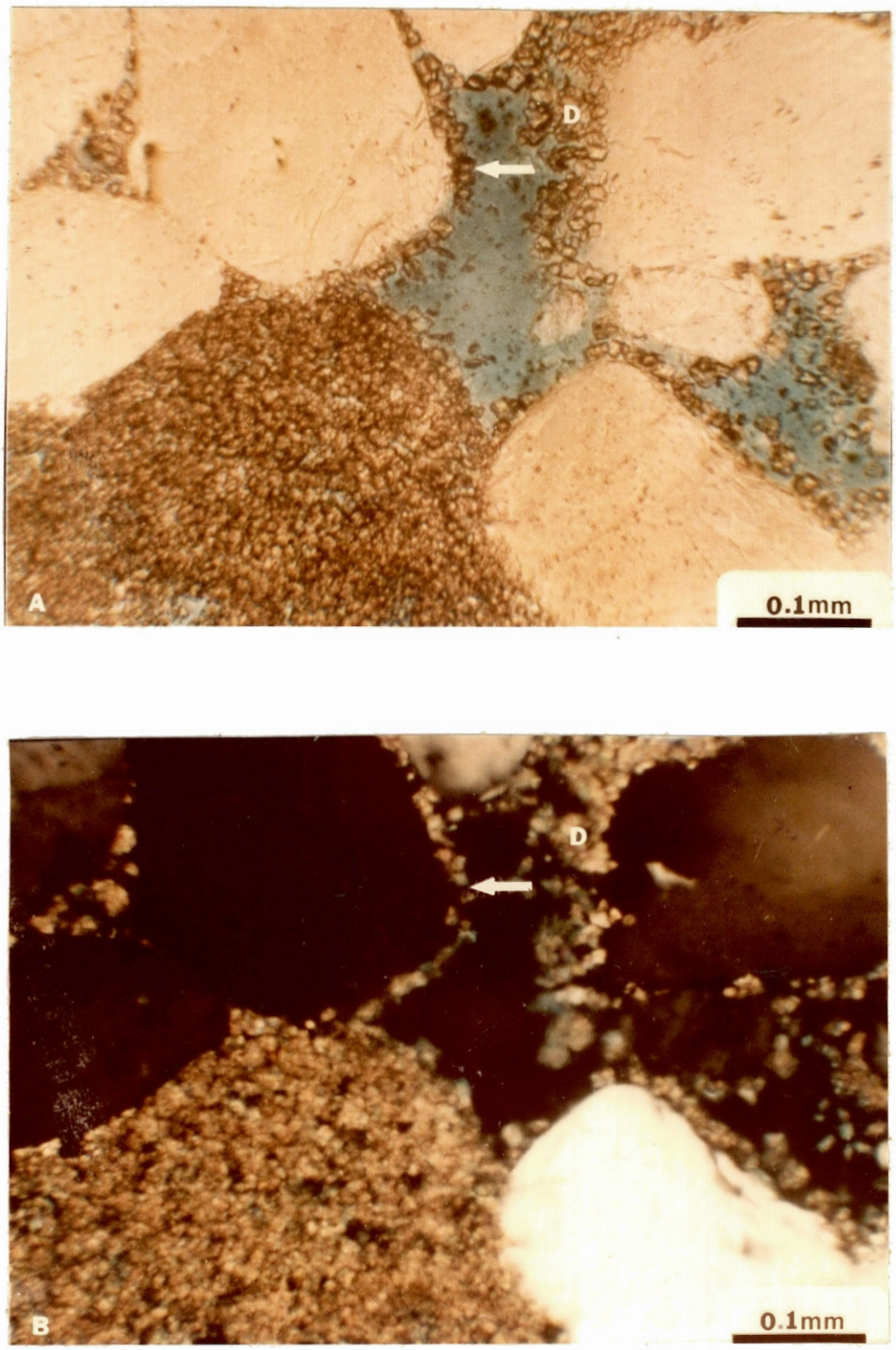

Fig. 12.--Light photomicrographs of pore-lining (arrow) dolomite (D). A. Plane light. B. Crossed polarizers.

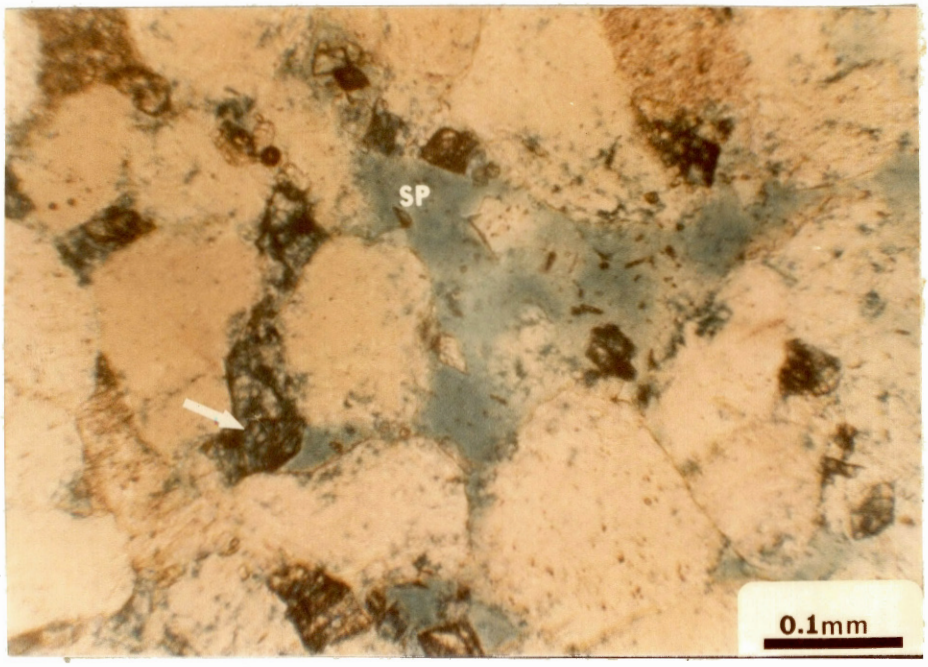

Fig. 13.--Light photomicrograph of ferroan dolomite (arrow) and secondary porosity (SP). Plane light.

mately 6.8, is representative of water character during the formation of authigenic dolomite, a strongly reducing environment was required to maintain elevated concentrations of Fe^{++} ions in solution (Hem and Cropper, 1959; Katz, 1971; Al-Shaieb and Shelton, 1978). The Fe^{++} ions represent a byproduct of the reduction of the Fe^{3+} in hematite which is a constituent of the Opeche shale. This reduction may be related to hydrocarbon migration.

Authigenic Clay Minerals

Authigenic clay minerals in representative samples of upper Minnelusa sandstones were identified by scanning electron microscopy and thin-section analysis, as mixed-layer illite-smectite and kaolinite. Mixed-layer illite-smectite occurs as pore-linings, pore-bridgings, and pore-fillings (Fig. 8, 14 and 15). Kaolinite booklets occur as pore-fillings. The delicate projections on these clays indicate their authigenic nature.

Extracted clay fractions were analyzed using x-ray diffraction analysis (Fig. 16). Quantitative estimates of the relative amounts of authigenic clay minerals were made on the basis of peak height and area under the peak (Appendix A). Mixed-layer illite-smectite is the most abundant authigenic clay mineral.

Although no detrital clays were observed in the Minnelusa sandstones, x-ray diffraction analysis indicated the presence of detrital illite in the rubble zone at the unconformity separating the Minnelusa from the overlying Opeche Shale (Fig. 17). The precipitation of authigenic dolomite and clay minerals reflects changes in the chemistry of the formation water. As a result of these changes, illite became unstable under a new equilibrium regime and authigenic kaolinite and mixed-layer illite-smectite were formed.

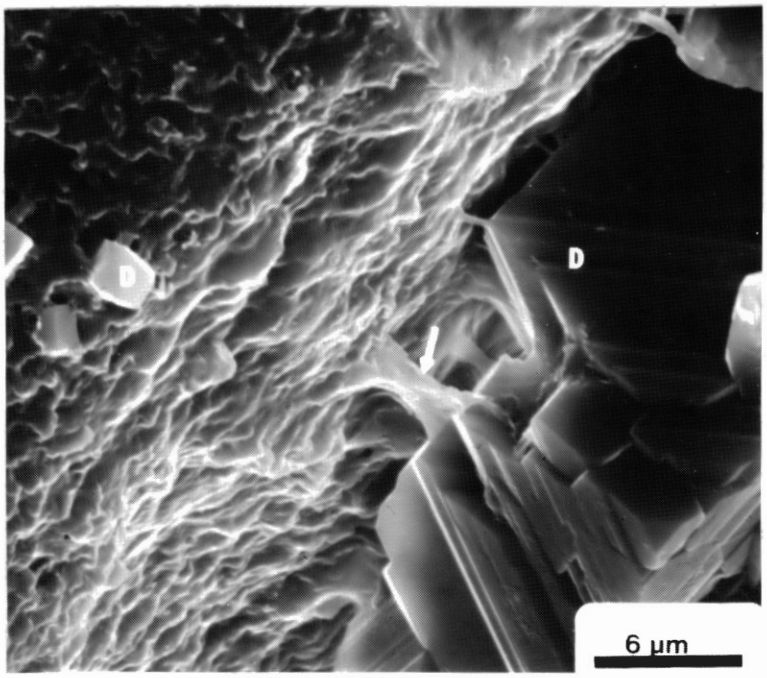

Fig. 14.--SEM photomicrograph of mixed-layer illite-smectite (arrow) bridging between detrital quartz and euhedral dolomite.

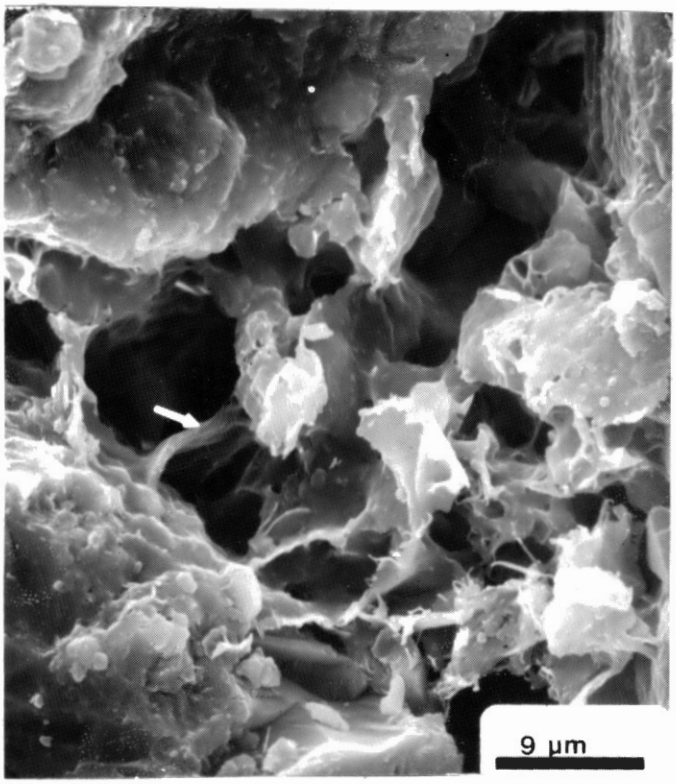

Fig. 15.--SEM photomicrograph of pore-bridging (arrow) and pore-filling mixed-layer illite-smectite.

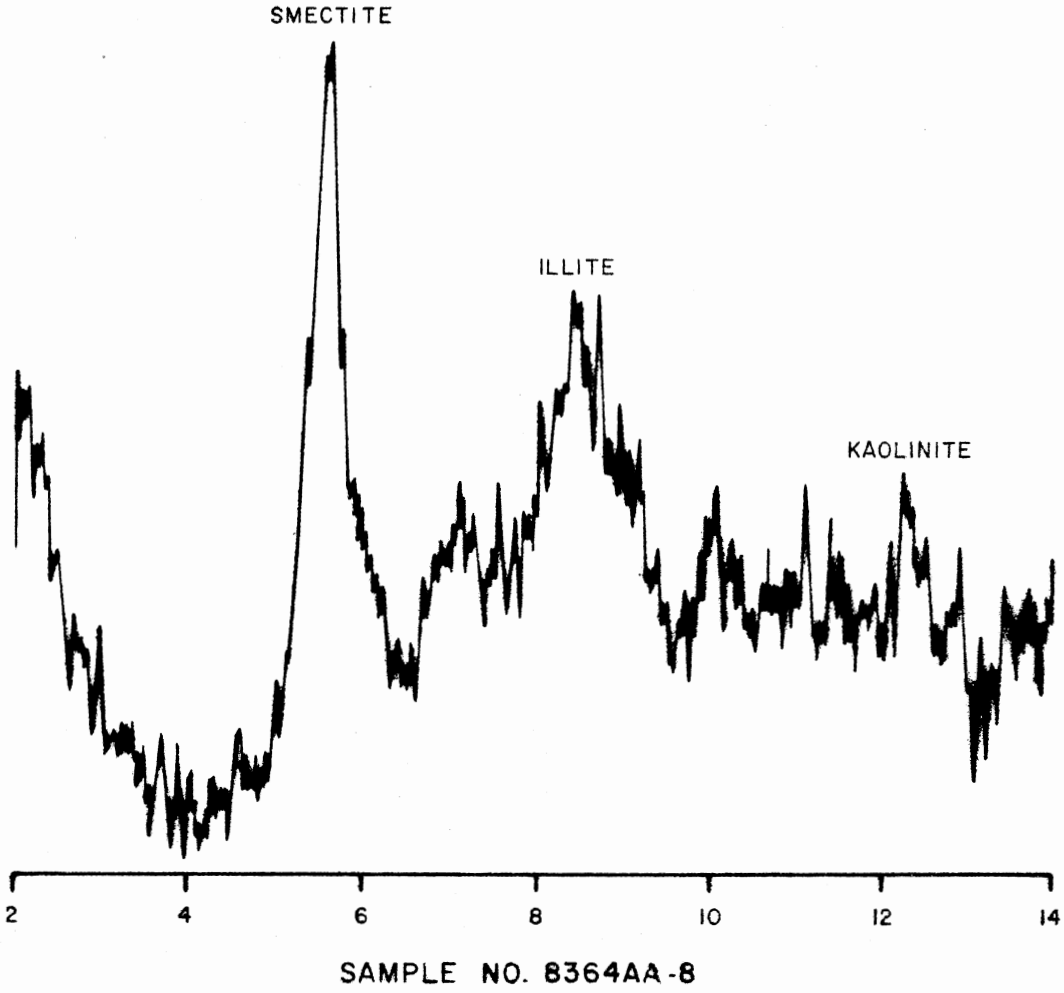

Fig. 16.--X-ray diffraction analysis of clay fraction from sample 8386AA-8. Upper Minnelusa sandstone.

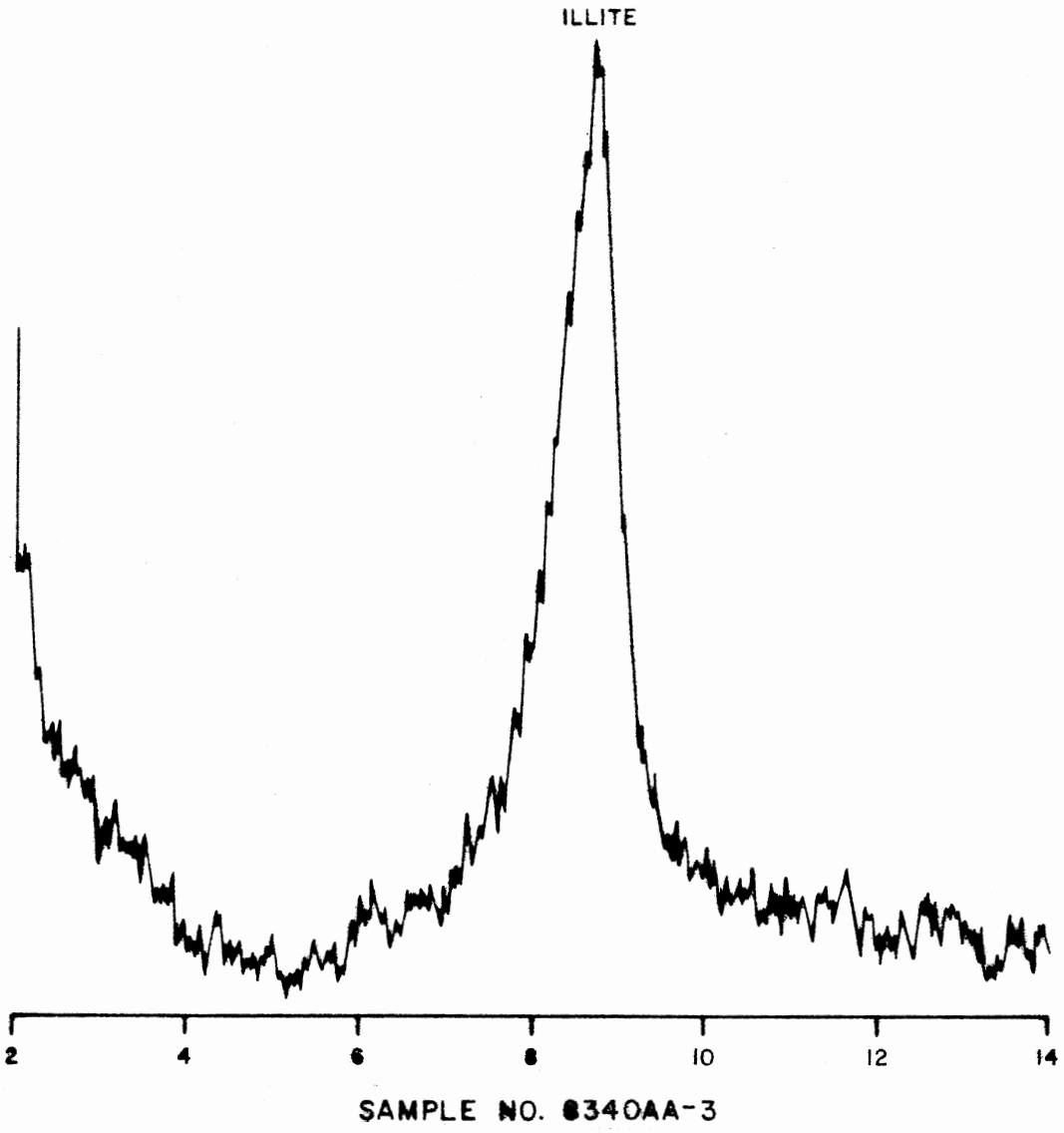

Fig. 17.--X-ray diffraction analysis of clay fraction from sample 8340AA-3. Rubble zone at the base of the Opeche Shale.

Benson and Aagaard (in Stanley and Benson, 1979) developed a model which is more accurate than the conventional activity diagrams in predicting saturation and equilibrium for different clay mineral phases. The model compensates for the effects of multi-component phases or solid solutions of variable composition. When plotted on a two-dimensional representation of this model (Fig. 18), the mean of the log (a_{K+}/a_{H+}) values calculated by the WATEQF program indicates that the formation waters are saturated with respect to illite, smectite, and kaolinite.

The following reactions may explain the transformation of detrital feldspar and illite to kaolinite and smectite, respectively:

$$\underset{\text{K-Feldspar}}{2KAlSi_3O_8} + 2H^+ + 9H_2O \quad \underset{\text{Kaolinite}}{H_4Al_2Si_2O_9} + 2H^+ + 4H_4SiO_4 \qquad (2)$$

$$\underset{\text{Mica}}{2KAl_3Si_3O_{10}(OH)_2} + 2H^+ + 3H_2 \quad \underset{\text{Kaolinite}}{3H_4Al_2Si_2O_9} + 2K^+ \qquad (3)$$

Boles and Franks (1979) proposed the following reaction for the transformation of smectite to illite:

$$4.5K^+ + 8Al^{3+} + \underset{\text{Smectite}}{KNaCa_2Mg_4Fe_4Al_4Si_{38}O_{100}(OH)_{20}} + 10H_2 \quad \underset{\text{Illite}}{K_{5.5}Mg_{12}Fe_{1.5}Al_{22}Si_{35}O_{100}(OH)_{20}} + Na^+ + 2Ca^{++} + 2.5Fe^{3+} + 2Mg^{++} + 3Si^{4+} + 10H_2O \qquad (4)$$

This reaction was based on the model developed by Hower et al. (1976):

$$\text{Smectite} + Al^{3+} + K^+ \quad \text{Illite} + Si^{4+} \qquad (5)$$

The activity diagram in Figure 19 may aid in the explanation of this transformation.

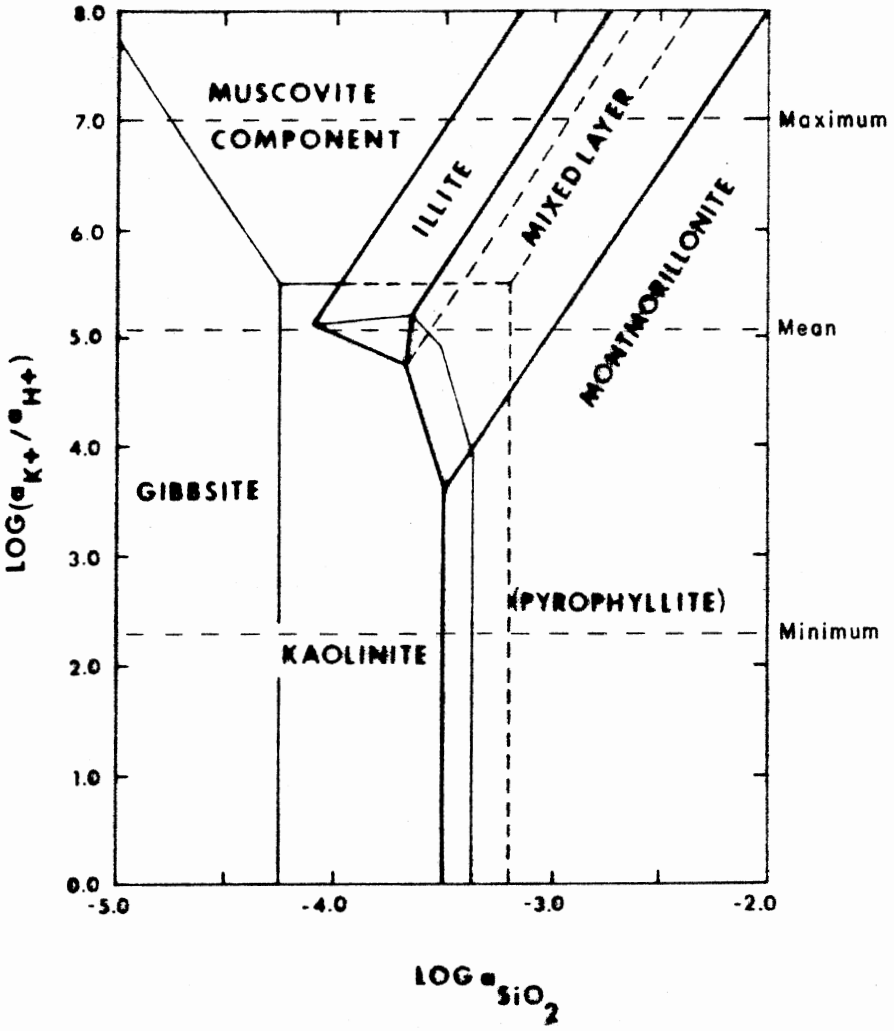

Fig. 18.--Activity diagram for the aluminosilicate system showing stability fields of naturally-occurring clay mineral groups (after Stanley and Benson, 1979). Shown are the mean, minimum, and maximum values of the log (a_{K^+}/a_{H^+}) of well waters from the Minnelusa.

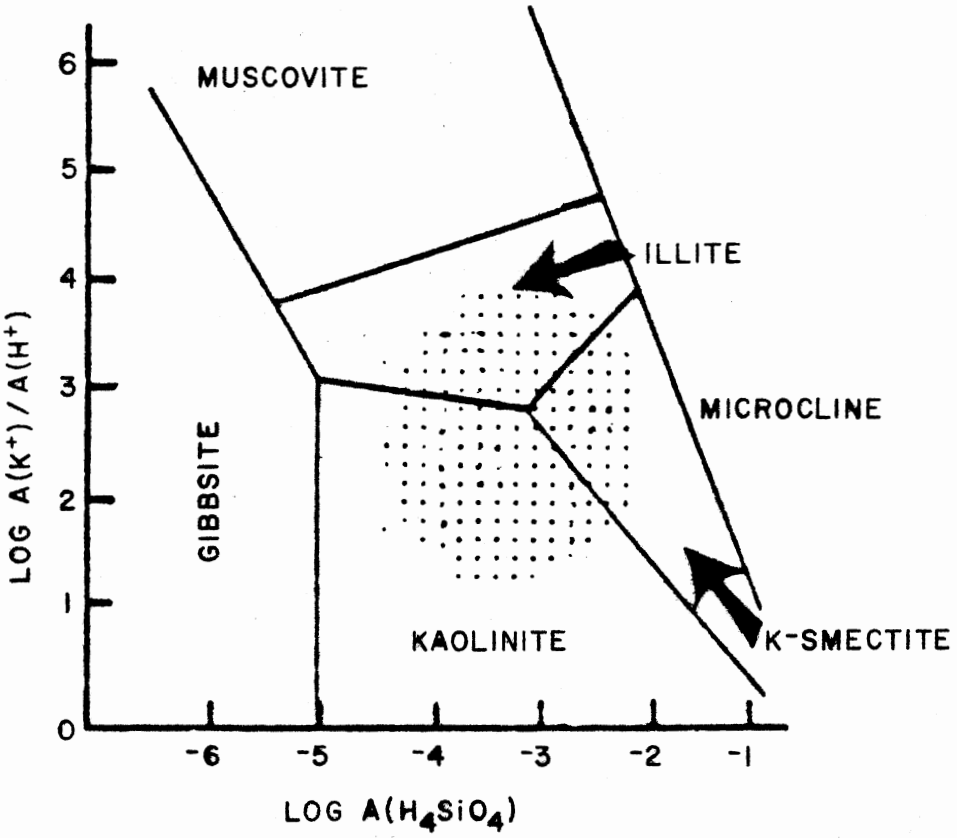

Fig. 19.--Stability field diagram for common minerals in K_2O-Al_2O_3-SiO_2-H_2O system (after Shvartsev and Bazhenov, 1978).

Miscellaneous Diagenetic Products

Secondary minerals which are somewhat less abundant than those described above but still important in the diagenetic history of upper Minnelusa sandstones include pyrite and silica.

Pyrite. Diagenetic pyrite is a minor constituent in upper Minnelusa sandstones. It occurs locally as small disseminated euhedral crystals. The formation of pyrite is the result of the reduction of iron by H_2S gas associated with hydrocarbons. Ferguson (1977), following Donovan (1972), used Eh-pH diagrams to demonstrate that pyrite could be formed in red beds by this mechanism. In this process the iron is altered from the ferric to ferrous state with the sulfur in the pyrite provided by the H_2S gas (Kartsev et al., 1959):

$$2H_2S + Fe_2O_3 \rightarrow FeS_2 + FeO + 2H_2O \qquad (6)$$

In the study area the iron needed for the reaction originated either from the hematite associated with the red Opeche shale, or by base exchange from clay minerals (Parker, 1973). The low concentration of pyrite is possibly due to the absence of sufficient volumes of H_2S gas. Hydrogen sulfide odors were not detected by Wells et al. (1979) in their investigation of formation waters in the Raven Creek and Reel oil fields.

Silica. Silica is a minor cementing agent in upper Minnelusa sandstones. It occurs as syntaxial quartz overgrowth boundaries, and the result is an interlocking mosaic of quartz (Fig. 20). Much of the silica was precipitated from migrating solutions rather than as the result of local pressure solution. This is shown by the paucity of sutured grain

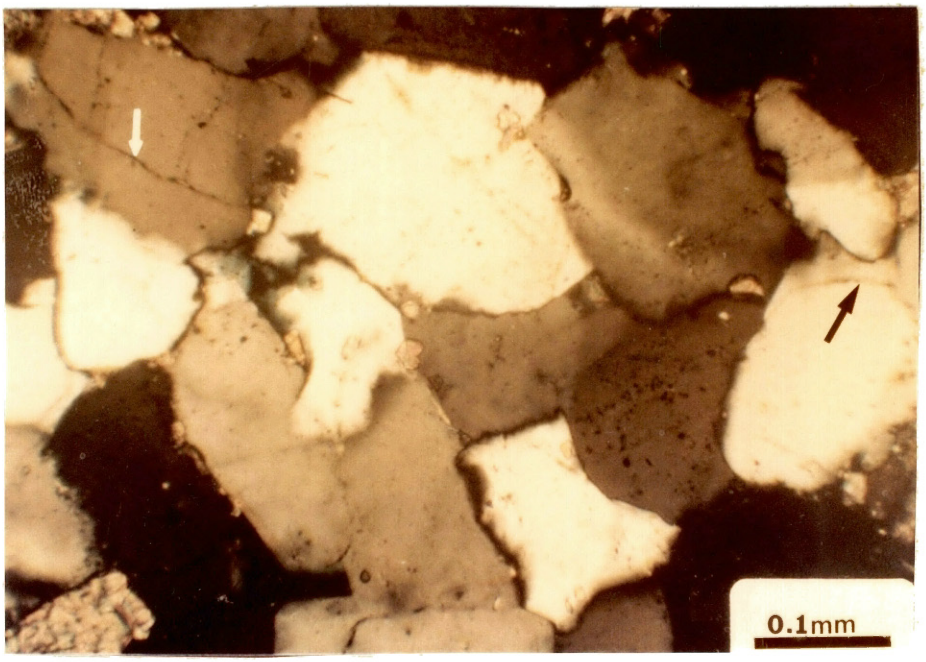

Fig. 20.--Light photomicrograph showing extreme silicification. Note quartz overgrowths and "dust" rims (arrows). Crossed polarizers.

contacts and the presence of prism faces on overgrowths. In addition to silica, traces of diagenetic chert were observed.

Autochthonous Sediments

Upper Minnelusa carbonate rocks are exclusively dense microcrystalline dolomites. They are gray to pink, and locally are arenaceous, stylolitized, and fractured and contain chert and anhydrite inclusions. Anhydrite beds are associated with dolomites or are interbedded with sandstones. The anhydrite is white to pink, microcrystalline to sucrosic in texture, and locally arenaceous. The autochthonous sediments are important in their contribution to the composition of the formation waters.

Opeche Shale

Opeche shales are red, anhydritic, and locally arenaceous. Locally, a rubble zone consisting of chert, dolomite, sandstone, and anhydrite pebbles in a red shale matrix is present at the base of the Opeche.

Hydrocarbon migration through red beds would probably result in an alteration in color caused by a reducing environment in the presence of hydrogen sulfide gas, and the formation of pyrite as a result of the reduction of iron oxide by hydrogen sulfide gas associated with petroleum (Lilburn, 1981). Pyrite was not observed in the Opeche samples examined. The red beds showed no evidence of bleaching. These observations suggest that hydrocarbon migration in the Minnelusa had no observable effect on the overlying Opeche shales.

Geochemistry of Formation Water

Subsurface formation waters generally reflect the mineral phases present in the rock (Mankiewicz and Steidtmann, 1979). Analyses of Minnelusa formation waters compiled by Wells et al. (1979) were analyzed using WATEQF (Truesdell and Jones, 1974; Plummer et al., 1976), a computer program which calculates the equilibrium distribution of all major species in the waters sampled. Using both analyzed and estimated data, the program calculated the activities of the major cations and anions, the activity product (IAP), and the saturation index (S = IAP/KT) for the dolomite, anhydrite, and gypsum phases. The solubility product for a particular mineral phase is represented by KT. Where the saturation index is one, greater than one, or less than one the water is defined as saturated, supersaturated, or undersaturated, respectively, with respect to a particular mineral phase. The results are summarized in Appendix B.

In the study area and surrounding Minnelusa oil fields the formation waters are slightly undersaturated with respect to anhydrite, extremely undersaturated with respect to gypsum, and supersaturated with respect to dolomite. It has been established that anhydrite and dolomite are the dominant secondary minerals in the study area. The saturation indices were calculated using approximated formation temperatures (Head et al., 1979). At these temperatures anhydrite is the more stable phase, at the expense of gypsum.

Dilution of formation waters by encroachment of meteoric waters resulted in the dissolution of anhydrite and an increase in Ca^{++} concentrations. Sulfate reduction increased the bicarbonate alkalinity

according to the following equation (Berner, 1971):

$$2CH_2O + SO_4^{=} \rightarrow 2HCO_3^{-} + H_2S \quad (7)$$

These two factors, in addition to high Mg^{++}/Ca^{++} ratios, favor dolomite over anhydrite as a mineral cement:

$$2HCO_3^{-} + 2Ca^{++} + 2Mg_{2-x}^{++} + Fe^{++} \rightarrow 2Ca(Mg_{1-x}, Fe_x) + (CO_3)_2 + 2H^{+} \quad (8)$$

Formation waters are neutral to slightly acidic, with pH values ranging from 4.5 to 9.1 and averaging 6.8. The pH values are controlled by the carbonate and sulfide systems. Disassociation of hydrogen sulfide tends to increase the hydrogen concentration and lower the pH according to the following equation (Mankiewicz and Steidtmann, 1979):

$$H_2S \qquad H^{+} + HS^{-} \quad pK_{eq} = 7.0 \quad (9)$$

The interaction between carbonate and sulfide equilibria, and possible variations in pK_{eq} with total concentration of dissolved solids result in variations from the calculated value of 7.0 (Goldhaber and Kaplan, 1975).

Saturation-index log values for anhydrite-gypsum and dolomite were plotted and contoured (Plates 2 and 3). A trend is noted where the values for saturation indices increase with increasing distance from the productive Minnelusa trend in the northeastern part of the Powder River basin. Increases in saturation index values may indicate increases in cementation.

Diagenetic History, Paragenesis, And Secondary Porosity

Examination of almost any thin section from the study area can leave little doubt that the state of the rock at the time of deposition was drastically different from its present state. The detrital grains have been corroded, embayed, altered, and replaced. Several stages of cementation have occurred. These changes have a direct influence on the reservoir potential of upper Minnelusa sandstones. The chronological sequence of diagenetic events (Fig. 21) is based on thin-section examination and scanning electron microscopy. Correlation of these events with the tectonic history of the Powder River basin is based on less direct lines of evidence.

The precipitation of quartz was the first major diagenetic event. Blatt (1979) suggested, on the basis of hydraulic and geochemical considerations, that the bulk of quartz cement in orthoquartzites is precipitated at very shallow depths. Precipitation probably occurred at temperatures ranging from 40° to 60°C. Flow rates of formation waters are too slow to result in significant silica cementation once the sand is buried to depths greater than a few hundred meters (Blatt, 1979). The presence of "floating" grains and the scarcity of sutured grain contacts implies that precipitation occurred soon after deposition and at a shallow depth.

The presence of poikilotopic masses of anhydrite enclosing and replacing unabraded quartz overgrowths indicates that anhydrite cementation followed silicification. Because of this sequence it is improbable that anhydrite cement was formed penecontemporaneously with deposition of the sand. Penecontemporaneous anhydrite may have preceded

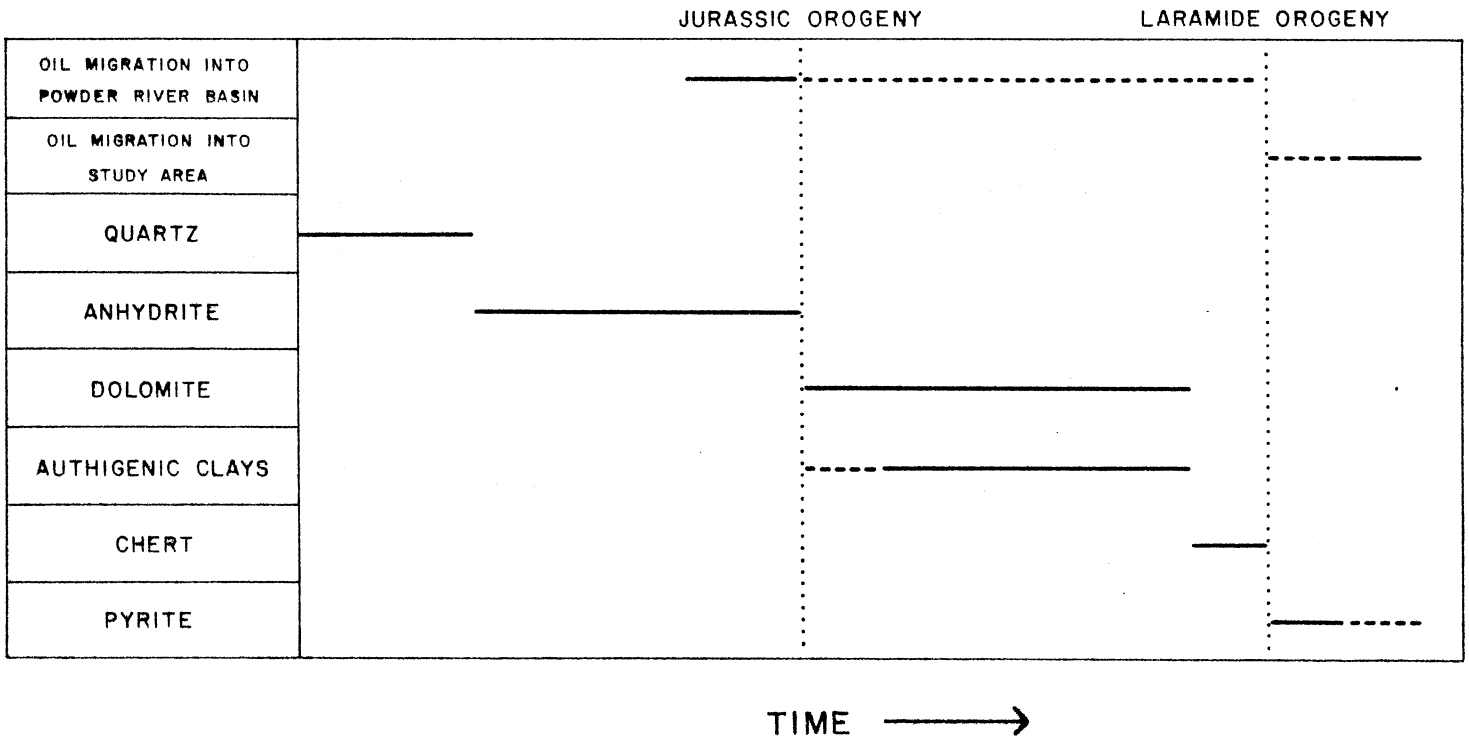

Fig. 21.--Paragenesis of diagenetic events.

silica cementation, but no evidence of such an occurrence was observed. The associated anhydrite units are the most probable source of the precipitate. Anhydrite cementation seems to have occluded all primary porosity.

Dissolution of anhydrite cement resulted in the development of significant secondary porosity (Fig. 22). This event was probably related to regional warping in the Jurassic or uplift initiated in the Early Cretaceous which brought about changes in basin hydrology. An influx of meteoric waters resulted in the dilution of formation waters and subsequently, the dissolution of anhydrite.

Pore-filling and pore-lining dolomite and dolomite replacing anhydrite represent late-stage diagenetic products. The conditions leading to anhydrite dissolution and dolomite precipitation are discussed in the preceding section. Dolomite precipitation did not completely occlude the secondary porosity created by anhydrite dissolution. In fact, localized concentrations of authigenic dolomite characterize the areas of greatest anhydrite dissolution. Authigenic illite-smectite mixed-layer clays and kaolinite were probably formed contemporaneously with diagenetic dolomite, although textural relationships suggest that dolomite precipitation may have slightly preceded the formation of authigenic clays. The precipitation of authigenic dolomite and clay minerals reflects changes in the chemistry of the formation water.

Hydrocarbons probably migrated into the Powder River basin during the Jurassic. Accumulation of hydrocarbons in the study area may have occurred during the Laramide Orogeny by remigration in response to basinward tilting of the Minnelusa strata.

Secondary chert appears to have formed late in the diagenetic

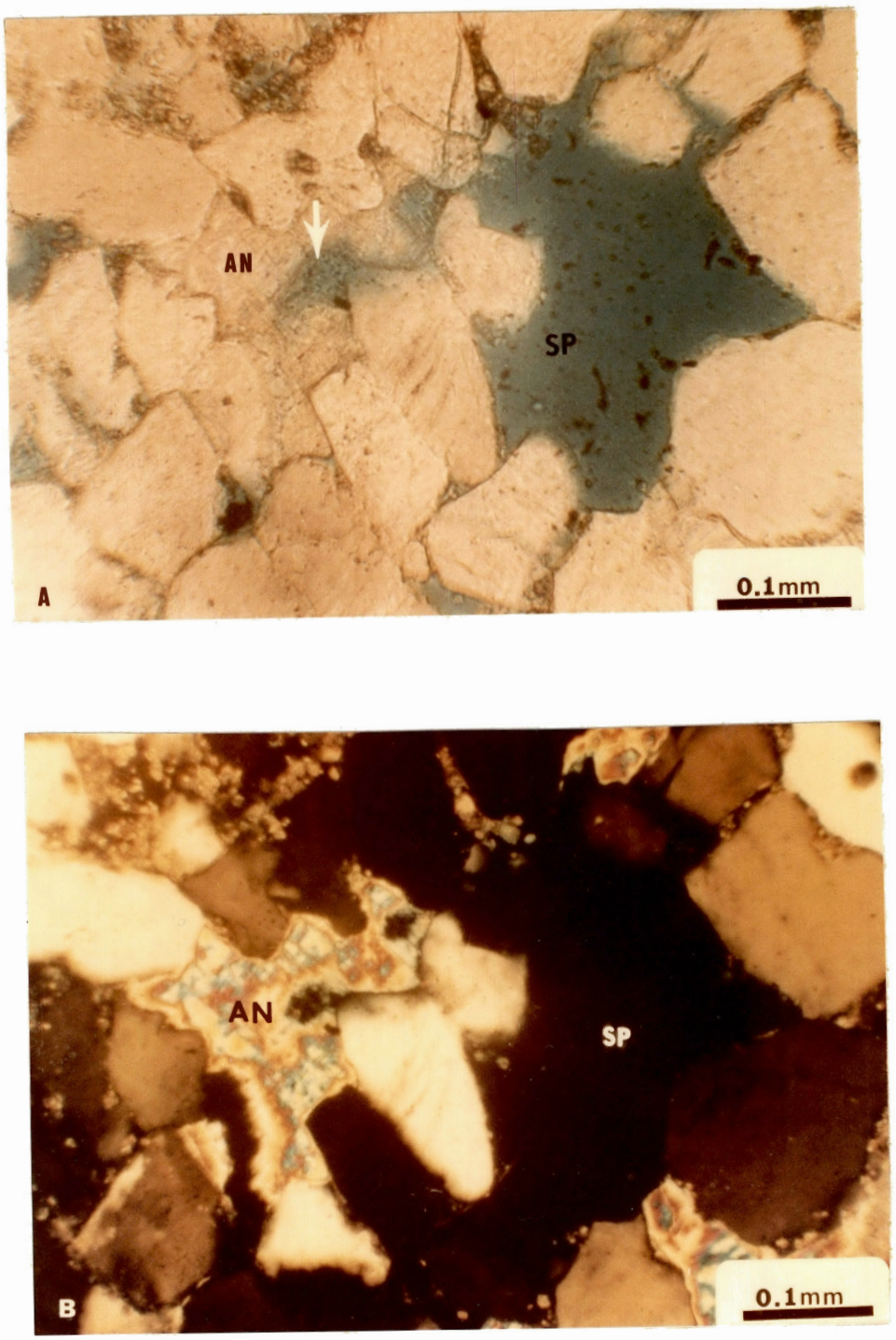

Fig. 22.--Light photomicrographs showing the dissolution of anhydrite (AN) and the formation of secondary porosity (SP and arrow). A. Plane light B. Crossed polarizers (B).

history of the Minnelusa, possibly before the precipitation of pyrite. Pyrite was the last authigenic mineral to form in upper Minnelusa sandstones. The development of pyrite is directly related to hydrocarbon migration.

The present porosity and permeability of upper Minnelusa sandstones is the result of diagenetic processes. Silica and anhydrite cementation occluded all primary porosity. Therefore, porosity in the sandstones can be attributed to anhydrite dissolution. The porosity created by the dissolution of anhydrite was partially destroyed by the formation of authigenic dolomite, clay, chert, and pyrite. Enough secondary porosity was preserved to allow upper Minnelusa sandstones to serve as commercially significant hydrocarbon reservoirs (Fig. 23).

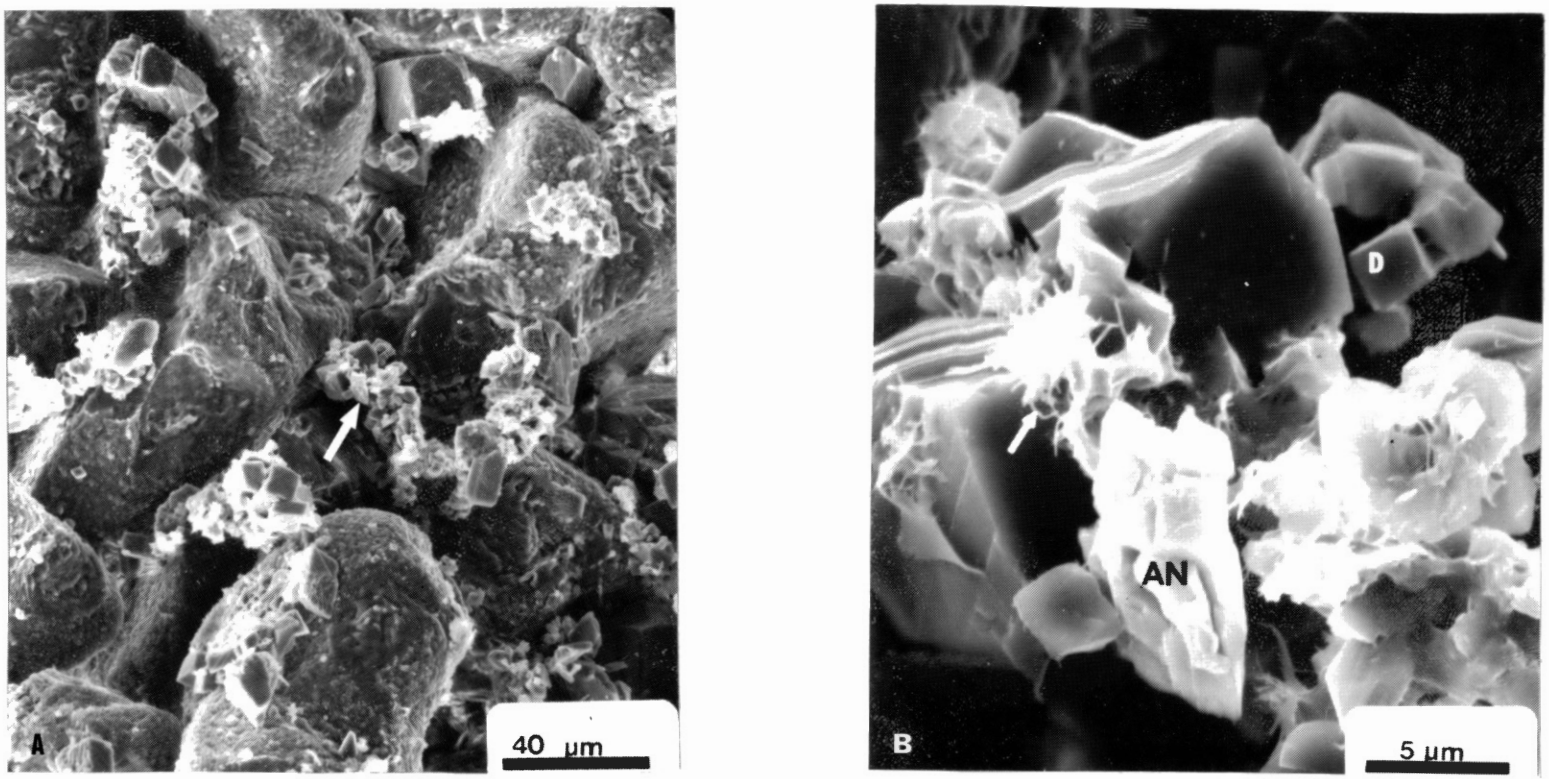

Fig. 23.--SEM photomicrographs showing textural features of upper Minnelusa sandstone. A. Textural relationships of detrital and authigenic minerals. B. Enlargement of a (arrow) showing textural relationships of authigenic minerals, anhydrite (AN), dolomite (D), and mixed-layer illite-smectite (arrow).

CHAPTER IV

HYDROCARBON SOURCE, MIGRATION, ENTRAPMENT, AND ALTERATION

The diagenetic effects of hydrocarbon migration depend, in part, on the physical and chemical properties of the hydrocarbons migrating through the reservoir. Petroleum composition is determined by source material, by depositional, generative, and transformational environments, by migrational processes, and by chemical changes within the reservoir after entrapment. The following chapter is a summary describing the source of the oil found in Minnelusa reservoirs, the mechanisms and paths of migration into the Powder River basin, the entrapment, and the changes that occur in hydrocarbon composition with migration and accumulation.

Hydrocarbon Source

Hunt (1953) and Curtis et al. (1958) suggested that the oil in Minnelusa reservoirs was derived locally from the dolomite-evaporite facies of the Minnelusa Formation. Barbat (1967, p. 1287) has observed that Minnelusa oils exhibit characteristics opposite those which would be expected if the source was the Minnelusa:

> The numerous occurrences of hematite, winnowed sandstone bodies, and shallow evaporite pans, and the general lack of pyrite in the carbonates of the Minnelusa, indicate a generally high state of oxidation. Hence, if any petroleum could have survived such a high state of oxidation, it would most likely be highly paraffinic and low in sulfur. The lack

> of phosphatic minerals would suggest also that any oil whose source was the Minnelusa probably would have a low nitrogen content.

In fact, Minnelusa oils are highly aromatic and have high sulfur and nitrogen contents.

Thin petroliferous beds of the Minnekahta are considered by some geologists to be the source of Minnelusa oils. Because the prospective source volume is very small, it is difficult to explain how the Minnekahta could have generated substantial amounts of oil. Red Opeche shales separate the Minnelusa from the Minnekahta at most places in the area where the Minnelusa is productive. This permeability barrier would have prevented the migration of oil from the Minnekahta to Minnelusa reservoirs (Barbat, 1967).

The source of most of the oil found in upper Paleozoic rocks in the northern and central Rocky Mountain region is believed to be the Permian Phosphoria Formation. Cheney and Sheldon (1959) speculated that the phosphatic shale beds of the Phosphoria were sources of petroleum found in the Park City Formation in southwestern Wyoming and northern Utah. Stone (1967) extended this concept to include most of the oil in Paleozoic reservoirs in the Big Horn basin. A similar source for the Paleozoic accumulations in the Wind River basin has been suggested by Keefer (1969). Barbat (1967), Sheldon (1967), and Momper and Williams (1979) concluded that the oil in upper Paleozoic rocks in the Powder River basin migrated eastward from the Phosphoria Formation.

The Phosphoria Formation and its partial stratigraphic equivalents of marine origin cover an area greater than 225,000 square miles in southwestern Montana, western Wyoming, northeastern Colorado, eastern Idaho, northern Utah, and northeastern Nevada (McKelvey et al., 1959).

In southeastern Idaho the Phosphoria is shale, phosphorite, and chert. These beds thin eastward from Idaho into western Wyoming and intertongue with the thin carbonate beds of the Park City Formation in central Wyoming. The Phosphoria and Park City also intertongue with the Shedhorn Sandstone in southwestern Montana and northwestern Wyoming (McKelvey et al., 1959; Sheldon, 1963). The Park City intertongues in central Wyoming with the predominately red bed Goose Egg Formation (Burk and Thomas, 1956).

In central and western Wyoming and eastern Idaho Permian rocks lie in the upper part of the Cordilleran geosynclinal wedge of Paleozoic and Mesozoic rocks. These rocks thin to the east on the craton in central and eastern Wyoming, and thicken to the west in the geosyncline in southeastern Idaho and western Wyoming (Sheldon, 1963). The Phosphoria Formation was deposited on the edge of the continental shelf in a large, open embayment adjacent to a bend in the geosynclinal axis.

The Phosphoria is composed of phosphatic shale and chert members. Each of the rock types within the Phosphoria represent parts of marine transgressive and regressive cycles (McKelvey et al., 1959). In western Wyoming two complete cycles are present. Each cycle is composed of a sequence of carbonate rock, chert, phosphorite, carbonaceous shale and then the reverse back to carbonate rock (Fig. 24). The Meade Park and Retort carbonaceous shale members represent the maximum transgression reached in each of these cycles.

Subsequent to deposition, Phosphoria strata were buried by increments to increasingly greater depths through the Mesozoic. Maximum burial of the Permian strata throughout most of the region is assumed to have occurred at the end of the Cretaceous (Claypool et al., 1978).

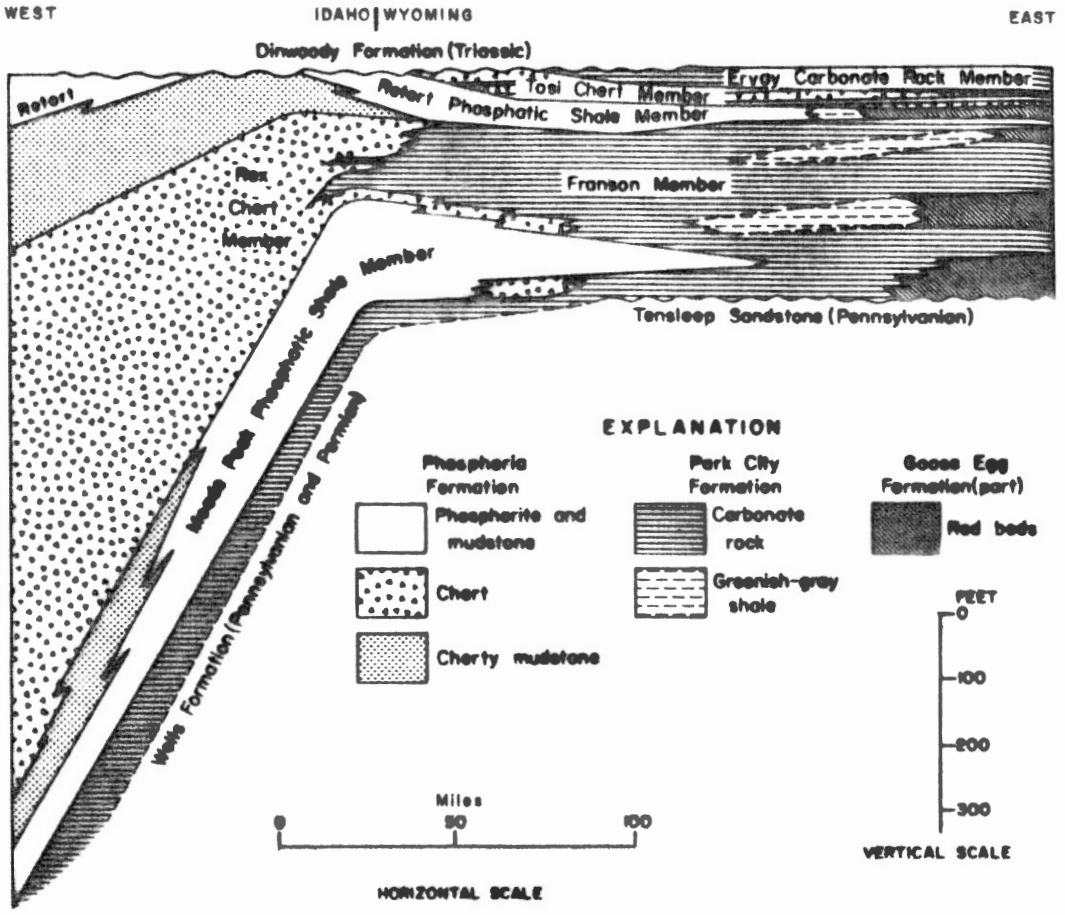

Fig. 24.--Stratigraphic relationships of the different lithologic units in the Phosphoria (Claypool et al., 1978).

During the Triassic and Jurassic there was a slow net accumulation of cover, despite frequent periods of nondeposition and erosion. Thick sediments were deposited during the Cretaceous. Cretaceous sediments generally provide most of the post-Permian accumulation.

Post-Permian sedimentation in the Cordilleran geosyncline in southeastern Idaho and western Wyoming was greater than on the craton in central and eastern Wyoming (Sheldon, 1967). The cover is markedly thicker west of a hinge line which separated the tectonically active geosynclinal trough from the more stable shelf and craton (Claypool et al., 1978).

In the Phosphoria Formation the sedimentary phosphorite has been considered a potential source rock. However, the carbonaceous shale is probably the better petroleum source rock (Claypool et al., 1978). The black shale members were deposited in an area of upwelling marine water (McKelvey et al., 1953). Upwelling currents bring mineral-rich water to shallow depths. The water supplies nutrients that enhance the production of organisms which flourish, die, and settle to the bottom. Subsequent burial and increases in temperature convert the accumulated matter to hydrocarbons (Maughan, 1975). Similarities in analyses of minor element composition of the carbonaceous matter in the black shales and the oils in Permian rocks in Wyoming suggest both were derived from the same original organic matter (Hyden, 1961).

If the dominant factor in the generation of hydrocarbons is the organic content, and the organic content at the time of hydrocarbon formation is proportional to the original content of organic matter, then the principal area of oil generation in the Phosphoria would have

been eastern Idaho, adjacent central-western Wyoming, and southwestern Montana (Maughan, 1975). Claypool et al. (1978) suggested that the petroleum-generation potential of the Phosphoria black shales is related to thermal maturity, which was a function of the thickness of overlying Mesozoic rocks and/or the proximity to the Idaho and Boulder batholiths. Maximum conversion of organic matter to petroleum occurs at temperatures corresponding to burial depths of 2.5 to 4.5 kilometers. Carbonaceous shales subjected to such temperatures occur on the platform east of the Cordilleran geosyncline across central Wyoming. At shallower depths the rocks contain an immature hydrocarbon assemblage which is unlike mature petroleum. At greater depths thermal destruction and expulsion result in the depletion of extractable hydrocarbons.

Hydrocarbon Migration

Sheldon (1967) and Barbat (1967) described the environmental-stratigraphic setting which is believed to have generated and preserved so much oil in Permian and Pennsylvanian strata across Wyoming. Oil now found in Minnelusa reservoirs migrated into the region from Phosphoria source areas as far west as several hundred miles. The hydrocarbons were squeezed out of the source rocks by overburden pressures into porous Permian and Pennsylvanian conduit beds. The vertical and lateral limits of migration were controlled by impermeable sealing beds (Fig. 25). Sheldon (1963, p. 159) concluded that:

> The source beds are a basinward facies of the reservoir beds which in turn are a basinward facies of the sealing beds. Transgressions and regressions of these facies give rise to an interfingering of source, reservoir, and sealing beds

Potential conduit and reservoir beds are the Permian Park City Formation and Shedhorn Sandstone, and the underlying Tensleep Formation and its

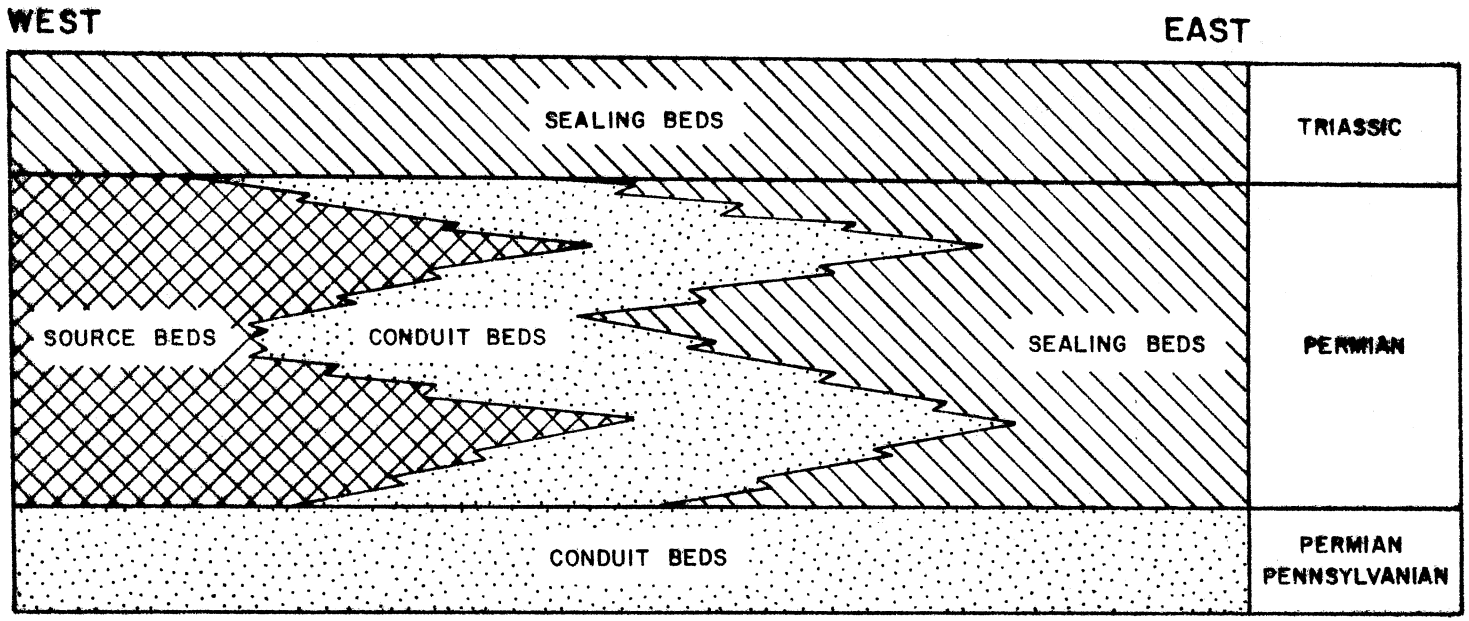

Fig. 25.--Idealized relationships between source, conduit, and sealing beds of Permian and Pennsylvanian rocks in Wyoming (after Sheldon, 1967).

stratigraphic equivalents. Sandstones equivalent to the Tensleep include the Minnelusa Formation in northeastern Wyoming, the Casper Formation in southeastern Wyoming, the Quadrant Quartzite in northwestern Wyoming, and the Wells Formation in western Wyoming and southeastern Idaho. The Permian Goose Egg Formation which is the stratigraphic equivalent of the Park City, acts as the sealing bed in central and eastern Wyoming. The Phosphoria, Shedhorn, and Park City Formations are overlain by Triassic shales which function as sealing beds.

Gussow (1954) suggested that approximately 2,000 feet of overburden are required before hydrocarbons are expelled from source rocks and primary "flush" migration can occur. Much of the Phosphoria source area was being subjected, or had already been subjected, to a critical load of 2,000 to 3,000 feet of burial by the end of the Jurassic (Barbat, 1967). This was sufficient to begin the expulsion and migration process. Sheldon (1967), Stone (1967), and Keefer (1969) concluded that the geological conditions in the Phosphoria source area were such that primary migration was initiated during Early Jurassic. Primary "flush" migration probably was complete by Early Jurassic (Stone, 1967) or Early Cretaceous time (Barbat, 1967).

The rate of post-Permian sedimentation was greatest in the geosyncline. Sedimentation rates decreased eastward, across the shelf and onto the craton in eastern Wyoming. The differences in overburden pressure, as well as the regional westward dip of strata off the positive cratonic area, would have induced an eastward migration of hydrocarbons toward central Wyoming (Sheldon, 1967). Regional southwestward tilting of approximately 10 feet per mile developed across the broad

shelf of central Wyoming during Late Jurassic (Fig. 26). Barbat (1967) speculated that secondary migration of oil from the Tensleep to the laterally contiguous Minnelusa may have occurred in response to this development.

Momper and Williams (1979) suggested that oil derived from the Phosphoria entered northeastern Wyoming across the Casper arch before the Powder River basin was formed. Initially, the oil migrated through Pennsylvanian Tensleep sandstones. Then, where Lower Permian Tensleep sandstones were preserved, it migrated through conduit beds of that age. A smaller amount of oil followed a second migration path to the northwestern margin of the basin, through middle Pennsylvanian sandstones.

Secondary migration continued until cementation impeded the paths of migration or tectonism broke them up (Sheldon, 1967). The Shedhorn Sandstone and the Tensleep and its equivalents are well sorted, and before cementation would have been ideal conduit rocks. Due to cementation by silica, carbonate, or anhydrite they now are largely impermeable. The carbonate rocks of the Park City also would have been excellent conduit rocks before cementation, but are now fairly impermeable.

The structural events leading to cessation of oil migration have been described by Sheldon (1967, p. 62):

> In southeastern Idaho, possible Jurassic orogeny (Armstrong and Cressman, 1963) broke up the earlier simpler structural pattern by folding and thrust faulting, and probably stopped further eastward migration of fluids. As time went on, tectonism increased and moved eastward. By Maestrichtian time, the ancestral Wind River Range began to emerge in central Wyoming, probably stopping the uninterrupted eastward migration of fluids.

Comparison of pre-Laramide and Laramide structural traps on the Casper arch indicates that migration had stopped by middle Cenozoic time

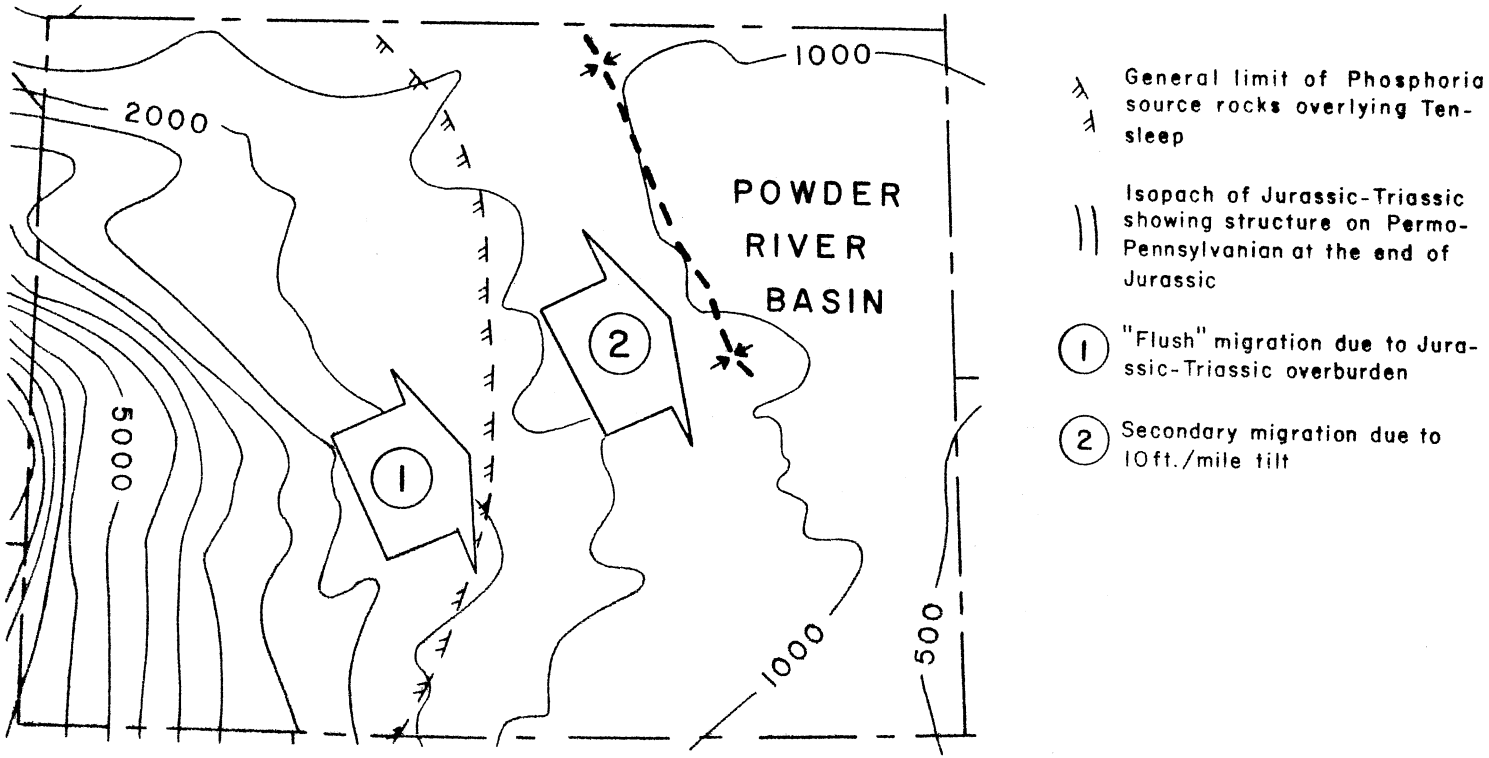

Fig. 26.--Regional geologic conditions that permitted migration of Phosphoria - source oils toward eastern Wyoming (after Barbat, 1967).

(Barbat, 1967; Sheldon, 1967). Pre-Laramide structural traps of small areal extent but relatively high relief contain oil derived from the Phosphoria. Large Laramide structures in the same area commonly have only minor Phosphoria-type oil accumulations or none at all.

Hydrocarbon Entrapment

Production from Minnelusa and Tensleep reservoirs in the Powder River basin is concentrated in three areas: the southeast rim of the basin, the southwest rim or Casper arch area, and the east-central part of the basin. In the southeast part of the basin oil derived from the Phosphoria is produced from upper and middle Minnelusa sandstone zones (Hubbell and Wilson, 1963). In the two other areas, upper Minnelusa and Tensleep sandstones produce oil (Berg and Tenney, 1967) derived from the Phosphoria (Momper and Williams, 1979). Middle Pennsylvanian, Tyler sandstone beds are productive on the northwest margin of the basin, but equivalents of this unit are very thin or absent in the basin proper (Kinnison, 1971).

The concentration of fields in the Powder River basin which produce from upper Minnelusa and Tensleep reservoirs forms a northeasterly trend (Fig. 27) across the central part of the basin (Mettler and Roehrs, 1968). Within this trend three types of trapping mechanisms control hydrocarbon accumulation in the Minnelusa and Tensleep (Berg, 1963). One type is structural closure, where the structure is generally of low relief, and actual closure generally does not exceed 100 feet. The second type of trap occurs where facies changes within the upper Minnelusa result in an updip permeability barrier. The third type of trap is an unconformity trap which is the result of post-Minnelusa topography and the updip

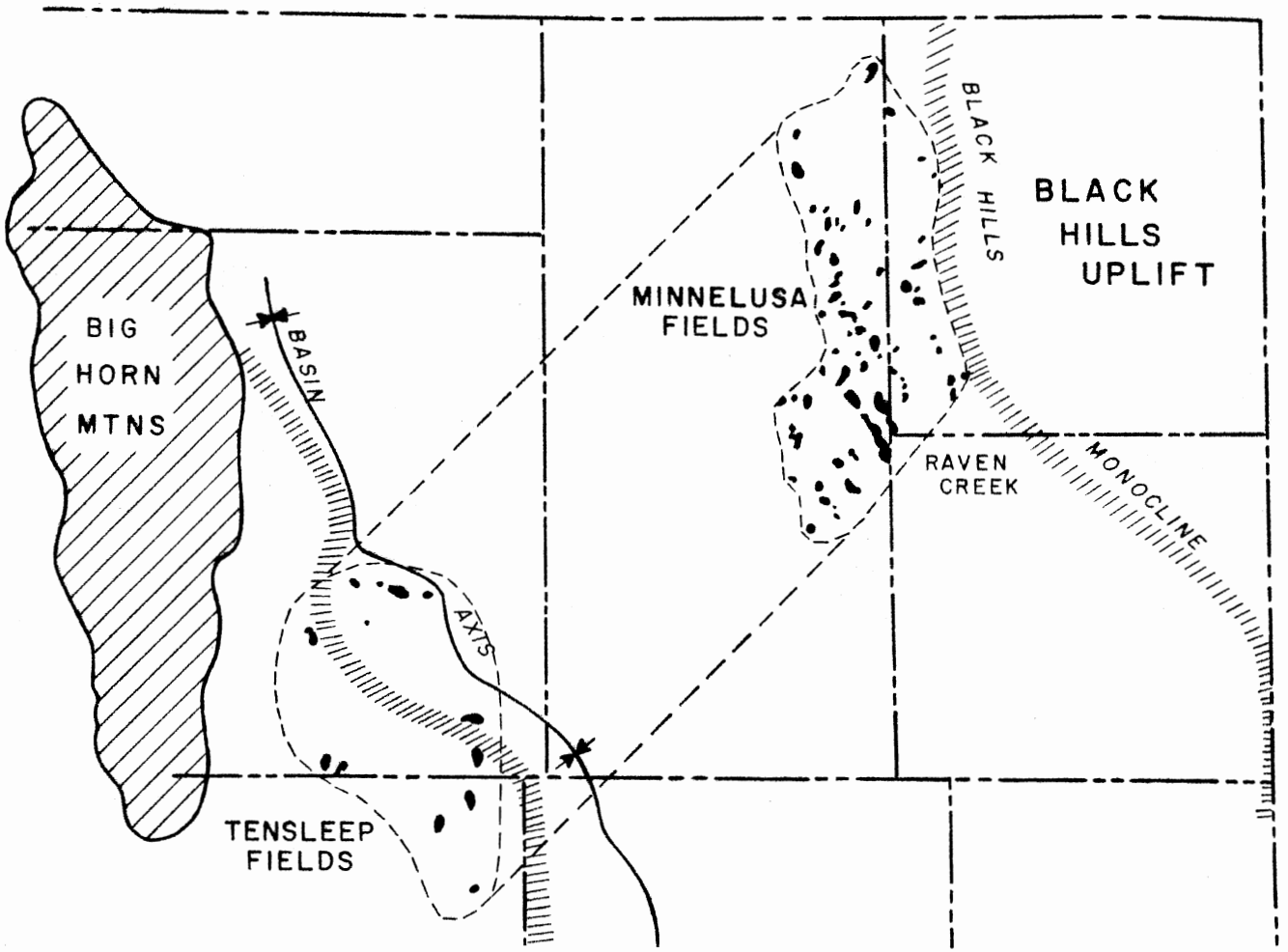

Fig. 27.--Regional productive trend in the Powder River basin (after Mettler and Roehrs, 1968).

presence of deep valleys which are filled with Opeche shale. Although other factors often play a secondary role in entrapment, most accumulations can be classified as belonging to one of these categories (Van West, 1972).

Most Minnelusa fields which occur east of the structural axis of the basin and within the productive trend are stratigraphic traps, although a few have minor structural modifications (Berg and Tenney, 1967). Tensleep fields west of the axis are largely structural traps, but post-Wolfcampian truncation may account for as much as half the closure.

By far the largest portion of the Minnelusa oil in place has been trapped by paleotopographic highs in the east-central part of the basin (Van West, 1972). These highs occur at the post-Minnelusa unconformity. Relief is considerably greater in the productive area than in the peripheral nonproductive regions. Slack (1981) suggested that the relief is related to paleotectonic movements, along northeast and locally northwest-trending structural lineaments that delineate the Belle Fourche arch. The arch extends through the productive trend delineated by Mettler and Roehrs (1968). Tensleep production on the southwest rim of the basin occurs directly on trend with the Belle Fourche arch. This suggests that the lineament pattern is continuous across the basin (Slack, 1981).

Local relief on the post-Minnelusa unconformity surface appears to be due in part to erosional modification and to depositional topography (Slack, 1981). Erosional channels trend approximately N25°W and N55°E (Mettler and Roehrs, 1968). These trends imply a relation to the nearly identical structural trends described by Slack (1981). The

consistency of topographic trend and the characteristic erosion pattern were controlled by regional pre-erosional tectonism that created conjugate fracture systems in the Minnelusa Formation (Mettler and Roehrs, 1968).

In the area of greatest Minnelusa production deposition of upper Minnelusa sediments probably occurred on a downthrown block. A downthrown block would have enhanced deposition of interbedded or reservoir-capping sabkha carbonate which would stabilize sandstone dune-form topography, as well as provide an updip permeability barrier (Slack, 1981). Dolomite and anhydrite are slightly more common in the producing area, suggesting that the block was depressed.

Upper Minnelusa rocks consist of dolomite and anhydrite interbedded with softer sandstones. The bedding of these rocks at the unconformity is essentially flat. These factors were partly responsible for the development of a mesa or tableland topography when the rocks were subjected to erosion. In western Crook County the paleotopographic highs tend to be relatively small and isolated within broad topographic depressions (Van West, 1972). The long axes of these paleotopographic highs tend to be oriented approximately to the northwest or to the northeast (Mettler and Roehrs, 1968). Relief of the paleotopographic highs decreased from east to north and west. In eastern Campbell County the paleotopographic highs merged into larger, elevated areas, and the valleys were better defined. The northwest orientation of the long axes of these hills appears to have been more prevalent here than to the east. Farther west, the paleotopographic highs coalesced more and more, showed no preferred orientation, and left shallow, isolated depressions between (Van West, 1972).

Erosion of the upper Minnelusa occurred before deposition of the overlying Opeche Shale. The time of this erosion was probably Late Wolfcampian to Early Leonardian (Tranter, 1963). Erosion proceeded westward and northward until the Opeche sea started to encroach upon the Minnelusa surface. Evaporites in the Minnelusa and Goose Egg Formations indicate that the Permian Period was very arid. Also, the wide, shallow depressions and the isolated paleotopographic highs in the eastern portion of the productive trend make it difficult to place these features within a logical drainage system. This factor, together with the presumably arid climate, indicates the occurrence of a desert-type erosion cycle during the hiatus (Van West, 1972).

The productive sandstone at Raven Creek, as at most other Minnelusa fields, has been eroded updip and its interval is occupied by an abnormally thick section of Opeche shale (Tranter, 1963; Trotter, 1963). Following the discovery of the field, two explanations of this Minnelusa-Opeche relationship were advanced (Trotter, 1963): The absence of the sandstone updip represented a local facies change to red shale; or the disappearance of the sandstone was the result of pre-Opeche erosion and the subsequent infilling by Opeche shale in topographic lows developed upon the eroded Minnelusa surface. Cores contain rubble at the Minnelusa-Opeche contact, thereby supporting the latter hypothesis.

At Raven Creek, and possibly at Reel field, the rock types and their association with a breached low-order anticline controlled the erosional pattern of the Minnelusa, hence the configuration of the trap (Trotter, 1963). The maximum amount of erosion occurred at the crest of the pre-Opeche anticline. The productive sandstone is overlain by a

dense dolomite which formed a protective dip slope. Erosion of the dolomite exposed the less resistant sandstone below. The sandstone was then eroded to the depth of the next resistant dolomite bed.

The eroded crest of the anticline was surrounded by topographic highs capped by resistant dolomite. The topographic lows on the surface of the structure were filled with Opeche shale. Where present, the productive sandstone unit was sealed. In the Raven Creek field the thickness of the Opeche Shale varies by as much as 70 feet. This variation is an indication of the amount of topographic relief prior to the deposition of the Opeche Shale.

The hypothesis that erosion of the Minnelusa surface was controlled by a pre-Opeche anticline is supported by the discrepancy between thinning of the upper Minnelusa compared to the thickening of the Opeche Shale (Tranter and Kerns, 1972). Thinning of the upper Minnelusa appears to be at least 50 feet greater than thickening of the overlying shale. Sometime after deposition of the Opeche Shale, structural closure was destroyed, probably by basinward tilting (Tranter, 1963). The western flank of the ancient structure formed a stratigraphic trap, where the productive sandstone, underlain by impermeable dolomite, is truncated against the Opeche Shale (Fig. 28).

Hydrocarbon Alteration

Although the crude oils of Wyoming vary widely in composition, they are generally divided into two groups, either on the basis of their general characteristics or on the age of their producing formations (Ball and Espach, 1948). There is a striking divergence in composition between Paleozoic and Mesozoic oils (Hunt, 1953). Oils produced from

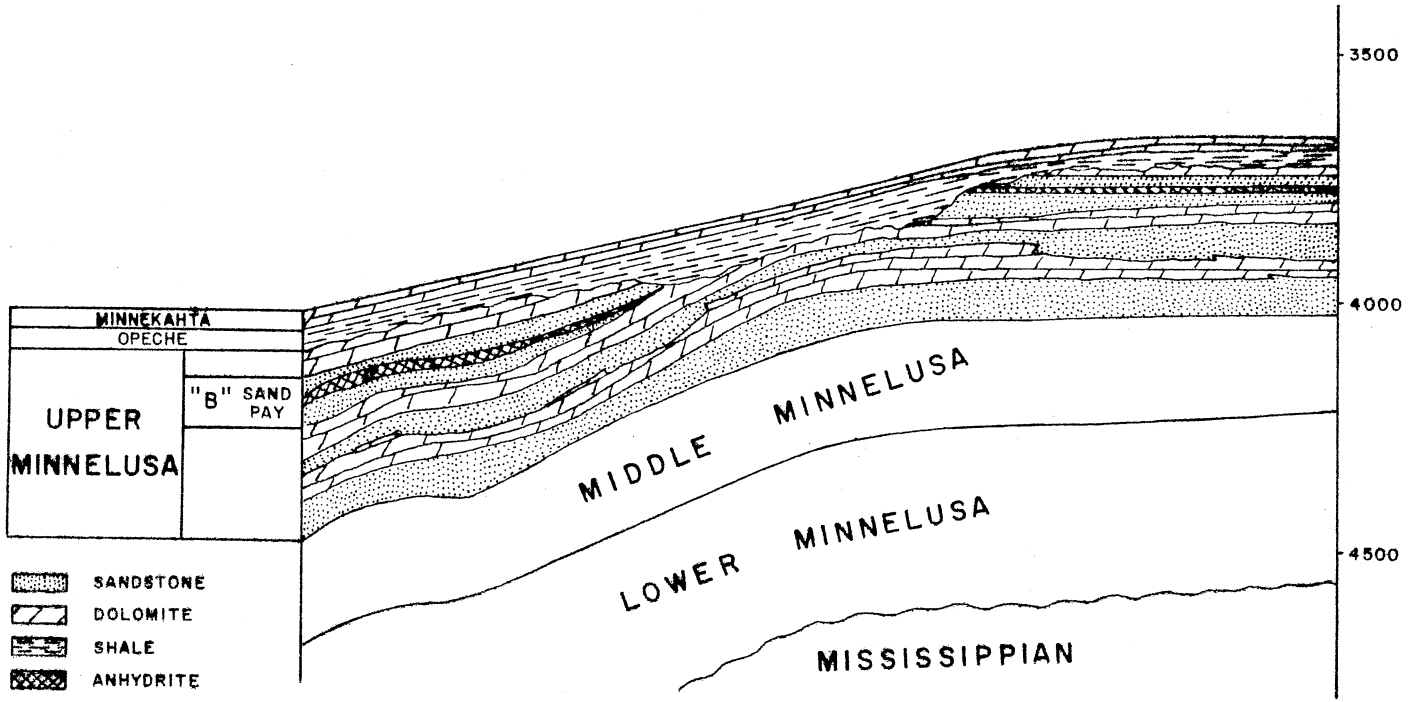

Fig. 28.--Cross section of the trap at the Raven Creek oil field (after Tranter, 1963).

Paleozoic formations are dark colored, have an aromatic-napthene base, low gasoline content, high sulfur, residue, and asphaltene content, and low A.P.I. gravity. Oils associated with Mesozoic rocks are light colored, have a paraffin-napthene base, high gasoline content, very low sulfur and asphaltene content, and high A.P.I. gravity.

These general correlations have been modified by Curtis et al. (1958), Strickland (1958), and Wenger and Reid (1958) to conform to conditions in the Powder River basin. Permian oils are produced from pre-Jurassic formations. These oils are similar in composition to the Paleozoic oils described by Hunt (1953). Cretaceous oils are similar in composition to oils which Hunt associated with Mesozoic rocks. Cretaceous oils are produced from Cretaceous and younger formations.

Oils produced from Jurassic formations are highly variable in composition. In some respects they appear to be mixtures of both Permian and Cretaceous oils. Production from Jurassic formations has been established in fields which produce Permian or Cretaceous oils or both (Curtis et al., 1958). Jurassic rocks seem to form the transition zone between the two major types of oil in the Powder River basin (Wenger and Reid, 1958).

Barbat (1967) has demonstrated that oils from similar source-rock environments which have been subjected to similar postgenetic influences are sufficiently alike that their common origin is easily established. However, when oils derived from a common source have been subjected to different time and temperature regimes, major changes in oil composition may occur (Orr, 1974). The process resulting from time-temperature effects is referred to as maturation. The Paleozoic oils in the Big Horn, Wind River, and Powder River basins occur in a region where

subsidence and tectonic history are complex; therefore, it is assumed that initially similar oils have been subjected to quite different temperatures during migration and entrapment.

The correlation index system devised by Smith (1940) provides a distinctive identity for oils based on the proportion of different hydrocarbon types in each distillation fraction. Paraffinic oils exhibit low correlation index values, whereas increasing the proportions of cyclic compounds results in increased index values. Barbat (1967) determined that the correlation index value of Phosphoria-source oils does not change appreciably with depth or distance from the source. The residuum after distillation usually contains most of the sulfurous, nitrogenous, and oxygenated organic compounds. Analyses of this fraction for Tensleep and Minnelusa oils show a remarkable consistency in the sulfur and nitrogen contents.

Three changes in oil composition are generally recognized as being characteristic of thermal maturation (Orr, 1974). A decrease in the molecular weight results in an increase in A.P.I. gravity. Secondly, heteroatoms (N, O, and S) decrease in content by thermal decomposition to gases (CO_2, H_2O, and H_2S). Finally, the gas/oil ratio increases as a result of thermal cleavages forming low-molecular-weight hydrocarbons.

In most basins in the world, oils from a single source exhibit an increase in A.P.I. gravity and a decrease in sulfur and nitrogen content with increasing depth. On the basis of these observations Barbat (1967, p. 1264) concluded that:

> Because the correlation indexes change little and the volumes of the respective distillation fractions also exhibit few differences with respect to each other as the A.P.I. gravity increases, the increase in gravity can be attributed largely to a decrease in residuum and an increase in gas content.

Because most of the sulfurous and nitrogenous compounds are contained in the residuum, the decrease in sulfur and nitrogen with increasing burial depth normally indicates a decrease in the proportion of the residuum in the system.

On the basis of thermal-cracking experiments conducted by McNab et al. (1952), Barbat (1967) concluded that mild thermal-cracking would reduce the residuum content, but probably would not affect the correlation index value. Extreme thermal-cracking would have an even greater effect on the residuum content, and would increase the correlation index value.

Hunt (1953) concluded that the Phosphoria was not the source of the oil in Minnelusa reservoirs on the basis of what he considered minor, but significant differences in composition. Minnelusa oils in the Powder River basin exhibit higher A.P.I. gravities and correlation index values than Tensleep oils in basins to the west. Minnelusa oils are also lower in sulfur and residue contents (Curtis et al., 1958).

These discrepancies can probably be attributed to thermal maturation. Phosphoria-source oils appear to have been very deficient in gas content at the time of generation (Barbat, 1967). However, thermal maturation may have generated significant quantities of gas during the migration of Phosphoria-source oils into the Powder River basin. The oils were redistributed during the Laramide Orogeny and now occur at depths of 15,000 feet or more (Momper and Williams, 1979). Such depths would enhance the thermal-cracking mechanism. Thermal maturation may account for the scattered occurrences of hydrogen sulfide gas associated with Minnelusa reservoirs in the northeastern part of the Powder River basin.

Orr (1974) classified Paleozoic oils in the Big Horn basin on the basis of maturity, which is a function of thermal history. The oils were classified into three maturity groups (Types I, II, and III) on the basis of a maturity index or "Z" value defined by the equation:

$$Z = 0.641(API°) + 1.34(S/N) + 15.1 \quad (10)$$

Ranges of A.P.I. gravity, percent sulfur, and sulfur/nitrogen ratio for the three maturity groups are shown in Figure 29.

Minnelusa oils in the study area have an A.P.I. gravity of 32, a sulfur content of 1.25 percent, and a sulfur/nitrogen ratio of approximately 12 (Fig. 29). The maturity index value of these oils is 52. The close correlation between these values and the values of Type II oils in the Big Horn basin indicates that both oils were subjected to a similar thermal history.

Orr (1974) noted that Paleozoic oil fields in the Big Horn basin contain little gas. Notable exceptions were some fields containing Type II and III oils, with the most gas observed in fields producing Type III oils. High hydrogen sulfide concentrations in the gas were detected in these fields, but were not detected in other fields.

The productive sandstones in the Raven Creek and Reel fields contain what appear to be two cycles of oil. The reservoirs contain streaks of black, dead oil trapped among sand grains which are evenly saturated with brown, live oil. Tranter and Kerns (1972) suggested that oil could have been trapped in a pre-Opeche structure, and seeped out when the sandstone was exposed by erosion. If this is the case, the black streaks are remnants of an inspissated pre-Opeche accumlation, whereas the producible oil migrated into the trap after deposition of

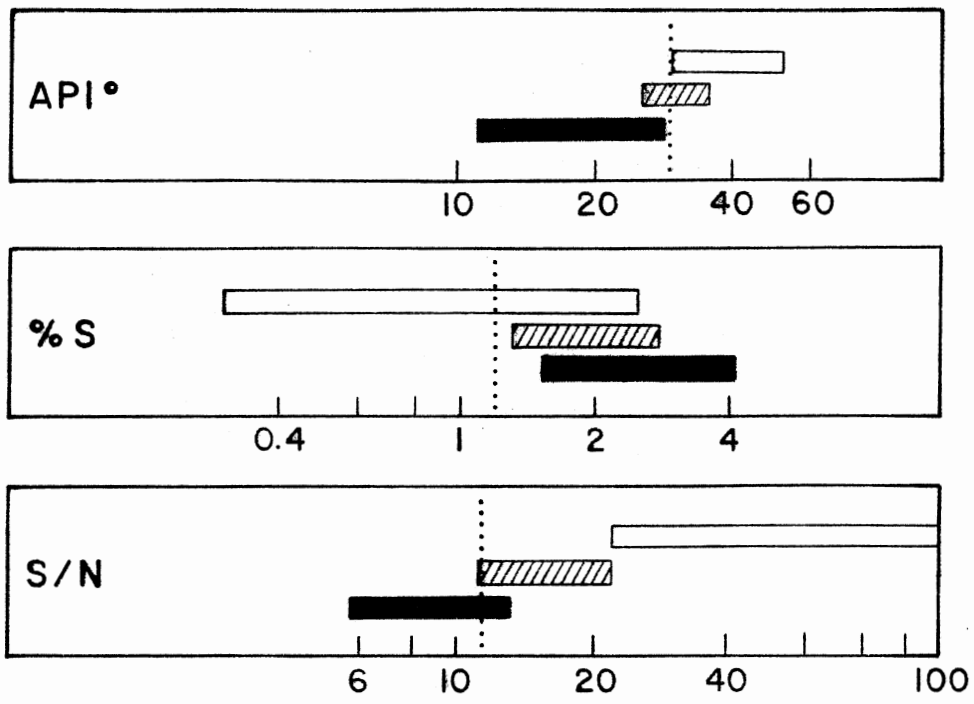

CORRESPONDING VALUES FOR OIL FROM STUDY AREA

Fig. 29.--Ranges of A.P.I. gravity, percent S, and S/N by oil maturity types in the Big Horn basin and corresponding values of oil in the Raven Creek and Reel oil fields (after Orr, 1974).

the Opeche Shale. Primary flush migration of oil from the Phosphoria probably did not begin until the Jurassic. If oil was in place in Minnelusa reservoirs before post-Minnelusa erosion occurred, it would have been derived from a source other than the Phosphoria.

An alternative to this hypothesis is that two generations of Phosphoria-source oils have occupied the reservoirs. The first cycle of oil may have been degraded by nonthermal alteration processes, such as biodegradation or water washing, before the Laramide Orogeny. The second generation of oil remigrated from other parts of the basin in response to the Laramide Orogeny.

CHAPTER V

ISOTOPIC COMPOSITION

During the preceding 25 years stable isotopes have been used extensively in the study of petroleum geochemistry. Only recently have sulfur, carbon, and oxygen isotopic compositions of the diagenetic minerals in reservoir rocks become an important tool in the study of hydrocarbon migration. This chapter examines the S^{34}, C^{13}, and O^{18} isotopes from diagenetic minerals in the Raven Creek and Reel oil fields and their relationship to hydrocarbon migration.

Sulfur Isotopes

Theory

Thode et al. (1958) established the basic framework for working with sulfur isotope data in crude oils. Later investigations have demonstrated that sulfur isotope ratios can be used to identify crude oil from specific source beds, to group oils into genetic families, to follow their migration, and less commonly, to monitor oil alteration processes (Harrison and Thode, 1958; Vredenburgh, 1968; Thode and Monster, 1970; Vredenburgh and Cheney, 1971; Monster, 1972; Orr, 1974; and Gaffney, 1979). The use of sulfur isotope ratios in petroleum exploration has been reviewed by Coleman (1975) and Krouse (1977).

Sulfur isotopic results are reported in terms of the quantity, δ which is defined by the S^{34}/S^{32} abundance ratio in the sample with

respect to the standard ratio in the troilite phase of the Canyon Diablo meteorite:

$$\delta S^{34} = \left[\frac{(S^{34}/S^{32})\ \text{Sample}}{(S^{34}/S^{32})\ \text{Standard}} - 1\right] \times 1000 \qquad (11)$$

with the values reported in per mil (0/00). Samples enriched in S^{34} relative to the standard are said to be isotopically heavy and have positive per mil values. The reverse is true for samples enriched in S^{32}.

The early work of Thode et al. (1958) showed that although there are wide sulfur isotope variations in terrestrial biogenic sulfur compounds, crude oils have a relatively narrow range of δS^{34} values. The range of δS^{34} values for crude oils in particular fields is even smaller (Thode and Monster, 1965). Thode and Monster (1965) reported an apparent relationship in the δS^{34} values between gypsum-anhydrite and petroleum sulfur of the same age. They noted a 15%o displacement in the δS^{34} content. Although Vredenburgh and Cheney (1971) supported this relationship, they claimed the difference to be 20%o for unaltered oils (Fig. 30). These observations suggest that sulfur in petroleum was derived from contemporary sea water, modified by bacterial reduction of sulfate in shallow source sediments before the sulfur was incorporated in the oil (Thode and Monster, 1965).

Thode et al. (1958) and Thode and Monster (1965, 1970) presented evidence that indicated stability of the sulfur isotope during the process of maturation. Analyses by other investigators later indicated that this interpretation was not universally applicable. Cheney (1964)

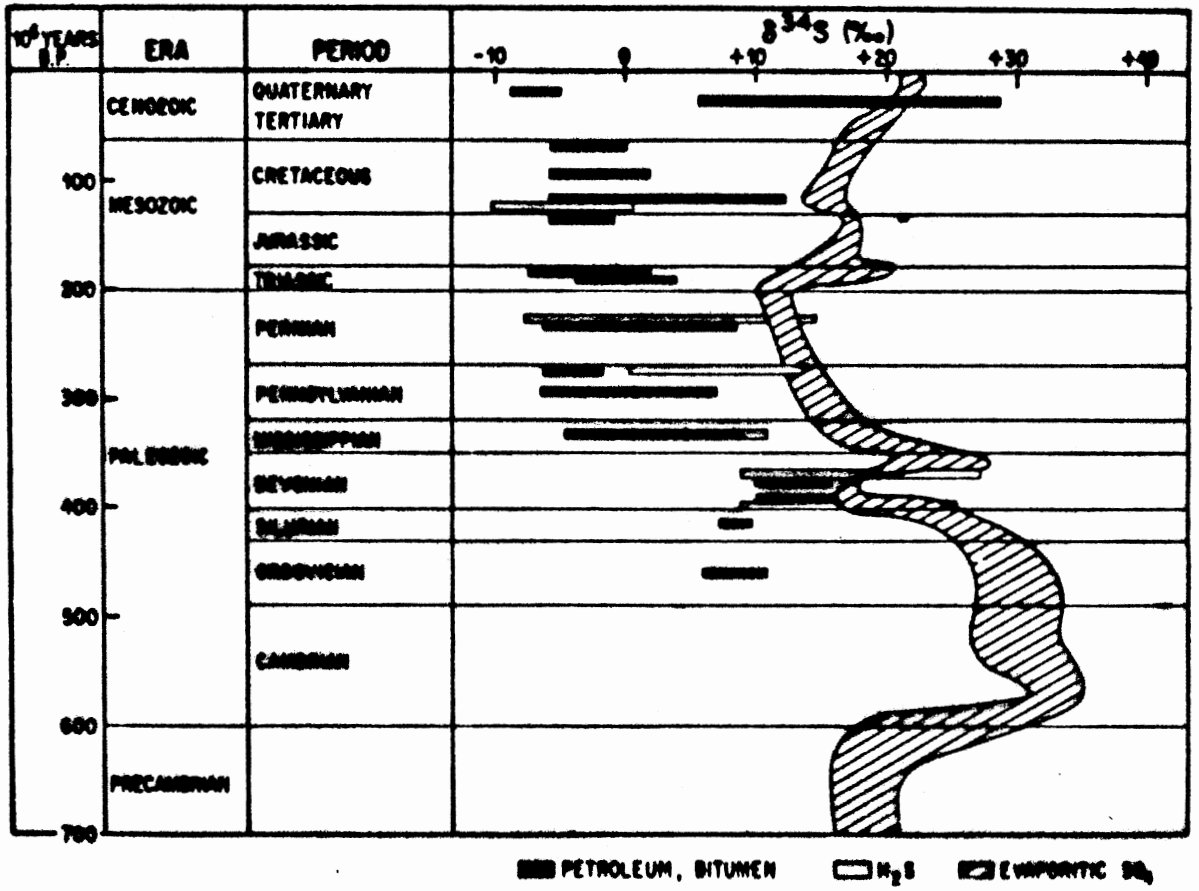

Fig. 30.--Comparison of sulfur isotopic abundances in reservoired petroleum and H_2S with evaporitic SO_4^{--} by geological age (Krouse, 1977).

identified sulfur isotope modifications resulting from petroleum maturation. This finding was later supported by the studies of Vredenburgh and Cheney (1971) and Orr (1974). Maturation results in fractionation which increases the δS^{34} values. As thermal maturation proceeds, the δS^{34} content of the oil continues to increase, and at temperatures greater than 80° to 120°C it approaches the value of sulfate of the same age (Orr, 1974).

The mechanism that results in increased δS^{34} values of the oil is probably related to the associated hydrogen sulfide gas (Orr, 1974). In his study, Orr noted that the values for the gas are similar to those of the oil but tend to be slightly heavier, while during maturation the oil itself becomes increasingly heavy. This led him to deduce that increases in δS^{34} values were due to competing sulfurization and desulfurization processes, and to propose two kinetically-controlled processes working in opposition. These reactions are the reduction of sulfate by hydrogen sulfide to release free sulfur, and the oxidation of hydrocarbons with the sulfur to give more hydrogen sulfide and carbon dioxide.

Thode et al. (1958) determined that although hydrogen sulfide gas had slightly larger isotopic variations, on the average it was enriched in δS^{34} by only 2‰ in comparison to its associated oil. Subsequently, Yeremenko and Pankina (1962) reported that hydrogen sulfide was not necessarily isotopically consistent with the organic sulfur in oil. This was verified by other investigators (Pankina and Mekhtiyeva, 1964; Thode and Monster, 1965; Vredenburgh and Cheney, 1971; Orr, 1974). A compilation of published data (Fig. 31) showed that the average value for the fractionation between hydrogen sulfide and associated oil is

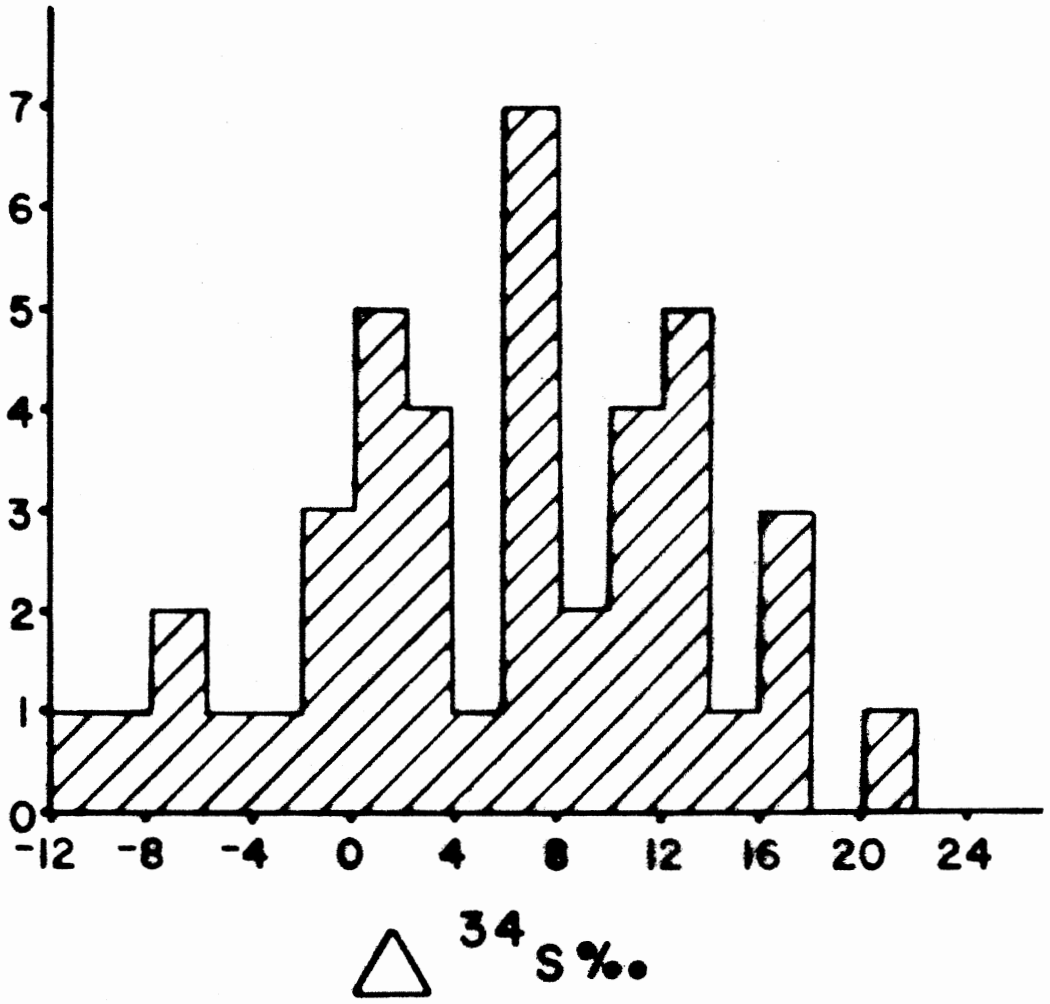

Fig. 31.--Sulfur isotope fractionation between oil and H_2S gas (Coleman, 1975).

approximately 8‰ (Coleman, 1975).

Goldhaber et al. (1978) constructed a histogram from published δS^{34} data of hydrogen sulfide associated with petroleum (Fig. 32). Their results show a range of +10 to -15‰ with a skewness to the positive side.

There are many examples in the literature where bitumens associated with pyrite demonstrate, by similar values, a common sulfur source (e.g., Harrison and Thode, 1958), or where the values of bitumens and pyrite show similar trends in a basin (Smith in Krouse, 1977). Ferguson (1977), followed by Lilburn (1981) presented evidence of pyrite formation as a result of the reduction of iron oxides in red beds by hydrogen sulfide gas derived from buried hydrocarbons. Goldhaber et al. (1978) and Reynolds and Goldhaber (1978) have related the formation of diagenetic pyrite to hydrogen sulfide gases associated with hydrocarbon reservoirs at depth.

Isotopic fractionation may occur when pyrite forms from hydrocarbon-derived hydrogen sulfide gas (Goldhaber et al., 1978). Fractionation controlled kinetically results in an enrichment in δS^{34} of 5 to 15‰. A study by Price and Shieh (1979), which is in disagreement with the previous study, demonstrated the fractionation of sulfur isotopes during laboratory synthesis of pyrite at low temperature. This experiment involved the reaction of hydrogen sulfide gas with goethite at 22° to 24° C for periods from 0.5 hours to 65 days. Within two days fine-grained pyrite formed and was isotopically 0.8‰ lighter than the hydrogen sulfide source. But, after a reaction time of 65 days, the isotopic values for the pyrite and the hydrogen sulfide were approximately the same.

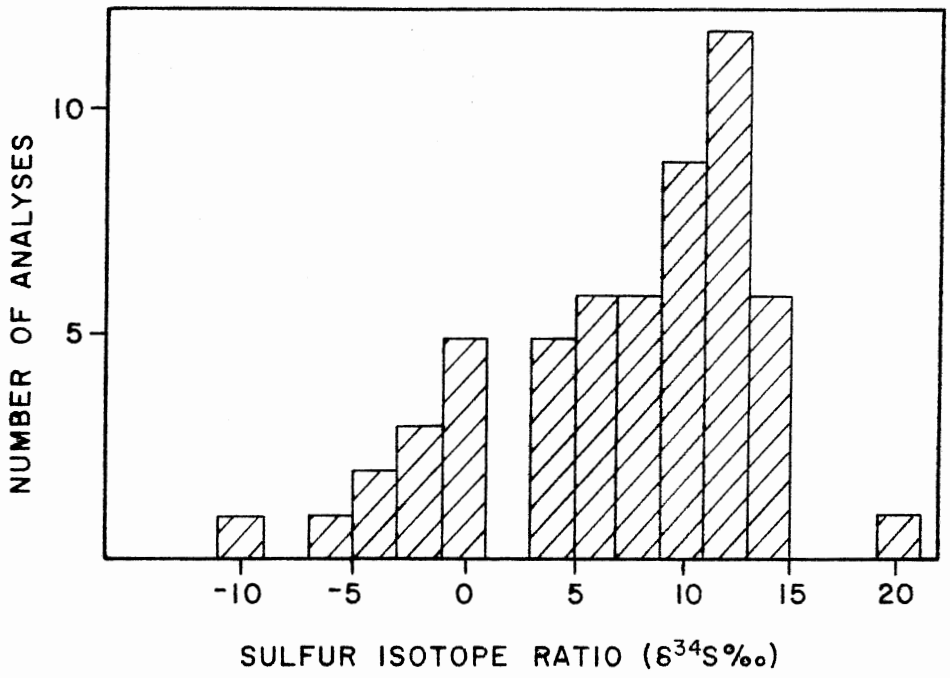

Fig. 32.--Frequency distribution for δS^{34} from H_2S gas associated with petroleum (after Goldhaber et al., 1978).

Results and Interpretations

Two pyrite samples and one anhydrite sample, collected from the subsurface, were analyzed for sulfur isotope composition. The pyrite samples were from upper Minnelusa sandstones in the Raven Creek and Reel oil fields. The anhydrite sample was also collected from the study area. Table II lists the results of sulfur isotope analyses. The frequency distribution of δS^{34} values of pyrite samples is shown in Figure 33.

Source of Sulfur in Oil. The ranges in δS^{34} values of Paleozoic oils from the Wind River and Big Horn basins, respectively, are -7.6 to +7.5‰ (Vredenburgh and Cheney, 1971) and -6.2 to +8.1‰ (Orr, 1974). It is suggested that oils from Paleozoic strata in the Powder River basin exhibit a similar range, although this has not been documented in the literature. It has been demonstrated that oil from the study area is similar in composition to Orr's (1974) Type II oil in the Big Horn basin. Therefore, oil from the study area should have a δS^{34} value approximately equal to that of Type II oils. The mean δS^{34} value for Type II oils in the Big Horn basin is -0.1‰. Using published data Orr (1974) determined that the mean δS^{34} value of Permian sulfate in Wyoming is +11.7‰. The δS^{34} value of anhydrite in the study area (+14.2‰) occurs within the range from which this mean was derived.

In comparing δS^{34} values of contemporaneous marine anhydrite and petroleum, ranging in age from Silurian to Permian, Thode and Monster (1965) found the δS^{32} in petroleum to be enriched by approximately 15‰. In their study of Wind River basin Permian oils, Vredenburgh and Cheney (1971) found this difference to be 20‰. This enrichment was attributed to the action of sulfate reducing bacteria

TABLE II

δS^{34} DISTRIBUTION IN PYRITE AND ANHYDRITE, AND δC^{13} AND δO^{18} DISTRIBUTION IN DOLOMITE

Well Number	Sample Number	Sample Description	δS^{34}	δC^{13}	δO^{18}
Govt F12-6-G	C-4	dolomite cement		+2.1	+23.7
Krause F21-2-P	C-9	dolomite cement		+0.5	+19.8
	C-11	dolomite bed		-3.6	+34.7
Krause F23-2-P	C-14	pyrite	+8.9		
Krause F32-3-P	C-10	dolomite cement		+2.9	+27.8
State F34-16-S	C-7	dolomite cement		+0.9	+22.4
	C-12	dolomite bed		-4.8	+33.9
Reel 1	C-3	pyrite	-3.5		
	C-5	dolomite cement		+2.1	+32.6
	C-13	anhydrite bed	+14.2		
Krause F14-34-P	C-8	dolomite cement		+2.7	+26.5
Krause F34-34-P	C-6	dolomite cement		+2.5	+25.9

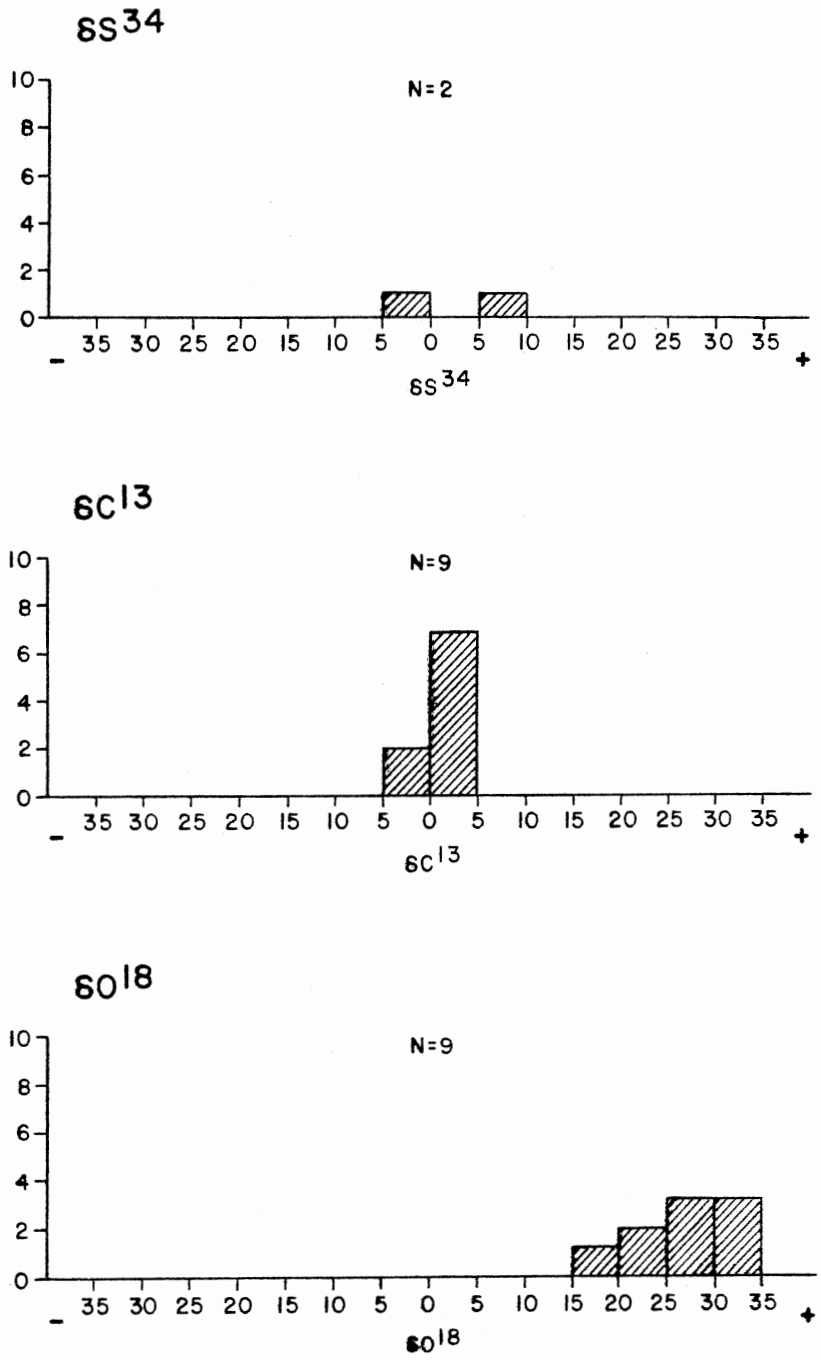

Fig. 33.--Frequency distribution of δS^{34}, δC^{13}, and δO^{18} from samples of pyrite and dolomite from the upper Minnelusa.

during deposition of source rocks and subsequent formation of petroleum. For the purpose of this study, it is assumed that the average δS^{34} value of the crude oil in the Raven Creek and Reel fields and Permian sulfates from the source area are -0.1‰ and +11.7‰, respectively. The difference in these values indicates that some degree of isotopic fractionation has resulted from thermal maturation. This conclusion is consistent with the evidence previously submitted in support of thermal maturation in the Powder River basin.

Source of Sulfur in Pyrite. Although no hydrogen sulfide samples were collected from the study area, the δS^{34} value of the gas is assumed to approximate the value of hydrogen sulfide associated with Type II oils in the Big Horn basin, or +5.9‰. Price and Shieh (1979) have shown that pyrite inorganically synthesized during the reaction of hydrogen sulfide and goethite in aqueous media at approximately 25°C, has the same isotopic composition as the hydrogen sulfide. Therefore, comparing the average value of δS^{34} of sulfur in the pyrite (+2.7%) and of sulfur in the hydrogen sulfide gas associated with Type II oil strongly suggests that the hydrogen sulfide associated with the oil is the source of sulfur in pyrite.

Orr (1974) suggested that at temperatures below 50°C microbial sulfate reduction is a common source of hydrogen sulfide gas in petroleum reservoirs, and that the contribution of hydrogen sulfide to the system by this process is negligible above approximately 60°C. McNab et al. (1952) demonstrated that crude oil would not generate hydrogen sulfide through thermal-cracking within geologic time if it remained below 65°C. Orr (1974) suggested that at temperatures above 80 to 120°C

non-microbial sulfate reduction may occur.

The present reservoir temperature in the study area is approximately 80°C (Fig. 34). However, the hydrocarbons may have been subjected to much greater depths and temperatures than those at which they presently occur. Hydrogen sulfide may have been generated prior to remigration of hydrocarbons into the study area. This conclusion, in conjunction with the evidence previously presented in support of thermal maturation, indicates that hydrogen sulfide gas in the study area was not bacterially generated.

Carbon Isotopes

Theory

Carbon isotopic data has long been utilized in the study of petroleum. This technique has also been applied to carbonate formations and cements. Carbon isotopic analyses are reported in δ terminology. This is defined by the C^{13}/C^{12} abundance ratio in the sample compared to the standard ratio in the Chicago PDB, a Cretaceous belmenite from the Peedee Formation:

$$\delta C^{13} = \left[\frac{(C^{13}/C^{12})\ \text{Sample}}{(C^{13}/C^{12})\ \text{Standard}} - 1\right] \times 1000 \qquad (12)$$

Values are expressed in per mil (0/00).

Variations in the sources of carbon analyzed in previous investigations have yielded the following generalizations. Coal, kerogen, oil, and natural gas have a carbon source, in plants which show a distinct

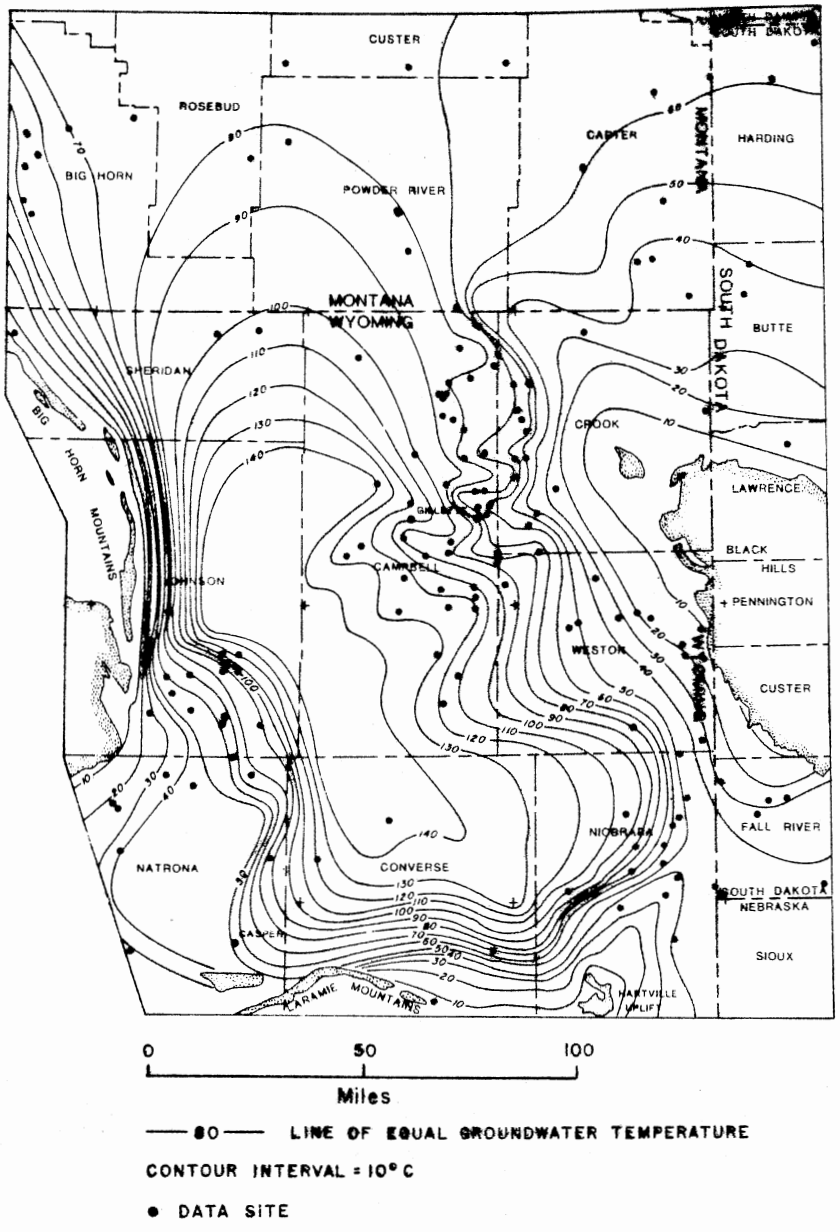

Fig. 34.--Ground water temperature in the Minnelusa Formation and equivalent strata (Head et al., 1979).

preference for the C^{12} isotope during photosynthesis (Murata et al., 1969). In contrast, carbonates formed in marine environments incorporate carbon from CO_2 in air or dissolved in water and show no isotopic preference. Carbonates that have been stabilized under meteoric water conditions contain carbon not only from the atmosphere but also from the CO_2 evolved during the decay of organic matter in soils.

The δC^{13} values of crude oils range between -22 and -33‰ (Smith, 1978). Methane associated with oil is isotopically lighter and has δC^{13} values that range from -35 to -55‰, while natural gas, which is composed chiefly of methane, has values that range from approximately -90 to -25‰ (Kirkland and Evans, 1976). Keith and Weber (1964) have demonstrated that the average δC^{13} values of marine and fresh-water carbonates, respectively, are +0.6 ± 2.8‰ and -4.9 ± 2.8‰. Carbonates whose major source of carbon is soil typically have δC^{13} values ranging from -9 to 12‰ (Salomons, 1975).

The occurrence of carbonate rocks and cements formed from the oxidation of hydrocarbons is well documented (Feely and Kulp, 1957; Hathaway and Degens, 1968; Mamchur, 1969; Donovan, 1974; Donovan and Dalziel, 1977; Lilburn, 1981). This mechanism involves the evolution of CO_2 which reacts with water to produce bicarbonate. The bicarbonate bonds with magnesium and calcium in the formation waters and a carbonate cement that has an isotopic signature matching the parent hydrocarbon is precipitated.

Results and Interpretations

Samples of diagenetic dolomite were analyzed for carbon isotope ratios in order to determine the origin of carbon and the carbonates

genetic relationship to a hydrocarbon source (Table II and Fig. 33). The mean value is +2.0‰. Values range from +0.5 to +2.9‰. Two samples from dolomite beds were analyzed for carbon isotope ratios. Their values are -3.6 and -4.8‰, with a mean value of -4.2‰.

Diagenetic dolomite is enriched in C^{13} and is probably not genetically related to hydrocarbon migration. The cement has about the same δC^{13} as marine carbonate. Hudson (1975) has suggested that late diagenetic carbonate cement forms during the compactional phase of burial diagenesis. This process involves the dissolution of carbonates originating in marine environments and their reprecipitation. Hudson (1975) noted that ancient limestones are fully cemented and that their isotopic compositions approximate those of modern carbonate sediments. Shales may be an important source of calcium carbonate for cementation of adjacent limestones and sandstones (Hudson, 1975).

An alternative hypothesis based on work by Murata et al. (1969) is proposed. It is possible to produce carbon isotopes in dolomite with values of +5‰ from methane with a δC^{13} value of -52‰ using an equilibration temperature of 80°C for methane-carbonate couplets as suggested by Bottinga (1968). However, evidence previously cited suggests that there are not sufficient volumes of methane associated with oil in the study area to allow such a mechanism to proceed.

The δC^{13} values of dolomite beds indicate that these units may have been subjected to diagenesis in the presence of meteoric formation waters. It was inferred from the formation water analysis that dolomite precipitation occurred in response to encroachment of meteoric waters. Diagenesis of dolomite beds may have occurred contemporaneously with dolomite precipitation in the sandstones. However, the mechanisms

involved in the contemporaneous formation of two types of dolomites in close proximity but with markedly different δC^{13} values cannot be explained. Keith and Weber (1964) suggested that the difference in δC^{13} values between marine and freshwater carbonates can be attributed to the contribution of carbon from land plants and humus which is deficient in C^{13}. Allan and Matthews (1977) observed Pleistocene limestones depleted in C^{13} as a result of subaerial diagenesis in the near-surface freshwater phreatic environment. Therefore, diagenesis of dolomite beds may have occurred very early in the diagenetic history of the upper Minnelusa.

Oxygen Isotopes

Theory

The oxygen isotopic composition of dolomite is expressed in terms of δ notation, which is defined by the O^{18}/O^{16} abundance ratio in the sample compared to the standard ratio of SMOW (standard mean oceanic water):

$$\delta O^{18} = \left[\frac{(O^{18}/O^{16})\ \text{Sample}}{(O^{18}/O^{16})\ \text{Standard}} - 1\right] \times 1000 \qquad (13)$$

with the values reported in per mil (0/00). In the literature the PDB standard has also been used to report the isotopic composition of oxygen in dolomite. This has resulted in two sets of numbers which are converted by means of the following equation (Land, 1980):

$$\delta_{SMOW} = 1.03086\delta_{PDB} + 30.86 \qquad (14)$$

Because the oxygen isotopes of carbonates are acquired from their depositional waters, the isotopic composition of dolomite is used to characterize the diagenetic fluid that has reacted with the formation (Land et al., 1975). Oxygen isotopes indicate whether the water had a fixed isotopic composition and temperature or if there was more than one episode of dolomite precipitation from different waters. Three factors are largely responsible for the isotopic composition of dolomite: (1) temperature of the depositional water, (2) mixing of waters, and (3) hydrocarbon induced evaporation of formation waters (Donovan and Dalziel, 1977; Goldhaber et al., 1979).

Epstein and Mayeda (1953) demonstrated that sea water has a constant isotopic composition of 0 ± 1 relative to SMOW. Because H_2O^{16} has a higher vapor pressure than H_2O^{18}, isotopic fractionation during the evaporation of sea water results in the depletion of O^{18}. The isotopic composition of water is latitude dependent, a factor governed largely by temperature.

The δO^{18} value of PDB calcite is +30.86‰. The δO^{18} values of Holocene marine limestones range from +28 to +30‰ (Faure, 1977). However, δO^{18} values decrease with increasing geologic age to approximately +20‰ for rocks of Cambrian age (Keith and Weber, 1964).

Murata et al. (1969) determined that δO^{18} values of freshwater and diagenetic carbonate vary from +9 to +36‰. Moore and Druckman (1981) suggested that carbonates precipitated under meteoric water conditions generally have δO^{18} values ranging from +25.7 to +30.9‰. Keith and Weber (1964) concluded that the average δO^{18} value for freshwater limestone is +21.9‰.

Mixing with brines or with meteoric waters can alter the δO^{18} composition of a subsurface carbonate forming solution (Donovan and Dalziel, 1977). Formation waters are often characterized by an enrichment in O^{18} (Clayton et al., 1966). The decrease in δO^{18} values with increasing age results in a complementary O^{18} enrichment in the formation water (Faure, 1977). The partial evaporation of pore water and isotopic equilibration with minerals in the surrounding rock are believed to be responsible for this enrichment.

Gas-induced evaporation of ground water can result in an enrichment in O^{18} in formation waters (Mills and Wells, 1919; Nisle, 1941; Donovan, 1972). This process is related to the expansion and separation from solution of natural gas as it ascends through ground water. The differing vapor pressures of H_2O^{18} and H_2O^{16} result in selective evaporation.

Results and Interpretations

Dolomite beds and dolomite cement in sandstone were analyzed for oxygen isotope ratios in order to determine the nature of their depositional waters (Table II). Figure 33 shows the frequency distribution of δO^{18} values. The δO^{18} values of the cement range from +19.8 to +32.7‰ with a mean value of +25.5‰. The δO^{18} values of samples from dolomite beds are +33.9 and +34.7‰, with a mean value of +34.3‰. The difference in the mean values indicates that the dolomite cement and the dolomite beds were formed in waters having markedly different isotopic compositions (Fig. 35).

The δO^{18} values of the dolomite cement are contradictory to what would be expected if gas-induced evaporation had a major influence on

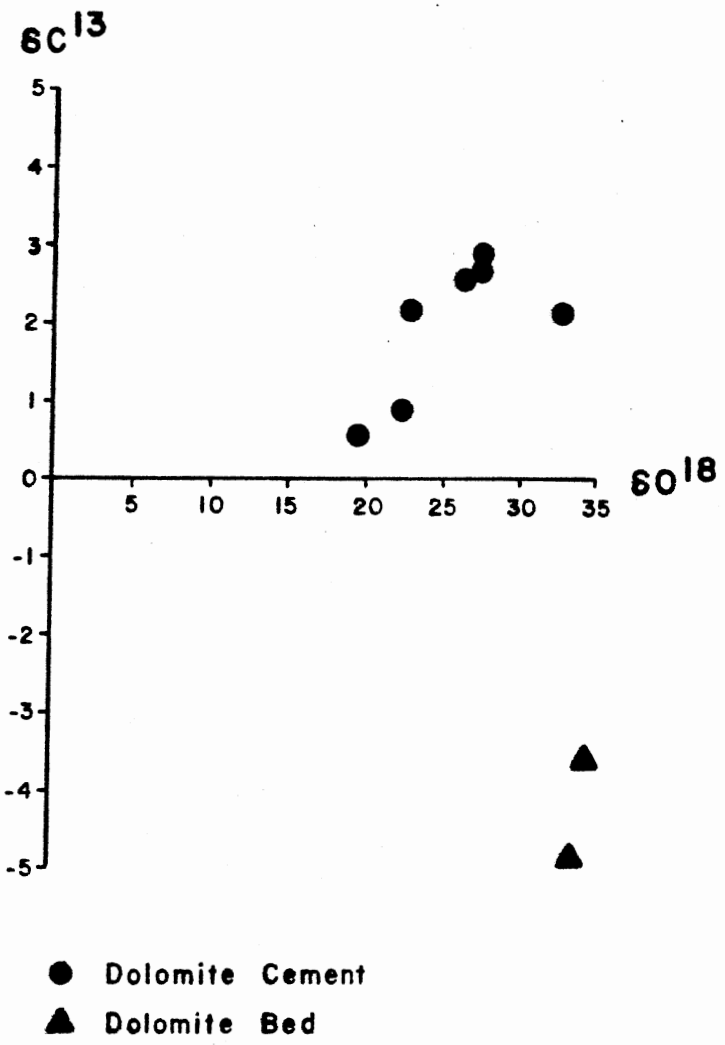

Fig. 35.--Relationship between δC^{13} and δO^{18} values of dolomite in the upper Minnelusa.

the isotopic compositon of the formation water. In addition, the driving force for this mechanism, gas related to petroleum, is notably absent in the study area. These lines of evidence suggest that hydrocarbon migration did not appreciably alter the isotopic composition of oxygen in the formation water.

The equilibrium value of δO^{18} for dolomite forming at 25°C probably ranges from +31.9 to +38.1‰. However, these values should decrease with increasing temperature (Land, 1980). Choquette (1971) noted the occurrence of ferroan dolomite cement with a δO^{18} value of +24.5‰. It was suggested that the cement originated late in diagenesis at advanced stages of induration and burial, and in the presence of heated and reducing subsurface waters. The ferroan dolomite cement in upper Minnelusa sandstones may have precipitated in a similar environment from water with approximately the same isotopic composition.

Dolomite beds in the study area are enriched in O^{18}. Lloyd (1966) predicted that the δO^{18} value of brines originating by evaporation in humid coastal environments would be increased to a maximum of +6‰. Dolomite beds in the study area were formed in waters having a δO^{18} value of approximately +3.3‰. The depositional environment in which these beds formed would probably have been conducive to O^{18} enrichment by evaporation of lagoonal or interdunal pond waters. Diagenesis subsequent to deposition did not appreciably alter the isotopic composition of oxygen.

CHAPTER VI

CONCLUSIONS

The upper member of the Minnelusa Formation in the Raven Creek and Reel oil fields in the Powder River basin consists of a sequence of interbedded sandstones, dolomites, and anhydrites of Wolfcampian age. This sequence was deposited in eolian and associated sabkha environments. Minnelusa sandstones are predominately moderate to well sorted, fine- to very fine-grained quartz arenites.

The dominant modifications of original depositional fabric are porosity reduction by the formation of authigenic anhydrite, dolomite, clay, and silica, and porosity enhancement by the dissolution of anhydrite. Saturations in the formation waters with respect to anhydrite-gypsum and dolomite increase with increasing distance from the productive Minnelusa trend, suggesting that the degree of sandstone cementation increases away from the trend.

Hydrocarbon migration had a limited influence on diagenetic mineralization in upper Minnelusa sandstones in the Raven Creek and Reel oil fields. Alteration of sandstones by hydrogen sulfide gas associated with petroleum resulted in the formation of disseminated euhedral pyrite crystals. The formation of pyrite resulted from the reduction of iron oxide by hydrogen sulfide. Petroleum in the study area is assumed to have been derived from the same source and subjected to a similar thermal history as petroleum from Tensleep reservoirs in the Big Horn basin.

Sulfur isotopes from hydrogen sulfide gas associated with petroleum from the Tensleep in the Big Horn basin and sulfur isotopes from diagenetic pyrite in the study area show a close relationship.

Carbon and oxygen isotopes indicate that dolomite cement formed late in diagenesis at advanced stages of burial, in the presence of heated and reducing subsurface waters, and that this cement did not form in response to hydrocarbon migration.

BIBLIOGRAPHY

Agatston, R. S., 1954, Pennsylvanian and Lower Permian of northern and eastern Wyoming: Am. Assoc. Petroleum Geologists Bull., v. 38, p. 508-583.

Allan, J. R., and R. K. Matthews, 1977, Carbon and oxygen isotopes as diagenetic and stratigraphic tools: Surface and subsurface data, Barbados, West Indies: Geology, v. 5, p. 16-20.

Al-Shaieb, Z., and J. W. Shelton, 1978, Secondary ferroan dolomite rhombs in oil reservoirs, Chadra sands, Gialo field, Libya: Am. Assoc. Petroleum Geologists Bull., v. 62, p. 463-468.

Armstrong, F. C., and E. R. Cressman, 1963, The Bannock thrust zone, southeastern Idaho: U.S. Geol. Survey Prof. Paper 374-J, 22 p.

Ball, J. S., and R. H. Espach, 1948, Crude oils in Wyoming: Petroleum Eng., v. 20, p. 229-234.

Barbat, W. N., 1967, Crude-oil correlations and their role in exploration: Am. Assoc. Petroleum Geologists Bull., v. 51, p. 1255-1292.

Barkley, C. J., and R. F. Gosman, 1958, Donkey Creek area, Crook County, Wyoming: Wyoming Geol. Assoc. Guidebook, 13th Ann. Field Conf., p. 174-179.

Berg, R. R., 1963, Powder River's Minnelusa play: Oil and Gas Jour., June 3, p. 168-176.

Berg, R. R., and C. S. Tenney, 1967, Geology of Lower Permian Minnelusa oil fields, Powder River basin, Wyoming: Am. Assoc. Petroleum Geologists Bull., v. 51, p. 705-709.

Berner, R. A., 1971, Principles of chemical sedimentology: New York, McGraw-Hill, 240 p.

Blackstone, D. L., Jr., 1963, Development of geologic structure in central Rocky Mountains: Am. Assoc. Petroleum Geologist Mem., v. 2, p. 160-179.

Blatt, H., 1979, Diagenetic processes in sandstones: Soc. Econ. Paleontologists and Mineralogists Spec. Pub. 26, p. 141-157.

Boles, J. R., and S. G. Franks, 1979, Clay diagenesis in Wilcox sandstones of southwest Texas: Implications of smectite diagenesis on sandstone cementation: Jour. Sed. Petrology, v. 49, p. 55-70.

Bottinga, Y., 1968, Isotopic fractionation in the system--calcite-graphite-carbon dioxide-methane-hydrogen-water: Ph.D. thesis, University of California, San Diego, 126 p.

Branson, C. C., 1939, Pennsylvanian formations of central Wyoming: Geol. Soc. America Bull., v. 50, p. 1199-1225.

Burk, C. A., and H. D. Thomas, 1956, the Goose Egg Formation (Permo-Triassic) of eastern Wyoming: Wyoming Geol. Survey Rept. Inv. 6, 11 p.

Cheney, E. S., 1964, Stable isotopic geology of the Gas Hills Uranium District, Wyoming: Ph.D. thesis, Yale University, 342 p.

Cheney, T. M., and R. P. Sheldon, 1959, Permian stratigraphy and oil potential, Wyoming and Utah: Intermountain Assoc. Petroleum Geologists, 10th Ann. Field Conf., p. 90-100.

Choquette, P. W., 1971, Late ferroan dolomite cement, Mississippian carbonates, Illinois basin: in O. P. Bricker (ed.), Carbonate cements: John Hopkins Univ. Studies Geology 19, p. 339-346.

Claypool, G. E., A. H. Love, and E. K. Maughan, 1978, Organic geochemistry, incipient metamorphism, and oil generation in black shale members of Phosphoria Formation, Western Interior, United States: Am. Assoc. Petroleum Geologists Bull., v. 62, p. 98-120.

Clayton, R. N., et al., 1966, The origin of saline formation waters-I, isotopic composition: Jour. Geophys. Research, v. 71, p. 3869-2882.

Coleman, M. L., 1975, The application of sulphur isotope geochemistry to oil, gas, and ore studies; a review: in M. L. Coleman and G. R. Davis (eds.), Proceedings of the forum on oil and ore in sediments: London, Imperial College, p. 53-92.

Curtis, B. F., J. W. Strickland, and R. C. Busby, 1958, Patterns of oil occurrence in the Powder River basin, Wyoming: in Habitat of oil, Am. Assoc. Petroleum Geologists, p. 268-292.

De Groot, K., 1973, Geochemistry of tidal flat brines at Umm Said, SE Qatar, Persian Gulf: in B. H. Purser (ed.), The Persian Gulf: New York, Springer-Verlag, p. 377-394.

Donovan, T. J., 1972, Surface mineralogical and chemical evidence for buried hydrocarbons, Cement field, Oklahoma: Ph.D. thesis, University of California, Los Angeles, 117 p.

Donovan, T. J., 1974, Petroleum microseepage at Cement, Oklahoma: Evidence and mechanism: Am. Assoc. Petroleum Geologists Bull., v. 58, p. 429-446.

Donovan, T. J., and M. C. Dalziel, 1977, Late diagenetic indicators of buried oil and gas: U.S. Geol. Survey Open-File Rept. 77-817, 44 p.

Epstein, S., and T. Mayeda, 1953, Variation of O^{18} content of waters from nautral sources: Geochim. et Cosmochim. Acta, v. 4, p. 225-240.

Faure, G. 1977, Principles of isotope geology: New York, John Wiley and Sons, 464 p.

Feely, H. W., and J. L. Kulp, 1957, Origin of Gulf Coast salt-dome deposits: Am. Assoc. Petroleum Geologists Bull., v. 41, p. 1802-1853.

Ferguson, J. D., 1977, The subsurface alteration and mineralization of Permian red beds overlying several oil fields in southern Oklahoma: M.S. thesis, Oklahoma State University, 95 p.

Foster, D. I., 1958, Summary of the stratigraphy of the Minnelusa Formation, Powder River basin, Wyoming: Wyoming Geol. Assoc. Guidebook, 13th Ann. Field Conf., p. 39-44.

Gaffney, J. S., E. T. Premuzic, and B. Manowitz, 1979, On the usefulness of sulfur isotope ratios in crude oil correlations: Geochim. et Cosmochim. Acta, v. 44, p. 135-139.

Glaze, R. E., and E. R. Keller, (co-chairmen Wyo. Geol. Assoc. Tech. Studies Committee), 1965, Geologic history of the Powder River basin: Am. Assoc. Petroleum Geologists Bull., v. 49, p. 1893-1907.

Goldhaber, M. B., and I. R. Kaplan, 1975, Apparent dissociation constants of hydrogen sulfide in chloride solutions: Marine Chemistry, v. 3, p. 83-104.

Goldhaber, M. B., R. L. Reynolds, and R. O. Rye, 1978, Origin of a south-Texas roll-type uranium deposit: I Sulfide petrology and sulfur isotope studies: Econ. Geology, v. 73, p. 1690-1705.

Goldhaber, M. B., R. L. Reynolds, R. O. Rye, and R. I. Grauch, 1979, Petrology and isotope geochemistry of calcite in a south-Texas roll-type uranium deposit: U.S. Geol. Survey Open-File Rept. 79-828, 21 p.

Gussow, W. C., 1954, Differential entrapment of oil and gas, a fundamental principle: Am. Assoc. Petroleum Geologists Bull., v. 38, p. 816-853.

Harrison, A. G., and H. G. Thode, 1958, Sulfur isotope abundances in hydrocarbons and source rocks of Uinta basin, Utah: Am. Assoc. Petroleum Geologists Bull., v. 42, p. 2642-2649.

Hathaway, J. C., and E. T. Degens, 1968, Methane-derived marine carbonates of Pleistocene age: Science, v. 165, p. 690-692.

Head, W. J., K. T. Kilty, and R. K. Knottek, 1979, Maps showing formation temperatures and configurations of the tops of the Minnelusa Formation and the Madison Limestone, Powder River basin, Wyoming, Montana, and adjacent areas: U.S. Geol. Survey Misc. Inv. Series, Map I-1159.

Hem, J. D., and W. H. Cropper, 1959, Survey of ferrous-ferric chemical equilibria and redox potentials: U.S. Geol. Survey Water-Supply Paper 1459-A, 31 p.

Henbest, L. G., 1954, Pennsylvanian foraminifera in Amsden Formation and Tensleep Sandstone, Montana and Wyoming: Billings Geol. Soc. Guidebook, 5th Ann. Field Conf., p. 50-53.

Henbest, L. G., 1956, Foraminifera and correlation of Pennsylvanian age in Wyoming: Wyoming Geol. Assoc. Guidebook, 11th Ann. Field Conf., p. 58-63.

Hower, J., et al., 1976, Mechanisms of burial, Part I mineralogical and chemical evidence: Geol. Soc. America Bull., v. 87, p. 725-737.

Hubbell, R. G., and J. M. Wilson, 1963, Lance Creek field, Niobrara County, Wyoming: Rocky Mountain Assoc. Geologists Guidebook, 14th Field Conf., p. 248-257.

Hudson, J. D., 1975, Carbon isotopes and limestone cement: Geology, v. 3, p. 19-22.

Hudson, R. E., 1963, Halverson Ranch field, Minnelusa production, Campbell County, Wyoming: Billings Geol. Soc. and Wyoming Geol. Assoc. Guidebook, 1st Joint Field Conf., p. 123-124.

Hunt, J. M., 1953, Composition of crude oil and its relation to stratigraphy in Wyoming: Am. Assoc. Petroleum Geologists Bull., v. 37, p. 1837-1872.

Hyden, H. J., 1961, Distribution of uranium and other metals in crude oils: U.S. Geol. Survey Bull. 1100-B, p. 17-99.

Katz, A., 1971, Zoned dolomite crystals: Jour. Geology, v. 79, p. 38-51.

Keefer, W. R., 1969, Geology of petroleum in Wind River basin, central Wyoming: Am. Assoc. Petroleum Geologists Bull., v. 53, p. 1839-1865.

Keith, M. L., and J. N. Weber, 1964, Carbon and oxygen isotopic composition of selected limestones and fossils: Geochim. et Cosmochim. Acta, v. 28, p. 1787-1816.

Kinnison, P. T., 1971, Future petroleum potential of Powder River basin, southeastern Montana and northeastern Wyoming: Am. Assoc. Petroleum Geologists Mem. 15, p. 591-612.

Kirkland, D. W., and R. Evans, 1976, Origin of limestone buttes, Gypsum Plain, Culberson County, Texas: Am. Assoc. Petroleum Geologists Bull., v. 60, p. 2005-2018.

Krouse, H. R., 1977, Sulfur isotope studies and their role in petroleum formation: Jour. Geochem. Exploration, v. 7, p. 189-211.

Land, L. S., 1980, The isotopic and trace element geochemistry of dolomite: The state of the art: Soc. Econ. Paleontologists and Mineralogists Spec. Pub. 28, p. 87-110.

Land, L. S., M. R. I. Salem, and D. W. Morrow, 1975, Paleohydrology of ancient dolomites: Geochemical evidence: Am. Assoc. Petroleum Geologists Bull., v. 59, p. 1602-1625.

Lilburn, R. A., 1979, Mineralogical, geochemical, and isotopic evidence of diagenetic alteration, attributable to hydrocarbon migration, Cement-Chickasha field, Oklahoma: M.S. thesis, Oklahoma State University, 88 p.

Lloyd, R. M., 1966, Oxygen isotope enrichment of seawater by evaporation: Geochim. et Cosmochim. Acta, v. 30, p. 801-814.

Love, J. D., P. O. McGrew, and H. D. Thomas, 1963, Relationship of latest Cretaceous and Tertiary deposition and deformation to oil and gas in Wyoming: Am. Assoc. Petroleum Geologist Mem. 2, p. 196-208.

Mallory, W. W., 1967, Pennsylvanian and associated rocks in Wyoming: U. S. Geol. Survey Prof. Paper 554-G, 31 p.

Mamchur, G. P., 1969, Isotopic composition of carbon in calcite paragenetic with sulfur: Geochem. International, v. 6, p. 660-670.

Mankiewicz, D., and J. R. Steidtmann, 1979, Depositional environments and diagenesis of the Tensleep Sandstone, eastern Big Horn basin: Soc. Econ. Paleontologist and Mineralogist Spec. Pub. 26, p. 319-336.

Maughan, E. K., 1975, Organic carbon in shale beds of the Permian Phosphoria Formation of eastern Idaho and adjacent states-a summary report: Wyoming Geol. Assoc. Guidebook, 27th Ann. Field Conf., p. 107-115.

Maughan, E. K., 1978, Pennsylvanian (Upper Carboniferous) System in Wyoming: U.S. Geol. Survey Open-File Rept. 78-377, 32 p.

McKelvey, V. E., R. W. Swanson, and R. P. Sheldon, 1953, The Permian phosphorite deposits of western United States: Internat. Geol. Cong., 19th, Algiers, 1952, Comptes rendus, sec. 11, pt. 11, p. 45-64.

McKelvey, V. E., et al., 1959, The Phosphoria, Park City, and Shedhorn Formations in the western phosphate field: U.S. Geol. Survey Prof. Paper 313-A, 47 p.

McNab, J. G., P. V. Smith, and R. L. Betts, 1952, The evolution of petroleum: Indust. and Eng. Chemistry, v. 44, p. 2556-2563.

Mettler, D., and R. C. Roehrs, 1968, Minnelusa: where next?: Oil and Gas Jour., Jan. 8, p. 96-100.

Mills, R. V. A., and R. C. Wells, 1919, The evaporation and concentration of waters associated with petroleum and natural gas: U.S. Geol. Survey Bull. 693, 104 p.

Momper, J. A., and J. A. Williams, 1979, Geochemical exploration in the Powder River basin: Oil and Gas Jour., Dec. 10, p. 129-134.

Monster, J., 1972, Homogeneity of sulfur and carbon isotope ratios S^{34}/S^{32} and C^{13}/C^{12} in petroleum: Am. Assoc. Petroleum Geologists Bull., v. 56, p. 941-949.

Moore, C. H., and Y. Druckman, 1981, Burial diagenesis and porosity evolution, Upper Jurassic Smackover, Arkansas and Louisiana: Am. Assoc. Petroleum Geologists Bull., v. 65, p. 597-628.

Murata, K. J., I. Friedman, and B. M. Madsen, 1969, Isotopic composition of diagenetic carbonates in marine Miocene formations of California and Oregon: U.S. Geol. Survey Prof. Paper 614-B, 24 p.

Nisle, R. G., 1941, Considerations on the vertical migration of gases: Geophysics, v. 6, p. 449-454.

Orr, W. L., 1974, Changes in sulfur content and isotopic ratios of sulfur during petroleum maturation-Study of Big Horn basin Paleozoic oils: Am. Assoc. Petroleum Geologists Bull., v. 58, p. 2295-2318.

Pankina, R. G., and V. L. Mekhtiyeva, 1964, The isotopic composition of sulfur in the hydrogen sulfide of natural gas of the Bobrikova zone in the Volga-Urals: Geokhimiya, v. 9, p. 866-871.

Parker, C. A., 1973, Geopressures in the deep Smackover of Mississippi: Jour. Petroleum Tech., v. 25, p. 971-979.

Plummer, L. N., B. F. Jones, and A. H. Truesdell, 1976, WATEQF-A-FORTRAN IV version of WATEQ, a computer program for calculating chemical equilibria of natural waters: U.S. Geol. Survey Water Resources Inv. 76-13, 61 p.

Price, F. T., and Y. N. Shieh, 1979, Fractionation of sulfur isotopes during laboratory synthesis of pyrite at low temperatures: Chem. Geology, v. 27, p. 245-253.

Reynolds, R. L., and M. B. Goldhaber, 1978, Origin of a south-Texas roll-type uranium deposit: I. Alteration of iron-titanium oxide minerals: Econ. Geology, v. 73, p. 1677-1689.

Robinson, C. S., W. J. Mapel, and M. H. Bergendahl, 1964, Stratigraphy and structure of the northern and western flanks on the Black Hills uplift, Wyoming, Montana, and South Dakota: U.S. Geol. Survey Prof. Paper 404, 134 p.

Sales, J. K., 1968, Regional tectonic setting and mechanics of origin of the Black Hills uplift: Wyoming Geol. Assoc. Guidebook, 20th Ann. Field Conf., p. 10-27.

Salomons, W., 1975, Chemical and isotopic composition of carbonates in recent sediments and soils from Western Europe: Jour. Sed. Petrology, v. 45, p. 440-449.

Schreiber, B. C., G. M. Friedman, A. Decima, and E. Schreiber, 1976, Depositional environments of Upper Miocene (Messinian) evaporite deposits of the Sicilian basin: Sedimentology, v. 23 p. 729-760.

Sheldon, R. P., 1963, Physical stratigraphy and mineral resources of Permian rocks in western Wyoming: U.S. Geol. Survey Prof. Paper 313-B, 273 p.

Sheldon, R. P., 1967, Long-distance migration of oil in Wyoming: Mountain Geologist, v. 4, p. 53-65.

Shvartsev, S. L., and V. A. Bazhenov, 1978, Geochemical conditions for the formation of illite in weathering crust products: Geochem. International, v. 15, p. 49-56.

Slack, P. B., 1981, Paleotectonics and hydrocarbon accumulation, Powder River basin, Wyoming: Am. Assoc. Petroleum Geologists Bull., v. 65, p. 730-743.

Smith, H. M., 1940, Correlation index to aid in interpreting crude-oil analyses: U.S. Bureau Mines Tech. Paper 610, 34 p.

Smith, J. W., 1978, Carbonates-a guide to hydrocarbons: Jour. Geochem. Exploration, v. 14, p. 103-107.

Stanley, K. O., and L. V. Benson, 1979, Early diagenesis of High Plains Tertiary vitric and arkosic sandstone, Wyoming and Nebraska: Soc. Econ. Paleontologists and Mineralogists Spec. Pub. 26, p. 401-423.

Stokes, W. L., 1968, Multiple parallel-truncation bedding planes - A feature of wind deposited sandstone formations: Jour. Sed. Petrology, v. 38, p. 510-515.

Stone, D. S., 1967, Theory of Paleozoic oil and gas accumulation in Big Horn basin, Wyoming: Am. Assoc. Petroleum Geologists Bull., v. 51, p. 2056-2114.

Stone, W. J., 1969, Stratigraphy of the Minnelusa Formation along western and northern flanks of the Black Hills, Wyoming and South Dakota: M.S. thesis, Kent State University, 254 p.

Strickland, J. W., 1958, Habitat of oil in the Powder River basin: Wyoming Geol. Assoc. Guidebook, 13th Ann. Field Conf., pp. 132-147.

Tenney, C. S., 1966, Pennsylvanian and Lower Permian deposition in Wyoming and adjacent areas: Am. Assoc. Petroleum Geologists Bull., v. 50, p. 227-250.

Thode, H. G., and J. Monster, 1964, Sulfur-isotope geochemistry of petroleum, evaporites, and ancient seas: Am. Assoc. Petroleum Geologists Mem. 4, p. 367-377.

Thode, H. G., and J. Monster, 1970, Sulfur isotope abundances and genetic relations of oil accumulations in Middle East basin: Am. Assoc. Petroleum Geologists Bull., v. 54, p. 627-637.

Thode, H. G., J. Monster, and H. B. Dunford, 1958, Sulfur isotope abundances in petroleum and associated materials: Am. Assoc. Petroleum Geologists Bull., v. 42, p. 2619-2641.

Thomas, H. D., 1963, Geologic history and structure of Wyoming: in Wyoming oil and gas fields, Wyoming Geol. Assoc., p. 15-23.

Tranter, C., 1963, Raven Creek field, Campbell County, Wyoming: Billings Geol. Soc. and Wyoming Geol. Assoc. Guidebook, 1st Joint Field Conf., p. 143-146.

Tranter, C. E., and C. K. Petter, 1963, Lower Permian and Pensylvanian stratigraphy of the northern Rocky Mountains: Billings Geol. Soc. and Wyoming Geol. Assoc. Guidebook, 1st Joint Field Conf., p. 45-53.

Tranter, C. E., and C. W. Kerns, 1972, Raven Creek field, Campbell County, Wyoming: Am. Assoc. Petroleum Geologists Mem. 16, p. 511-519.

Trotter, J. F., 1963, The Minnelusa play of the northern Powder River, Wyoming and adjacent areas: Billings Geol. Soc. and Wyoming Geol. Assoc. Guidebook, 1st Joint Field Conf., p. 117-122.

Truesdell, A. H., and B. F. Jones, 1975, WATEQ, a computer program for calculating chemical equilibria of natural waters: U.S. Geol. Survey Jour. Research, v. 2, p. 233-248.

Van West, F. P., 1972, Trapping mechanisms of Minnelusa oil accumulations, northeastern Powder River basin, Wyoming: Mountain Geologist, v. 9, p. 3-20.

Verville, G. J., 1957, Wolfcampian fusulinids from the Tensleep Sandstone in the Big Horn Mountains, Wyoming: Jour. Paleontology, v. 31, p. 349-352.

Vredenburgh, L. D., 1968, Sulfur isotopic investigation of petroleum, Wind River basin, Wyoming: Ph.D. thesis, University Washington, 108 p.

Vredenburgh, L. D., and E. S. Cheney, 1971, Sulfur and carbon isotopic investigation of petroleum, Wind River basin, Wyoming: Am. Assoc. Petroleum Geologists Bull., v. 55, p. 1954-1975.

Wells, D. K., J. F. Busby, and K. C. Glover, 1979, Chemical analyses of water from the Minnelusa Formation and equivalents in the Powder River basin and adjacent areas, northeastern Wyoming: Wyoming Water Planning Program Rept. 18, 27 p.

Wenger, W. J., and B. W. Reid, 1958, Characteristics of petroleum in the Powder River basin: Wyoming Geol. Assoc. Guidebook, 13th Ann. Field Conf., p. 148-156.

West, W. E. Jr., 1964, The Powder River basin: Wyoming Geol. Assoc. Tech. Studies Committee, Highway Geol. Wyoming, p. 22-28.

Yeremenko, N. A., and R. G. Pankina, 1962, Isotopes of sulfur in oil and gas field of the Volga-Ural regions of the Soviet Union: Geol. Nefti Gaza, v. 6, p. 554-560.

APPENDIX A

COMPOSITION OF SANDSTONES FROM THIN-SECTION EXAMINATION AND X-RAY DIFFRACTION ANALYSIS

TABLE III

COMPOSITION OF SANDSTONES (THIN SECTION)

Well Number	Sample Number	Quartz	Feldspar	Mica	Anhydrite	Dolomite	Clays	Pyrite	Misc.
Government									
F12-6-G	8058B-22	76	tr	--	2	22	ob	--	ob-Z
Krause	8352B-53	78	2	tr	12	8	ob	--	--
F12-2-P	8340B-25	79	1	tr	3	17	tr	tr	--
Krause	8349B-6	75	1	tr	19	5	tr	tr	--
F21-2-P	8530B-55	69	1	tr	13	17	ob	--	ob-Z
	8595B-14	71	3	tr	2	24	--	--	ob-Z
Krause	8348B-64	83	1	tr	3	13	--	tr	--
F23-2-P	8370B-19	82	1	tr	5	12	--	tr	--
Krause	8373B-50	80	1	tr	7	12	tr	--	tr-C
F41-3-P	8390B-49	75	2	tr	8	15	tr	--	tr-C
Krause	8385B-16	71	1	tr	5	23	--	--	--
F32-3-P	8394B-20	80	1	--	1	18	--	--	ob-Z
	8415B-57	83	3	tr	4	10	--	--	--
Talley 1	8655B-45	80	2	tr	1	17	--	ob	--
	8670B-44	85	1	tr	3	11	--	--	ob-Z
Krause	8425B-60	67	4	tr	17	12	--	--	--
C-1	8471B-26	85	1	--	2	12	--	tr	--
Krause	8370B-52	76	5	--	5	14	ob	--	tr-Z
F12-11-P	8388B-51	69	2	--	25	4	tr	--	tr-Z

TABLE III (Continued)

Well Number	Sample Number	Quartz	Feldspar	Mica	Anhydrite	Dolomite	Clays	Pyrite	Misc.
Krause F34-11-G	8340B-48	76	4	--	15	5	--	--	--
Clark	8491B-46	85	1	tr	2	12	--	ob	--
F-48-69-13-C4	8520B-47	80	3	tr	3	14	tr-K,I	--	--
Norman 1	8350B-38	87	3	--	23	6	tr	--	--
	8390B-39	71	4	tr	17	2	tr	--	ob-Z
	8430B-40	80	2	tr	13	1	tr	--	ob-Z
Government	8320B-41	77	2	tr	11	10	tr	tr	ob-Z
Bell 1	8360B-42	83	1	tr	9	7	ob	--	--
	8410B-43	77	2	tr	11	lo	tr	tr	ob-Z
Clark	8395B-37	50	1	tr	44	5	tr	tr	--
F-48-69-24-B1	8485B-36	81	2	tr	3	14	--	--	ob-Z
Pickrel	8995B-33	72	5	tr	13	10	tr	--	--
P-48-69-29-A4	9025B-32	80	2	tr	2	16	--	--	ob-Z
Bishop 1-31	9017B-21	78	1	tr	4	17	--	--	ob-Z
	9052B-54	69	1	tr	13	17	tr	--	ob-Z
Government	9380B-18	76	2	tr	21	1	--	--	ob-Z
Neuen. 1	9420B-58	80	2	--	5	13	--	--	--
State F34-16-S	8505B-63	76	1	--	14	9	--	--	--
Reel	8530B-61	75	1	tr	15	9	--	--	--
F14-21-P	8550B-10	79	1	tr	8	11	tr-I/S	--	--

TABLE III (Continued)

Well Number	Sample Number	Quartz	Feldspar	Mica	Anhydrite	Dolomite	Clays	Pyrite	Misc.
Reel 1	8467B-1	79	1	tr	16	3	--	1	tr-Z,T
	8484B-62	79	4	tr	2	15	--	--	--
Wolfe 1	8345B-31	77	4	tr	5	14	ob	--	ob-Z
	8385B-30	75	8	--	5	12	tr	--	--
Bryant P-49-69-27-A4	8459B-29	79	2	tr	3	16	ob	--	ob-C
Reel	8555B-34	77	1	--	8	14	--	--	--
Government 23-28A	8575B-35	77	6	tr	10	7	tr	--	--
Reel	8530B-28	75	2	tr	19	4	--	--	--
Government 21-28A	8550B-27	75	3	tr	5	17	ob	--	--
Krause F14-34-P	8480B-24	77	1	tr	7	15	ob	--	ob-Z
Krause	8405B-8	79	2	tr	3	16	tr-I/S	tr	tr-Z
F34-34-P	8435B-56	68	tr	tr	30	2	--	--	--
Government 14-1	9055B-59	68	tr	tr	30	2	--	--	--
Averages		77%	2%		10%	11%			

Note: tr = trace, ob = observed, I = illite, S = smectite, K = kaolinite, Z = zircon, T = tourmaline, C = chert.

TABLE IV

COMPOSITION OF SANDSTONES (X-RAY DIFFRACTION)

Well Number	Sample No.	Quartz	Feldspar	Anhydrite	Dolomite
Government F12-6-G	8054A-1	56	2	12	30
	8056A-2	84	2	1	30
	8056A-3	64	2	1	13
Krause F12-2-P	8348A-4	59	3	36	2
	8352A-5	81	1	16	2
	8354A-6	70	4	7	19
	8356A-7	80	2	2	16
	8358A-8	84	--	--	16
	8360A-9	70	--	27	3
	8362A-10	79	2	16	3
	8364A-11	69	1	19	11
	8366A-12	88	--	1	11
	8368A-13	71	1	13	15
	8380A-14	67	2	31	--
	8382A-15	76	2	9	13
	8386A-16	76	2	1	21
	8388A-17	94	2	--	4
	8390A-18	76	3	1	20
	8392A-19	83	3	2	12
Krause F21-2-P	8340A-20	83	3	12	2
	8350A-21	67	12	21	--
	8530A-22	84	2	--	14
	8550A-23	70	1	8	21
	8575A-24	75	1	--	24
	8585A-25	81	3	--	16
	8595A-26	78	4	7	11
	8610A-27	81	9	--	10
	8620A-28	56	1	8	35
	8636A-29	59	5	36	—
Krause F23-2-P	8348A-30	92	--	2	6
	8357A-31	94	2	--	4
	8367A-32	90	3	1	6
	8377A-33	85	3	--	12
	8383A-34	73	1	23	3
Krause F41-3-P	8365A-35	74	3	21	2
	8373A-36	78	1	18	3
	8391A-37	73	1	19	7
Krause F32-3-P	8385A-38	78	--	16	6
	8395A-39	88	1	1	10
	8405A-40	72	2	23	3
	8415A-41	87	3	4	6
Talley 1	8655A-42	89	--	1	10
	8660A-43	92	--	1	7
	8665A-44	74	3	22	1
	8670A-45	86	2	4	8

TABLE IV (Continued)

Well Number	Sample No.	Quartz	Feldspar	Anhydrite	Dolomite
Krause C-1	8425A-46	67	5	20	8
	8435A-47	68	13	15	4
	8446A-48	89	--	--	11
	8455A-49	86	--	14	--
	8465A-50	67	11	20	2
	8475A-51	79	4	14	3
	8485A-52	70	--	30	--
	8507A-53	55	--	32	13
Krause F12-11-P	8367A-54	82	--	--	18
	8370A-55	82	4	5	9
	8374A-56	80	5	10	5
	8379A-57	72	1	22	5
	8388A-58	64	3	30	3
Krause F34-11-G	8335A-59	77	6	13	4
	8349A-60	78	5	14	3
F-48-69-13-C4	8491A-61	91	--	1	8
	8520A-62	82	5	2	11
Norman 1	8350A-63	83	5	3	9
	8360A-64	57	--	41	2
	8370A-65	93	--	2	5
	8390A-66	65	3	30	2
	8402A-67	45	--	54	1
	8410A-68	71	6	14	9
	8420A-69	787	--	22	--
	8430A-70	81	3	16	--
Government Bell 1	8320A-71	76	4	14	6
	8350A-71	94	--	1	5
	8360A-73	90	--	5	5
	8370A-74	70	--	27	3
	8380A-75	61	2	35	2
	8390A-76	81	4	10	5
	8400A-77	80	--	2	18
	8410A-78	83	3	7	7
	8420A-79	83	3	5	9
	8395A-80	44	2	52	2
	8405A-81	68	--	31	1
	8485A-82	87	--	--	13
Pickrel P-48-69-29-A4	8995A-83	72	9	12	7
	9005A-84	91	2	6	1
	9015A-85	70	--	29	1
	9025A-86	78	--	5	17
Bishop 1-31	9019A-87	91	--	--	9
	9029A-88	88	4	--	8
	9039A-89	71	3	4	22
	9059A-90	82	--	--	18
	9064A-91	85	4	--	11
Government	9380A-92	63	--	37	--

TABLE IV (Continued)

Well Number	Sample No.	Quartz	Feldspar	Anhydrite	Dolomite
Neuenschwander 1	9390A-93	60	3	29	8
	9410A-94	73	6	11	10
	9420A-95	84	--	5	11
State F34-16-S	8485A-96	66	1	26	7
	8495A-97	67	--	14	19
	8505A-98	78	2	17	3
	8525A-99	78	5	10	7
	8535A-100	71	1	17	11
	8545A-101	55	2	21	22
Reel F14-21-P	8530A-102	73	--	12	15
	8540A-103	59	2	39	--
	8550A-104	67	7	8	18
	8560A-105	72	3	19	6
	8570A-106	57	1	39	3
Reel 1	8454A-107	94	2	--	4
	8464A-108	85	2	6	7
	8467A-109	68	3	28	1
	8474A-110	80	--	1	19
	8479A-111	82	2	1	15
	8484A-112	86	2	--	12
Wolfe 1	8345A-113	72	5	4	19
	8355A-114	68	2	27	3
	8365A-115	90	--	10	--
	8375A-116	86	--	4	10
	8385A-117	74	14	3	9
Bryant P-49-69-27-A4	8459A-118	84	--	6	10
Reel Government	8546A-119	84	--	6	10
23-28A	8555A-120	82	--	9	9
	8565A-121	84	--	10	6
	8575A-122	75	8	11	6
	8584A-123	50	2	45	3
Reel Government	8530A-124	70	3	25	--
21-28A	8540A-125	74	1	25	--
	8550A-126	77	2	8	20
Krause F14-34-P	8476A-127	70	2	8	20
	8486A-128	83	4	1	12
	8496A-129	92	2	1	5
Krause F34-34-P	8395A-130	86	--	2	12
	8405A-131	90	2	--	8
	8415A-132	88	2	3	7
	8425A-133	70	4	26	--
	8445A-135	70	4	26	--
	8485A-136	85	4	4	7
Government 14-1	9055A-138	60	--	39	1
	9075A-138	53	2	45	--
	9095A-139	90	2	--	8
Averages		77%	2%	13%	8%

TABLE V

COMPOSITION OF CLAY FRACTION IN SANDSTONES (X-RAY DIFFRACTION)

Well Number	Sample Number	Kaolinite	Illite	Smectite
Government F12-6-G	8054AA-1	--	80	20
	8058AA-2	--	--	--
Krause F12-2-P	8340AA-3	--	100	--
	8348AA-4	20	--	80
	8356AA-5	--	100	--
	8364AA-6	6	49	45
	8380AA-7	--	28	72
	8386AA-8	34	66	--
	8392AA-9	9	91	--

Note: Percentages given as percent of total clay in sample.

APPENDIX B

WATQF: ANALYSIS OF FORMATION WATERS

TABLE VI

WATEQF: ANALYSIS OF FORMATION WATERS

Sample Location	IAP/K_{ANH}	IAP/K_{GY}	IAP/K_{DOL}
SE NW Sec. 26 - T45N - R71W	-0.41	-1.03	2.13
SW NE Sec. 7 - T46N - R69W	0.12	-0.47	1.49
NW SE Sec. 12 - T46N - R70W	0.22	-0.37	1.50
Sec. 6 - T47N - R69W	-0.21	-0.76	2.12
SW SE	-0.19	-0.74	2.69
SW SE 7	-0.17	-0.72	1.98
NE SE Sec. 5 - T47N - R70W	-0.16	-0.69	1.80
NE SE 10	0.41	-0.07	----
SW NE 16	-0.01	-0.58	0.89
NE SW	-0.03	-0.59	1.86
	-0.27	-0.84	1.65
NE SE	-1.14	-1.63	1.82
	-0.52	-1.05	2.21
	-0.23	-0.80	1.49
	-0.47	-1.05	1.76
	-0.42	-1.00	2.41
	-0.36	-0.90	1.42
SW SE	-0.22	-0.77	1.68
	-0.24	-0.80	0.97
NE NE 21	-0.23	-0.82	1.70
SW NE 22	0.36	-0.15	1.57
NE NE 28	-0.05	-0.62	2.40
NE NW 35	-0.44	-0.99	-2.99
NE NE Sec. 2 - T47N - R71W	-0.44	-0.95	1.05
NW NE	-0.38	-0.90	1.27
SW SW Sec. 12 - T47N - R72W	-0.19	-0.76	1.44
SW SE	-0.17	-0.70	2.06
SW NW 14	-0.49	-1.01	-0.41
	0.26	-0.29	2.60
NW SW Sec. 2 - T48N - R69W	-0.07	-0.44	2.33
SW SW	-0.14	-0.49	1.84
SW SW 13	-0.47	-0.79	0.88
NE NE 14	-0.06	-0.47	2.33
SW NW	-0.05	-0.51	3.15
NE NE 15	-0.67	-0.53	1.88
SE NW 18	-0.09	-0.58	0.58
SE SE	-0.21	-0.71	1.88
SW NE 23	-0.14	-0.57	0.71
SW NE 24	-0.12	-0.54	1.96
NE SW Sec. 23 - T48N - R70W	-0.13	-0.64	1.63
SW SW	-0.17	-0.68	1.72
SE SW 25	-0.20	-0.73	0.08
NW SE Sec. 1 - T48N - R71W	-0.18	-0.64	1.66
SW NW 12	-0.14	-0.60	1.17
SE SE 35	-0.18	-0.70	1.90

TABLE VI (Continued)

Sample Location	IAP/K_{ANH}	IAP/K_{GY}	IAP/K_{DOL}
SE NE Sec. 7 - T48N - R72W	-1.97	-2.50	2.57
NW SW Sec. 2 - T49N - R69W	0.16	-0.21	0.56
SW NW 6	-0.07	-0.52	2.48
NE NE 7	-0.13	-0.38	-0.57
NE SW 8	-0.04	-0.44	2.27
SW SW	0.00	-0.43	0.58
SW NE 10	0.42	0.16	3.56
SE NE 11	0.17	-0.07	1.91
SW SW	-0.30	-0.55	2.08
SE NW 14	0.15	-0.12	3.59
NE SW 16	0.03	-0.30	1.27
SW NW 17	-0.06	-0.41	2.29
NE SW 21	-0.64	-0.86	1.95
SW SW	0.00	-0.33	2.27
SE SE 24	-2.23	-2.41	-7.08
NE SW 28	0.04	-0.28	2.63
NE SW Sec. 8 - T49N - R70W	-0.01	-0.44	2.67
NW 14	-0.42	-0.81	1.58
NW NW 23	-0.09	-0.52	2.88
SE SW Sec. 1 - T49N - R71W	-0.10	-0.52	2.54
SE SE 10	-0.02	-0.46	3.19
	-0.04	-0.49	1.91
NW NW 12	-0.13	-0.62	0.99
SE NE 24	-0.03	-0.44	2.15
NW NW Sec. 25 - T49N - R72W	-0.12	-0.54	2.90
SW SE Sec. 14 - T49N - R74W	-0.04	-0.58	2.76
SE NE Sec. 7 - T50N - R69W	0.07	-0.14	2.94
NW SW 19	0.06	-0.25	2.93
SW SW 21	-0.28	-0.57	0.78
SW SE 23	-0.26	0.09	1.49
	0.26	0.09	2.56
SE SE	0.26	0.09	2.56
NE NW 27	0.27	0.05	3.20
NW 30	-0.26	-0.60	2.54
NE SE Sec. 10 - T50N - R70W	0.14	-0.24	2.73
11	-0.13	-0.38	-0.73
	-0.04	-0.35	1.63
SW SW 25	0.07	-0.40	2.74
NE NW 26	-0.08	-0.44	2.19
27	-0.14	-0.54	2.05
SW NE 34	-.21	-0.22	2.96
SW NW 35	-1.04	-1.40	2.01
NW SE Sec. 20 - T50N - R71W	-0.05	-0.52	1.49
SE SE 34	0.26	-0.23	1.79
SW NW 35	-0.39	-0.08	2.79
SW SW Sec. 3 - T51N - R69W	-0.18	-0.08	1.38
SE NW 28	-0.30	-0.46	2.56

TABLE VI (Continued)

Sample Location	IAP/K_{ANH}	IAP/K_{GY}	IAP/K_{DOL}
SE NW 29	0.15	-0.01	2.74
SW SE 32	-0.20	-0.34	-1.30
SW SW 33	0.13	-0.02	2.63
	0.10	-0.04	3.11
SE SW 34	0.26	0.05	-2.55
SE SW Sec. 10 - T51N - R70W	-0.03	-0.32	3.32
SE SE 12	0.05	-0.24	2.66
NW NW 15	0.06	-0.20	1.95
22	-0.35	-0.58	3.49
SE NW	0.20	-0.05	2.32
NE SW 35	-0.16	-0.37	1.51
SW SW Sec. 25 - T51N - R71W	0.05	-0.34	1.68
	0.16	-0.25	3.13
NW SW Sec. 35 - T51N - R72W	0.11	-0.41	1.54
	-0.30	-0.83	-0.05
NE NE Sec. 1 - T52N - R69W	0.05	-0.11	1.87
SW SW 11	0.06	-0.25	-0.18
NW NW 15	0.20	-0.08	2.40
NW SE 28	0.21	-0.13	2.29
SE SE SE 29	-0.78	-1.15	-2.78
NE NW 33	-0.05	-0.30	2.71
NW SE 36	0.25	-0.07	2.55
NE SE Sec. 15 - T52N - R70W	0.21	-0.10	3.66
SE SE 16	0.20	-0.12	3.13
SE SE 20	0.07	-0.28	1.29
SE NE Sec. 12 - T52N - R72W	-0.03	-0.42	2.55
NE SW 24	0.01	-0.42	2.34
SW NW 25	0.44	0.02	2.07
	0.04	-0.39	2.35
	-0.07	-0.49	2.31
	-0.10	-0.53	-0.99
SW NE Sec. 5 - T53N - R69W	0.10	-0.12	2.59
SE SE 9	0.22	-0.01	3.44
NW NW 16	0.20	0.00	2.43
NW SW 18	0.05	0.16	2.32
SE SE 21	0.07	-0.11	2.62
	0.08	-0.10	3.24
24	0.11	-0.05	1.82
SE SE 36	0.02	-0.12	2.04
SE SE Sec. 3 - T53N - R70W	-1.09	-1.35	-1.90
SE NW 5	0.10	-0.18	1.91
SE SE 10	-0.02	-0.29	1.21
SE NE 13	-0.08	-0.32	-0.59
	0.00	-0.24	3.01
NE NE 14	0.06	-0.20	2.05
SE NE 24	0.12	-0.12	2.29
SE NW 27	0.07	-0.18	1.79

TABLE VI (Continued)

Sample Location	IAP/K_{ANH}	IAP/K_{GY}	IAP/K_{DOL}
NW SW	0.03	-0.22	-1.07
SE NW SW 28	0.08	-0.19	2.18
SW NE 33	0.48	0.21	1.98
NW NW 34	0.11	-0.16	1.98
	0.07	-0.18	1.95
SW SE	0.18	-0.09	2.28
SW SE Sec. 1 - T54N - R69W	0.07	-0.12	1.32
NE SE 11	0.08	-0.13	1.83
SE SE 13	0.05	-0.15	1.70
NW SE 14	0.41	0.19	3.44
SW SW 16	0.09	-0.13	2.16
NE SW 32	0.13	-0.09	1.50
NE SE	0.12	-0.10	2.94
	0.13	-0.09	2.05
NW NW Sec. 2 - T54N - R70W	0.02	-0.22	1.75
NE SW 6	-0.14	-0.43	2.89
NE SW 18	-0.08	-0.37	2.39
SE SW 34	-0.10	-0.37	2.18
NE NE Sec. 7 - T54N - R71W	-0.33	-0.68	2.35
	-0.20	-0.55	2.47
NW SW 11	0.04	-0.27	3.44
NW NW Sec. 25 - T55N - R69W	-0.09	-0.12	3.27
NW NW 30	0.01	-0.23	2.26
SW NE Sec. 26 - T55N - R71W	0.07	-0.22	2.32
SW NW Sec. 3 - T56N - R69W	0.02	-0.23	1.49
SW NW 34	0.02	-0.21	1.47
NW NW Sec. 21 - T57N - R69W	-0.03	-0.24	1.14
SE 34	0.01	-0.23	1.96
NW SE	0.00	-0.24	2.84
Sec. 4 - T49N - R67W	0.33	0.23	0.96
SW SE 5	0.17	0.06	3.63
SE SE	0.16	0.05	0.42
SE SW 8	-0.53	-0.70	3.05
SW SE	-0.18	-0.35	2.70
NW SE Sec. 8 - T49N - R68W	0.28	0.11	3.32
NE NE 10	0.05	-0.11	3.29
NE NW 14	0.42	0.26	1.96
NW NE 31	0.41	0.13	3.51
SE NW	-2.53	-2.81	-1.66
NW SW	-0.02	-0.28	2.49
NW NW Sec. 35 - T50N - R65W	-0.07	0.20	1.22
NE NE Sec. 7 - T50N - R66W	0.08	0.19	0.85
NE NW 21	0.16	0.27	2.88
SW NW Sec. 6 - T50N - R67W	-0.06	00.03	2.93
NE NW 7	-0.06	-0.07	3.82
SE SW 17	0.07	0.05	2.06
NE SE	0.04	0.02	2.42

TABLE VI (Continued)

Sample Location				IAP/K_{ANH}	IAP/K_{GY}	IAP/K_{DOL}
SW	NW		22	0.08	0.06	2.27
NW	NE		27	0.03	-0.01	1.78
NE	NW		28	0.09	0.05	0.49
				0.14	0.09	0.92
SW	NW			0.08	0.03	2.46
			29	0.16	0.10	0.50
NW	SE			-0.10	-0.17	2.04
			32	0.17	0.07	2.29
				0.17	0.07	2.76
				0.19	0.09	3.02
				0.10	0.00	2.12
NW	NE			0.15	0.06	1.27
				0.16	0.07	1.68
SW	NE			0.29	0.19	3.03
NE	SE	Sec.	1 - T50N - R68W	-0.01	-0.01	2.06
SE	SE		6	0.31	0.20	2.45
			18	0.44	0.32	3.07
				0.24	0.12	3.26
				0.41	0.27	3.58
SW	SW			0.35	0.21	0.49
NE	SW		19	0.29	0.10	1.76
SE	NE		27	0.31	0.14	2.44
SE	SE		32	0.37	0.24	3.49
				0.28	0.16	2.77
NW	SE	Sec.	9 - T51N - R66W	-0.02	0.18	2.49
	NE	Sec.	2 - T51N - R68W	-0.30	0.16	3.17
SW	NW			0.33	0.15	2.54
SW	NW		3	0.35	0.13	1.81
SE	SE		9	0.17	-0.02	1.53
NW	NW		15	0.14	-0.02	3.70
SE	SW		20	0.17	0.03	3.98
SE	NW		29	0.13	0.02	2.99
SE	NE		30	0.21	0.08	2.02
SW	NE		36	-0.01	0.02	2.72
SE	NW			-0.02	0.00	2.55
NE	NE	Sec.	19 - T52N - R67W	0.23	-0.20	4.36
SW	SW	SW		0.22	0.19	1.40
SE	NW		31	0.17	0.13	1.21
NW	NE	Sec.	1 - T52N - R68W	0.06	0.02	4.49
NE	SW		2	0.17	0.11	3.25
SW	SE			-0.24	-0.30	1.30
NE	NE		7	0.19	-0.03	2.90
NW	NW		18	0.23	0.04	3.56
SE	SE		20	0.20	0.01	3.54
SW	NE		24	0.34	0.24	2.85
			28	0.15	-0.05	3.64
SE	SE		30	0.41	0.16	2.93

TABLE VI (Continued)

Sample Location	IAP/K_{ANH}	IAP/K_{GY}	IAP/K_{DOL}
NE NE 31	0.20	-0.06	2.60
NW NE	0.20	-0.06	2.60
SW SE 34	0.36	0.13	1.87
NW NW 35	0.18	0.03	2.28
SW NE NW Sec. 18 - T53N - R65W	-0.57	-0.25	0.07
NW NW Sec. 7 - T53N - R67W	0.18	0.07	3.07
NE NW 31	-2.25	-2.26	-3.58
SW SW Sec. 11 - T53N - R68W	0.11	-0.02	2.49
SW SE 19	0.13	-0.02	3.00
NE SW 23	0.34	0.23	3.39
	0.31	0.20	2.38
	0.18	0.07	3.76
NW NW NW Sec. 21 - T54N - R60W	-0.13	0.56	-0.37
Sec. 24 - T54N - R63W	-0.50	-0.15	2.09
SE Sec. 12 - T54N - R65W	-1.46	-1.12	-0.24
13	-1.24	-1.34	2.21
SE NW	-1.24	-1.35	2.21
SE SE 29	-1.20	-0.88	-0.68
	-1.28	-0.97	0.04
SW NW Sec. 10 - T54N - R66W	-0.14	0.02	1.61
NW Sec. 7 - T54N - R67W	0.09	-0.03	2.52
NE NW	0.23	0.12	2.19
SW NW	0.07	-0.04	0.62
NW SE Sec. 13 - T54N - R68W	0.08	-0.07	1.16
NE NE 19	0.07	-0.12	1.35
SE SE 35	0.00	-0.14	1.32
	0.03	-0.11	3.96
SW SW Sec. 9 - T55N - R67W	0.02	0.0	0.95
NW NW 10	-0.57	-0.55	3.15
NE Sec. 35 - T55N - R68W	0.06	-0.12	2.68
NE NW Sec. 14 - T56N - R61W	0.09	.24	2.09
NE SW Sec. 15 - T57N - R64W	0.12	0.20	2.21
SW NW NW Sec. 18 - T41N - R77W	-0.44	-0.31	0.90
NE SE Sec. 16 - T41N - R81W	-0.44	-0.31	0.13
SW SW 23	-0.76	-0.67	2.26
26	-1.00	-0.91	2.92
	-0.99	-0.91	1.12
NE NE 27	-1.14	-1.03	0.95
NW NW	-1.38	-1.28	-0.80
NE SE SE Sec. 35 - T42N - R78W	0.09	-0.22	0.91
SE SW Sec. 35 - T43N - R82W	-0.30	-0.19	3.39
NW NW Sec. 26 - T43N - R84W	-3.65	-3.32	0.85
NE SW SW Sec. 13 - T44N - R82W	-0.30	-0.40	2.42
SE NE 24	-0.62	-0.71	1.80
NE NE NW	-0.63	-0.72	1.17
SW SW 26	-0.75	-0.79	2.00
NW SW Sec. 19 - T45N - R79W	-0.41	-0.94	1.47

TABLE VI (Continued)

Sample Location	IAP/K_{ANH}	IAP/K_{GY}	IAP/K_{DOL}
NW 23	-0.25	-0.78	0.12
SE Sec. 24 - T45N - R80W	-0.28	-0.81	0.63
SW SW Sec. 5 - T46N - R81W	-0.10	-0.39	1.40
SW SE Sec. 27 - T49N - R83W	-2.95	-2.56	0.74
SW NW Sec. 5 - T35N - R65W	0.03	-0.32	1.43
35	-0.80	-0.80	-0.58
NE SE NE Sec. 26 - T36N - R64W	-0.18	-0.28	0.25
NE SE	-0.21	-0.32	2.30
SW SW Sec. 19 - T38N - R61W	0.10	0.03	2.34
NW NW 30	0.09	-0.02	3.31
SW NW	0.03	-0.04	1.72
NE NE Sec. 25 - T38N - R62W	-4.33	-4.36	2.30
NE SE	-0.11	-0.14	3.54
SW Sec. 19 - T39N - R60W	0.27	0.21	0.64
NE SW 24	0.13	-0.21	1.02
NE NW Sec. 28 - T28N - R66W	-2.67	-2.19	0.10
SW NW SE Sec. 24 - T29N - R69W	-2.10	-1.62	-1.97
	-2.62	-2.14	-0.26
SW NW NE	-2.67	-2.19	-1.04
NE NW 33	-2.72	----	-1.74
NE SE Sec. 9 - T54N - R77W	-0.12	-0.73	1.89
SW SW Sec. 7 - T55N - R85W	-1.04	-0.67	-0.48
Sec. 28 - T45N - R61W	-0.05	0.21	0.29
NE NE Sec. 4 - T47N - R68W	-0.10	-0.52	1.99
NW SE 31	-0.19	-0.66	3.08
	-0.35	-0.82	3.02
NW SW NW Sec. 6 - T48N - R68W	0.03	-0.23	1.98

VITA

John Conrad Markert

Candidate for the Degree of

Master of Science

Thesis: MINERALOGICAL, GEOCHEMICAL, AND ISOTOPIC EVIDENCE OF DIAGENETIC ALTERATION, ATTRIBUTABLE TO HYDROCARBON MIGRATION, RAVEN CREEK AND REEL FIELDS, WYOMING

Major Field: Geology

Biographical:

Personal Data: Born in Shawnee, Oklahoma, December 8, 1950, the son of Dr. and Mrs. G. Conrad Markert.

Education: Graduated from Stroud High School, Stroud, Oklahoma, in May, 1969; received Bachelor of Science degrees in Zoology and Geology from Oklahoma State University in December, 1974, and December, 1979; completed the requirements for the Master of Science degree in Geology at Oklahoma State University in May, 1982.

Professional Experience: Development geologist, Cities Service Company, Oklahoma City, Oklahoma, May, 1980 to August, 1980; teaching assistant, Department of Geology, Oklahoma State University, Stillwater, Oklahoma, August, 1980 to May, 1981; research assistant, Department of Geology, Oklahoma State University, Stillwater, Oklahoma, August, 1980 to August, 1981; junior member of the American Association of Petroleum Geologists; student member of the American Institute of Mining Engineers.